

INFORMATION TO USERS

This was produced from a copy of a document sent to us for microfilming. While the most advanced technological means to photograph and reproduce this document have been used, the quality is heavily dependent upon the quality of the material submitted.

The following explanation of techniques is provided to help you understand markings or notations which may appear on this reproduction.

1. The sign or "target" for pages apparently lacking from the document photographed is "Missing Page(s)". If it was possible to obtain the missing page(s) or section, they are spliced into the film along with adjacent pages. This may have necessitated cutting through an image and duplicating adjacent pages to assure you of complete continuity.
2. When an image on the film is obliterated with a round black mark it is an indication that the film inspector noticed either blurred copy because of movement during exposure, or duplicate copy. Unless we meant to delete copyrighted materials that should not have been filmed, you will find a good image of the page in the adjacent frame.
3. When a map, drawing or chart, etc., is part of the material being photographed the photographer has followed a definite method in "sectioning" the material. It is customary to begin filming at the upper left hand corner of a large sheet and to continue from left to right in equal sections with small overlaps. If necessary, sectioning is continued again—beginning below the first row and continuing on until complete.
4. For any illustrations that cannot be reproduced satisfactorily by xerography, photographic prints can be purchased at additional cost and tipped into your xerographic copy. Requests can be made to our Dissertations Customer Services Department.
5. Some pages in any document may have indistinct print. In all cases we have filmed the best available copy.

University
Microfilms
International

300 N. ZEEB ROAD, ANN ARBOR, MI 48106
18 BEDFORD ROW, LONDON WC1R 4EJ, ENGLAND

7911160

OZOMARD, CHRISTIAN OLUFEMI
ANALYSIS OF COKE COMBUSTION DURING IN-SITU
OIL RECOVERY.

THE UNIVERSITY OF OKLAHOMA, PH.D., 1978

University
Microfilms
International 300 N. ZEEB ROAD, ANN ARBOR, MI 48106

PLEASE NOTE:

In all cases this material has been filmed in the best possible way from the available copy. Problems encountered with this document have been identified here with a check mark .

1. Glossy photographs _____
2. Colored illustrations _____
3. Photographs with dark background _____
4. Illustrations are poor copy _____
5. Print shows through as there is text on both sides of page _____
6. Indistinct, broken or small print on several pages _____ throughout

7. Tightly bound copy with print lost in spine _____
8. Computer printout pages with indistinct print _____
9. Page(s) _____ lacking when material received, and not available
from school or author _____
10. Page(s) _____ seem to be missing in numbering only as text
follows _____
11. Poor carbon copy _____
12. Not original copy, several pages with blurred type _____
13. Appendix pages are poor copy _____
14. Original copy with light type _____
15. Curling and wrinkled pages _____
16. Other _____

University
Microfilms
International

300 N. ZEEB RD., ANN ARBOR, MI 48106 /313/ 761-4700

THE UNIVERSITY OF OKLAHOMA
GRADUATE COLLEGE

ANALYSIS OF COKE COMBUSTION
DURING IN-SITU OIL RECOVERY

A DISSERTATION
SUBMITTED TO THE GRADUATE FACULTY
in partial fulfillment of the requirements for the
degree of
DOCTOR OF PHILOSOPHY

By
CHRISTIAN OLUFEMI OZOMARO
Norman, Oklahoma
1978

ANAYLSIS OF COKE COMBUSTION DURING IN-SITU OIL RECOVERY

Approved By:

Key C. Carter
A.W. Mc. Cray
J. H. Day
S. E. Mearns
J.M. Townsend

ACKNOWLEDGMENT

The author wishes to express his appreciation to Dr. H. B. Crichlow, who served as advisor in this research, for his continued support, interest and guidance in the completion of this effort.

Appreciation is also extended to Professor A. W. Aldag, Professor D. E. Menzie, Professor F. M. Townsend and Professor A. W. McCray for their valuable discussion and constructive criticism of this dissertation.

Recognition is extended to Mr. W. L. Martin, Mr. J. D. Alexander and management of Conoco Research and Development Division for their time, encouragement and the use of their facilities.

Special thanks go to the Nigerian Federal Government for its financial support.

Finally, the author wishes to express his indebtedness to his wife Monica, for her encouragement, patience and devotion, and also, to his son Omoyefe and daughter Orowo.

TABLE OF CONTENTS

	Page
LIST OF TABLES	vi
LIST OF ILLUSTRATIONS	vii
Chapter	
I. INTRODUCTION	1
II. LITERATURE REVIEW	5
Statement of Problem	12
III. MATHEMATICAL MODELS	13
3.1 Chemical Rate Control Analysis	13
3.1.1 Differential Method of Analysis	17
3.1.2 Non-Linear Optimization	26
3.2 Diffusion Control Analysis	30
IV. EXPERIMENTAL APPARATUS AND MATERIALS	36
4.1 Apparatus for Process Simulation	36
4.1.1 Fire Flood Pot Pressure Jacket	38
4.1.2 Fire Flood Pot Liner	38
4.1.3 Temperature Control System	41

Chapter	Page
4.1.4 Gas Flow System	46
4.1.5 Auxiliary Systems	47
4.2 Apparatus for Combustion Studies	47
4.2.1 Reactor	47
4.2.2 Gas Sampling and Analysis	49
4.3 Materials	54
V. EXPERIMENTAL PROCEDURE	55
5.1 Process Simulation.	55
5.1.1 Weight Measurements	60
5.1.2 Saturating Porous Medium with Water	60
5.1.3 Water Displacement in the Porous Medium	61
5.1.4 Simulation of Various Discrete Regions	62
5.2 Fuel Concentration.	65
5.3 Combustion Process.	65
5.3.1 Preparation of Sample	65
5.3.2 Initiation of Reaction.	66
5.3.3 Sample Collection	67
5.3.4 Sample Analysis	67
5.3.5 Calibration of Gas Chromatograph.	69
5.3.6 Termination of Combustion	70
VI. PRESENTATION AND DISCUSSION OF RESULT.	71
VII. CONCLUSION	91

	Page
BIBLIOGRAPHY	94
NOMENCLATURE	98
APPENDICES	100
A. Algebraic Illustration of Steepest Descent Non-Linear Optimization Technique.	100
B. Data and Results of Experimental Runs (Oxygen Utility).	104
C. Hydrogen Carbon Ratio Computations . .	108
D. Data and Results of Experimental Runs (Coke Combustion)	111

LIST OF TABLES

Table		Page
3.1	Comparison of Non-Linear Solution Technique With Statistical Method	25
4.1	Main Components in Process Simulation Apparatus	36
5.1	Computation of Initial Oil, Water and Gas Saturation in Porous Media.	63
5.2	Temperature History Experienced by Porous Media	64
	Appendix B: Experimental Results and Data:	
B-1	Effect of Channeling on Oxygen Utility.	105
B-2	Effect of Coke Concentration and Combustion Temperature on Oxygen Utility	106
B-3	Effect of Combustion Temperature on Oxygen Utility	107
	Appendix D: Data and Results of Runs (Coke Combustion)	

LIST OF ILLUSTRATIONS

Figure		Page
3.1	Carbon Oxides in Exit Gases Vs Combustion Time	20
4.1	Schematic Diagram of Process Simulation Experimental Apparatus	37
4.2	Fire Flood-Pot Pressure Jacket Showing Construction	39
4.3	Assembled Pressure Heating Jacket, Mating Flange Assembled Reactor	40
4.4	Drawing of Fire-Pot Liner.	42
4.5	Controller Wiring.	43
4.6	Electrical Wiring of Temperature Control System	44
4.7	Weight Measurement of Pot Liner Using Heavy Duty Ohaus Scale	48
4.8	Combustion Reactor	50
4.9	Model 550 Gow Mac Chromatograph.	52
5.1	Various Views of Combustion Experimental Apparatus.	56
5.2	Process to be Simulated in Model	59
5.3	Schematic Diagram of Combustion Process Apparatus.	68
6.1	Effect of Channelling on Oxygen Utility.	72
6.2	Effect of Coke Concentration and Temperature on Oxygen Utility.	76

6.3	Effect of Temperature and Channelling on Oxygen Utility.	79
6.4	Best Values of K Vs Gas Flow Rate	80
6.5	Reaction Rate Vs Carbon Concentration	83
6.6	Variable in Diffusion Equation Vs H/C	85
6.7	Best Values of K Vs Combustion Temperature. . .	87
6.8	Variable in Diffusion Equation Vs Time.	89

CHAPTER I

INTRODUCTION

After primary production of crude oil from a reservoir, a considerable amount of oil is left behind and this necessitates the application of secondary recovery techniques. The choice of, and time to initiate such secondary mechanism will be determined by a host of variables. These include: quantity of residual oil, the formation characteristics, physical and chemical properties of the crude, and production history of the field, etc. For most reservoirs, the percentage of crude oil remaining after primary and secondary recovery methods presents an attractive potential for enhanced oil recovery.¹ The term enhanced or improved or tertiary oil recovery is used to describe oil production after waterflooding or that initial flow of gas or oil from reservoirs as yet unproducibile in the light of present economic conditions and/or existing technology. The latest estimates of American Petroleum Institute indicate there are 299 billion barrels² of known resources that will never be produced under existing economic conditions and known technology, and this value is approximately 68 percentage³

of O.O.I.P. The difficulty of finding new reserves to replace produced oil could be minimized by employing better and more efficient recovery techniques since more than 50% of the oil in the reservoir is usually left behind. The challenging task has resulted in the development of newer recovery techniques several of which show promise of commercial applications in the oil field. Some of these techniques are out of the laboratories and into the field for pilot testing with possible large scale field operations. The prominent ones are miscible flooding,⁴ ⁵, ⁶ micellar-polymer flooding, carbon dioxide flooding⁷ and in-situ combustion. The major drawbacks to existing enhanced recovery methods range from high cost and limited availability of material to poor sweep efficiency.

In-situ combustion is one of the thermal recovery techniques employed in recovering medium to low gravity viscous crude oil (12° API to 35° API). This mechanism consists of igniting the crude oil in the porous rock by means of an igniter and the combustion front is propagated through the reservoir rock by continuously injecting air and/or combustion gases. The heat generated lowers the oil viscosity thereby resulting in a more favorable mobility ratio that permits more efficient displacement to producing wells.

In forward combustion, the combustion front moves from the injection well towards the producing well in the same direction as the injected air. The fuel for this

process is a residual material known as coke and its concentration and rate of combustion at the front are important factors governing the air requirement for the forward combustion process. As much as 300 barrels per acre⁸-foot of hydrocarbon may be consumed by the burning front and the heat transport associated with the exothermic reaction is a key and unique feature of this process. Fuel availability has been reported as one of the most critical parameters governing in-situ combustion performance⁹ because this highly reactive hydrocarbon residuum produced in the evaporation and cracking region must be completely burned before the combustion front can propagate to the producing well. Thus, the ability to maintain self sustained combustion, advance rate of the combustion front, and total air requirement for the in-situ process are all related to the fuel nature and its concentration. The coke formation and its subsequent combustion add a new dimension to the complexity of this process since we now have to consider simultaneous hydrodynamics of three phase flow coupled with heat, mass and chemical reaction kinetics. Thus, an adequate mathematical description of the forward combustion process will require adequate description of the coke combustion process.

As noted by some authors,^{10, 11} lack of complete oxygen consumption has been most troublesome. The vented oxygen from producing wells represent a waste and thereby making the process ineffective and in most cases, uneconomical.

Such poor oxygen utilization which is most critical at low combustion temperatures could be speculatively attributed to insufficient fuel deposition or explained in terms of the reaction kinetic process.

The main purpose of this study was two fold:

1. To investigate the adequacy of the model describing oxygen carbon reaction of various types of coke formed under conditions that simulate field conditions during in-situ combustion and also, to determine the controlling mechanism of the coke combustion.

2. To conduct experiments to explain the low oxygen utility that is observed during low temperature combustion.

CHAPTER II

LITERATURE REVIEW

When combusting thermal energy is introduced into underground formations to recover oil, the process is known as in-situ combustion. The combustion process is most useful in recovering low to medium gravity crude oils because of the significant effect of temperature on cracking and vaporizing the oil; lowering the crude viscosity and causing fluid expansion. The thermal energy is introduced into the formation by igniting the underground crude and the generated combustion front is propagated by continuous air injection. In forward combustion which is referred to in this work, the fuel for the combustion process is a residual material known as coke which is deposited on the sand grains during distillation and cracking of the oil ahead of the combustion front.

The effectiveness of this process depends on the rate of heat generation by combustion process and efficiency of the heat utilization. The rate of heat generation depends on the reaction rate which depends on coke (fuel) concentration, oxygen partial pressure and air injection rate. The fuel

concentration in turn depends on the formation and crude oil characteristics. The efficiency of heat utility on the other hand depends on reservoir fluid saturation distribution, thermal properties of the reservoir rock matrix and its surrounding rock. One can at this stage, begin to understand the intricate interdependence between the various process variables and it is no surprise then that the history of mathematical description and performance prediction of in-situ recovery technique has been centered on emphasizing single factors such as thermal or hydrodynamic or kinetic aspects.^{12, 13, 14} Likewise, laboratory research works have only concentrated on simple models in which all the process variables are held constant except the one under investigation.^{9, 11, 15} Although these experimental works do not reflect real world situations where most of the variables vary both with time and distance, they do however provide comprehensive description of these subprocesses which aid in adequate formulation of a comprehensive mathematical model.

The mathematical models proposed by Baily and Larkin,¹³ Thomas¹⁶ and Chu¹⁴ emphasized the heat transfer by convection and conduction and vertical heat losses aspects. The following assumptions were made:³

1. The effect of heat transfer due to flow of oil and gas.

2. The effect of condensation of vapors ahead of the combustion front and

3. Formation of vapor at the combustion front

were all neglected. In other words, the hydrodynamic and kinetic effects were all neglected.

Wilson et al.¹² concentrated on the hydrodynamic aspect and they developed a model for predicting the fluid flow rates and their saturations in the different regions ahead of an advancing combustion front. A steady state assumption between the fluids was made and the concept of three phase relative permeability was used. They ignored heat transfer and kinetic effects.

The first serious attempt to consider kinetic effects was by Tadema,¹⁷ who presented a differential thermal analysis study. The apparatus used was adapted for measuring the temperature difference between an oil sand sample in an air stream and a blank sand sample where both samples were being heated under the same conditions. Two different combustion reactions were observed to occur at about 270°C and 400°C and analysis of the exhaust gas indicated that at 270°C, most of the oxygen was taken up from the feed gas leaving behind a coke-like residue. Most of the oxygen reacted to form water with small percentage traced as CO₂ and CO. At the high temperature peak of 400°C, mainly CO₂ and some CO were formed with little water production and no residue left behind. Thus, Tadema's kinetic analysis was

mostly qualitative and also, devoid of other process variables which were considered separately.

The first comprehensive model to incorporate the effects of conductive-convective heat transfer with convective external heat loss, phase change in water component, three phase fluids flow and chemical reaction was by Gottfried.¹⁸ The chemical aspect of his model was most lacking since it neglected hydrocarbon phase change and variation in fuel concentration. The model assumed a non-volatile liquid oil in which the reaction rate is proportional to the amount of oil present and an Arrhenius type rate expression was arbitrarily assumed but interestingly enough, he rightly indicated that the correct procedure would be to write an additional partial differential equation representing a mass balance on the fuel (coke). Such an expression would account for both the rate of coke formation and the rate at which it is subsequently burned. However, quantitative information describing the above rates are scarce and sometimes contradictory. Bousaid et al.¹⁹ pointed out the scanty existence of quantitative work on reaction kinetics in forward combustion but noted the extensive work on combustion of carbon, oils and carbonaceous residue from cracking catalyst pellets. Dart et al.²⁰ demonstrated that the combustion rate for oxidation of carbonaceous residue on clay catalyst pellets was first order with respect to carbon and oxygen partial pressure for carbon concentration greater than 2% by weight of

catalyst but second order with respect to carbon concentration for values less than 2%. The variation in order of carbon dependence on the rate studies were attributed to the aging effect²¹ of the fuel during combustion. Lewis et al.²² studied oxidation of charcoal coke in fluidized bed and indicated a rate expression that showed first order dependence on both carbon concentration and oxygen partial pressure. Both Dart et al. and Lewis et al. concluded that the oxidation reaction of carbon in porous beds was chemically rate controlled and that the rate constant could be correlated by Arrhenius equation. Determination of the controlling mechanism by these authors was based on reaction rates derived from power law type model describing coke-oxygen reaction.

On the other hand, Strijbos²³ used cylindrical pills made of inert ceramic material (pyrolith) that were impregnated with Rhoplex, dried and heated to 600°C in a nitrogen atmosphere to form carbonaceous residue. He showed that above 660°C, the combustion process was controlled by diffusion. Weisz and Goodwin²⁴ conducted some combustion studies on a porous catalyst and at high temperature (625°C), found the process to be controlled by diffusion. These authors^{23, 24} used unreacted²⁵ core analysis model in their solution approach to the problem. The above studies and results were very revealing and important but their applicability was no doubt intended for the relevant subjects

studied and their applicability in the in-situ recovery process is questionable.

More relevant data were provided by Ramey¹⁹ et al. who studied oil oxidation on two crude types at low temperature in a rocking bomb apparatus and found the rate to be first order with respect to oxygen partial pressure. They also reported that on the coke combustion studies, for the same two types of crude investigated, a combustion rate that indicated a first order dependency with respect to both carbon concentration and oxygen partial pressure was observed. They also showed that the activation energy depended on formation type and the presence of clay reduced its value from 26,600 to 20,800 Btu/lb-mole. Here again, these authors assumed a power law type rate expression model and concluded that the coke combustion process is controlled by chemical reaction. Some of the limitations of the work presented by Bousaid et al. could be summarized as:

1. The condition under which the work was done do not simulate the sequence of hydrodynamic and thermal effects occurring in the reservoir fluids during in-situ combustion.

2. The cokes were made by mixing crude oil and sand and then heated in the presence of nitrogen only. This is a representation of coke formed by pyrolysis and they do not represent coke formed from low temperature oxidation (L.T.O.) of the crude oil.

The most recent work by Dabbous and Fulton²⁶ has strongly indicated the need for more research efforts on resolving the controlling mechanism during coke combustion. Their primary interest was on evaluating the coke formation reaction rate with peripheral interest on its combustion process. They also reported that the coke combustion process was controlled by chemical reaction but they also suspected some diffusion effects at high carbon concentration above 0.5 gmC/100 gm sand.

The lack of agreement in the published literature as to the controlling mechanism of the coke combustion reaction as demonstrated by these authors^{19, 20, 21, 22, 23, 26} is a further indication that more extensive work is required in this area.

STATEMENT OF THE PROBLEM

At low temperatures the reaction between crude oil and oxygen in a porous medium, leaves a residual material known as coke. The reaction kinetics of this coke combustion is the least investigated subprocess of in-situ oil recovery process and adequate description of the process is essential for complete mathematical modeling of this recovery mechanism. Depending on the line of attack, conflicting results could be obtained in trying to determine the controlling mechanism of this subprocess as indicated in the literature review section of this work.

This work addresses itself to the task of determining the controlling mechanism by considering two different mathematical approaches to the problem.

Furthermore, this work also addresses itself to the problem of high percentage of oxygen appearing unreacted especially at low temperatures during coke combustion.

CHAPTER III

MATHEMATICAL MODELS

3.1 Chemical Rate Control Analysis

The reaction between the coke and oxygen in a porous bed is a heterogeneous flow reaction. There are a number of transport processes occurring within the reaction zone and the slowest step has the highest resistance to reaction. Therefore, such slowest process is the controlling process in determining the overall observed reaction rate. These subprocesses can be described as:

1. Transport of oxygen from the bulk gas stream through a thin boundary layer to the coke interface by a process of diffusion.
2. Absorbtion into active sites.
3. Reaction with coke at the active sites.
4. Desorbtion of combustion products into pores of the coke matrix.
5. Transport of combustion products back into the bulk gas stream.

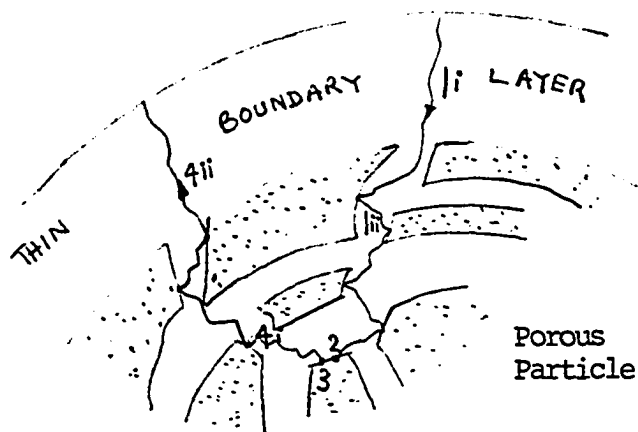


ILLUSTRATION OF PHYSICAL AND CHEMICAL STEPS
IN HETEROGENEOUS REACTION

- Step 1(i) Transport of oxygen through thin boundary layers surrounding the particle.
- Step 1(ii) Diffusion through blanket of ash to surface of unreacted core.
- Step 2 Adsorption at active site.
- Step 3 Reaction of oxygen with coke at reaction surface.
- Step 4(i) Diffusion of gaseous product through ash back to exterior surface of solid.
- Step 4(ii) Diffusion of gaseous product through gas film back into gas stream.

According to Levenspiel,²⁵ when no gaseous products are formed or if the reaction is irreversible, Steps 4(i) and 4(ii) will not contribute to the resistance to reaction. A comprehensive overall reaction rate can be formulated in which the above steps are all considered but such formulation will be quite

complex and will contain so many variables, resulting in questionable utility for such formulation.

Previous authors^{19, 20, 26, 27} studying the combustion of coke in a porous bed had started with a model describing carbon burning rate to be directly proportional to carbon concentration and oxygen partial pressure. Mathematically, this could be expressed as

$$-r = \frac{dc}{dt} = Kc^n p^m \text{ - - - - - (3.1)}$$

Some of these authors^{19, 20, 22} concluded that such combustion process was chemically rate-controlled and that the rate constant could be correlated by the Arrhenius equation.

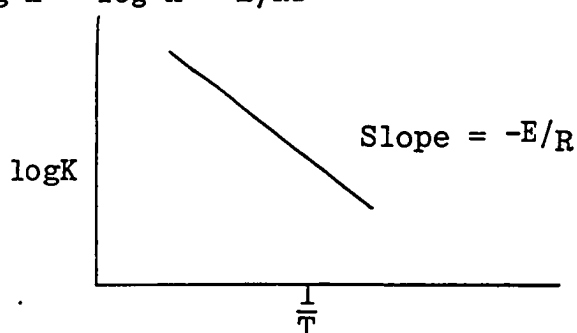
Thus equation (3.1) now becomes

$$r = A e^{-E/RT} c^n p^m \text{ - - - - - (3.2)}$$

Although not implicitly indicated in any of the previous research works, conditions that enhanced diffusion process should have been employed and by using the model depicted by equation (3.2), observed experimental data should not match this proposed model if indeed the overall reaction rate was controlled by diffusion. On the other hand, if we do not have a diffusion limiting process, provision for enhancing diffusion conditions will be immaterial and ineffective and observed overall reaction rate data will closely correlate the proposed chemically rate controlled theory. In this case, the following result should be expected.

$$K = Ae^{-E/RT}$$

$$\log K = \log A - E/RT$$



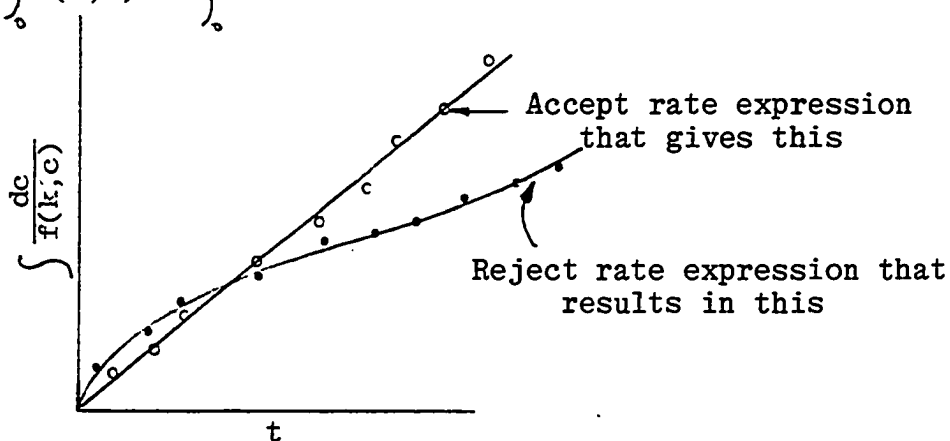
The above mathematics are rather trivial but the complexity of analysis is in trying to determine the value of K (specific rate coefficient). In the following sections, detailed analysis on the determination of the variables r , c , p , K is discussed.

The burning of a layer of coked sand in a combustion cell should strictly speaking be considered as an integral reactor and the kinetic data obtained, treated as integral data. Levinspiel²⁵ indicated that when variation in reaction within a reactor is very large then we account for such variation in the method of analysis. This is the basis of an integral reactor. Since reaction rates are concentration dependent, such large variations in rate may be expected to occur when the reactant composition changes significantly in passing through the reactor. For the integral analysis, the rate expression to be tested is integrated and the resulting concentration time curve is compared with experimental concentration data. If the fit is unsatisfactory,

another rate expression is proposed and tested. To illustrate this, suppose $r = -\frac{dc}{dt} = f(k, c)$

$$\text{Then } -\frac{dc}{f(k, c)} = dt$$

$$\int_0^c \frac{dc}{f(k, c)} = \int_0^t dt = t$$



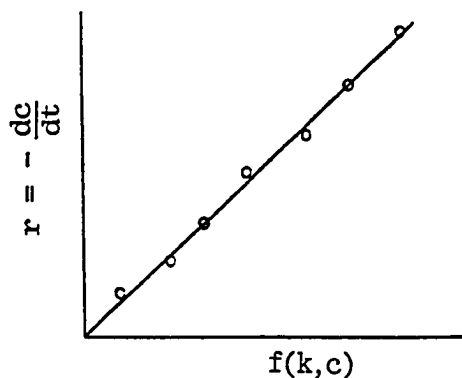
If the physical situation involved in burning a layer of coked sand is such that the reaction rate can be considered to be constant at all points within the reactor, then differential method of analysis will be justifiable. Such a physical situation is representative of the conditions involved in burning thin layer of coked sand in a shallow small reactor. This is the basis on which the differential method of analysis was chosen.

3.1.1 Differential Method of Analysis

In this method of analysis, we deal directly with the differential rate equation to be tested. The entire procedure can be summarized below.

1. Hypothesize a mechanism and obtain a rate expression from it.
2. Obtain raw data in the form of concentration vs. time for all the variables in the rate expression.
3. Draw a smooth curve through the concentration-time data and determine the slope at selected concentration intervals. This represents the reaction rate.
4. Plot the value of this reaction rate (slope of curve) against evaluated values of the expression describing the reaction rate.

As an illustration, suppose $r = -\frac{dc}{dt} = f(k,c)$ then from raw C vs t data, obtain $\frac{dc}{dt}$ by differentiating C vs. t curve. The slope obtained from the above is plotted against $f(k,c)$



The expression $f(k,c)$ which yields a straight line is accepted as the correct expression describing the reaction rate under investigation.

The following procedural steps are involved in applying the above concept to coke-oxygen reaction.

1. The hypothesized rate equation under investigation is $r = - \frac{dc}{dt} = KC_p^m$.
2. The raw data describing volume % CO, CO₂ and O₂ with time are illustrated by Figure 3.1. Convert the volume % measurement to carbon concentration C as indicated below.

Detected oxides of carbon produced during carbon combustion are CO and CO₂. Therefore, at any instant, volume of carbon products produced =

$$[CO(t) + CO_2(t)] F(t)$$

Total mass of carbon burnt after t minutes = CB(t)

$$CB(t) = \int_0^t [C.F. (CO(t) + CO_2(t)) F(t)] dt \quad \text{--- (3.3)}$$

where CB is gmC/100 gm sand.

C.F. = Conversion factor (from volume to mass)

$$= \frac{12 \text{ gmC/mol.} \cdot 100 \text{ gm sand}}{\text{G.M.V.} \cdot \text{wt of clean sand (gm)}}$$

G.M.V. = Gram molecular volume of gases at room

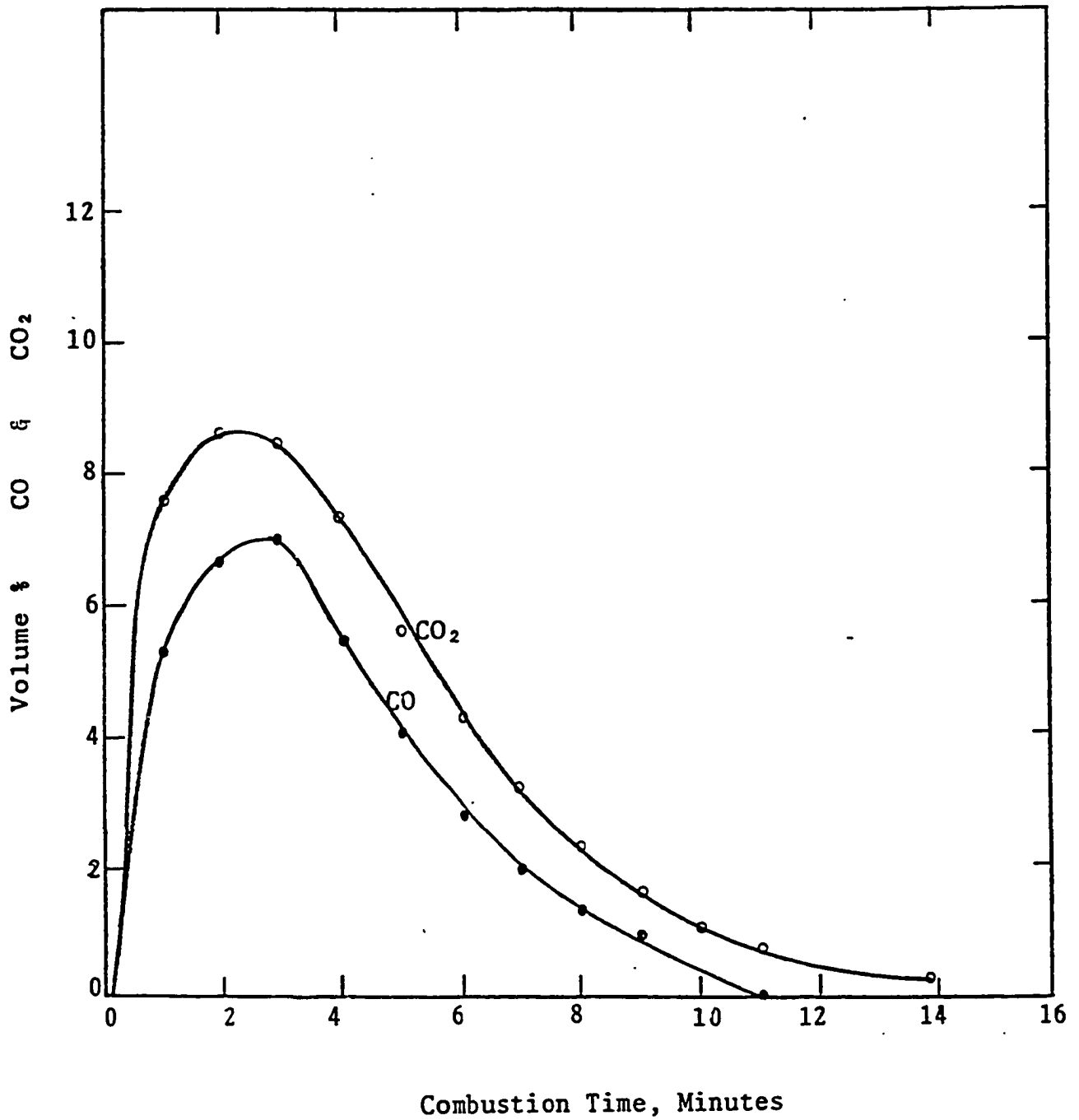
temperature = 22,900 cc/mol at 72°F

By using C.S.M.P.²⁸ integrator (Continuous system modelling program), equation 3 was integrated for the duration of the run and this yielded the initial carbon concentration C_I. The instantaneous carbon concentration at any time C(t) is thus C_I-CB.

$$C(t) = \int_0^{t_{\text{end}}} [C.F. (CO(t) + CO_2(t)) F(t)] dt - \int_0^t [C.F. (CO(t) + CO_2(t)) F(t)] dt$$

$t_{\text{end}} = \text{time to end of run}$

Figure 3.1
Carbon Oxides in Exit Gas
Vs
Combustion Time



The oxygen partial pressure P was evaluated as follows:

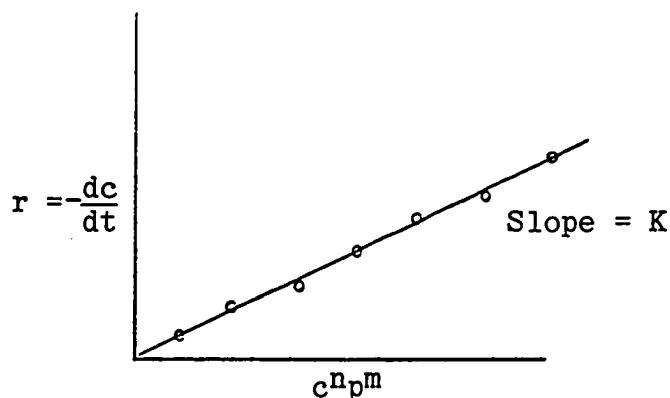
$$P = \frac{P_{in} + P_E}{2} \quad \text{where } P_{in} \text{ and } P_E \text{ represent the inlet}$$

and exit oxygen partial pressures respectively.

$$P_{in} = \frac{\text{Vol. \% of inlet O}_2}{100\%} * \pi \quad \text{where } \pi = \text{reactor pressure in atmosphere}$$

$$P_E = \frac{\text{Vol. \% of unreacted oxygen}}{100\%} * \pi$$

3. By using C.S.M.P. derivative program, the slope of the concentration time curve was evaluated at each time level to yield reaction rate r .
4. Plot $\frac{-dc}{dt}$ versus $f(C,P)$ where $f(C,P)$ is $c^n p^m$ and if a straight line through the origin is obtained, then the rate equation is consistent with the data.



The task at this stage is to evaluate the function $f(C,P)$ that will yield a straight line as indicated above. A non linear optimization technique was developed to give optimum values of n , m and K . The reasons for using non linear optimization technique are discussed later. With various K values for different isothermal combustion temperatures, the Arrhenius plot can then be tested to determine

if reaction controls the combustion process.

For a reaction control process, $K = Ae^{-E/RT}$ thus $\log K$ vs. $\frac{1}{T}$ will yield a straight line.

As can be seen from the above discussion, determining the controlling mechanism from this type of analysis is quite complex. Since:

1. The correct rate expression is assumed to be accurately known.
2. It is assumed that the global rate which we observe and compute is the same as the intrinsic rate which we seek to determine. For a heterogeneous system, one would be ill advised to make such assumption a priori.

As previously noted, the complexity of this analysis lies in determining the value of K from the hypothesized reaction rate involved in oxygen coke reaction:

$$r = \frac{-dc}{dt} = k C^n p^m$$

The following section describes methods that could be used to determine the constants K , n , m .

In 1956, Levenspiel, Weinstein et al.²⁹ published a solution technique which involves linearizing the above equation such that the dependent variable is a linear function of the three independent variables: K , n , m . By logarithmic transformation, the above equation becomes

$$\log r_i = \log K + n \log C_i + m \log P_i$$

Let $Y_i = \log r_i$, $b_0 = \log K$, $X_{1i} = \log C_i$, $X_{2i} = \log P_i$

$$Y_i = b_0 + nX_{1i} + mX_{2i} \text{ -----(a)}$$

Summing equation (a) from $i = 1$ to N (total number of data points on each run)

$$\sum_{i=1}^N Y_i = Nb_0 + n \sum_{i=1}^N X_{1i} + m \sum_{i=1}^N X_{2i} \text{ - - - - - (1)}$$

Multiply (A) by X_{1i} and sum

$$\sum_{i=1}^N Y_i X_{1i} = b_0 \sum_{i=1}^N X_{1i} + n \sum_{i=1}^N (X_{1i})^2 + m \sum_{i=1}^N X_{2i} X_{1i} \text{ - - - (2)}$$

Multiply (A) by X_{2i} and sum

$$\sum_{i=1}^N Y_i X_{2i} = b_0 \sum_{i=1}^N X_{2i} + n \sum_{i=1}^N X_{1i} X_{2i} + m \sum_{i=1}^N (X_{2i})^2 \text{ - - - (3)}$$

Equations 1, 2 and 3 can now be solved simultaneously and the values of K , n , m determined. This was done by using

LEQTLF³⁰ subroutine and the following matrices were provided:

$$\vec{A} = \begin{bmatrix} N & \sum_{i=1}^N X_{1i} & \sum_{i=1}^N X_{2i} \\ \sum_{i=1}^N X_{1i} & \sum_{i=1}^N (X_{1i})^2 & \sum_{i=1}^N X_{2i} X_{1i} \\ \sum_{i=1}^N X_{2i} & \sum_{i=1}^N (X_{1i} X_{2i}) & \sum_{i=1}^N (X_{2i})^2 \end{bmatrix}$$

$$\vec{B} = \begin{bmatrix} 1 & 0 & 0 & \sum_{i=1}^N Y_i \\ 0 & 1 & 0 & \sum_{i=1}^N (Y_i X_{1i}) \\ 0 & 0 & 1 & \sum_{i=1}^N (Y_i X_{2i}) \\ 0 & 0 & 0 & 1 \end{bmatrix}$$

The output solution was modified vector B

$$\vec{B} = \begin{bmatrix} - & - & - & b_0 \\ - & - & - & n \\ - & - & - & m \\ 0 & 0 & 0 & 1 \end{bmatrix} \quad \text{where } b_0 = \log K$$

$$\underline{K = 10^{b_0}}$$

The above statistical solution technique is a standard procedure for analyzing data but unfortunately, this technique failed to yield reasonable and acceptable results. (See Table 1) The shortcomings of this technique could be attributed to the fact that the method minimizes the root mean square deviation of the logarithm of the variables rather than the variables themselves.

Previous authors^{19, 26} tackled this problem of evaluating K, n, m from a very simplistic approach. They rearranged the linearized form of the rate equation to obtain

$$\log \frac{\left(\frac{dc}{dt}\right)}{p^m} = \log K + n \log C$$

By assuming $m = 1$, $\frac{(-dC/dt)}{p}$ was plotted against C on log-log paper and the values of n and K evaluated. The initial assumption that $m = 1$ is verified by now plotting $\log \frac{(-dc/dt)}{C^n}$

against $\log P$ from which the slope of the resultant line should equal 1. The success of this graphical technique depends on experience and is subject to unavoidable bias. If the initial assumption $m = 1$ could not be verified by the second plotted graph, further trial and error attempts will be made to zero

TABLE 1
COMPARISON OF NON-LINEAR SOLUTION TECHNIQUE
WITH STATISTICAL METHOD

Run #	# of Data Points	OPTIMUM VALUES OF K, N, M							
		NON-LINEAR METHOD				STATISTICAL METHOD			
		K	n	m	$\sum_{i=1}^N (\xi_i)^2 =$ (min ⁻¹) ²	sum of error ² (min ⁻¹)	K	n	m
1		min ⁻¹							
2	(7)	1.1	.94	.79	.3790E-04	(3.32)10 ⁻⁷	-1.2	-5.1	
3	(8)	1.2	.6	.8	.9358E-04	27.1	.87	2.2	
4	(19)	.4	.6	1.3	.1072E-04	.000952	.31	-2.0	
5	(7)	1.5	1.1	.5	.2493E-04	2.91	1.2	.75	
7	(12)	1.7	1.0	1.3	.1683E-04	.128	.8	.1	
8	(7)	1.84	.9	1.2	.213E-04	2411.6	1.2	5.2	
10	(10)	1.2	.95	.74	.2689E-03	.0000888	-.2	-3.1	
15	(11)	.97	.74	1.1	.3152E-04	6298	1.2	5.7	
16	(7)	1.9	.9	1.0	.1610E-04	.605	.86	.4	
17	(8)	2.0	1.3	.9	.2705E-04	20.77	1.5	2.1	
19	(8)	1.1	.8	.6	.4894E-04	.145	.65	.26	
20	(10)	1.1	1.1	.74	.6194E-04	4.586	1.26	1.43	
21	(12)	.4	.4	1.3	.5004E-05	.00546	.32	-1.2	
22	(11)	.96	.77	1.1	.7002E-05	.561	.73	.80	
23	(13)	1.23	.9	.8	.3467E-04	.106	.7	-.4	

TEST DATA*

	K=	n=	m=	$\sum_{i=1}^N (E_i)^2 =$	K=	n=	m=
(8)	.01285	.892	.4168	.4946E-06	.0135	.933	.4588

*Data from Hydrogen-Bromide reaction $H_2 + Br_2 = 2HBr$

Page 79 Chemical Reaction Eng. 2nd Edition by Levenspiel.

on the correct value of m and this would entail considerable amount of work especially as there is no scientific approach towards finding best m value.

3.1.2 Non-Linear Optimization

A new solution technique had to be developed to evaluate the variables of interest. In developing this new technique that has never been used for experimental data, some theories were hypothesized:

1. The values of K , n , m are not true constants. This implies that K , n , m vary with time during the course of a run, and since r , c , P also vary with time, then the hypothesized rate expression describing oxygen coke reaction is highly non-linear.
2. K , n , m are also functions of temperature and to simplify our analysis, each experimental run will be conducted under isothermal conditions.
3. An objective function to be defined later can be visualized to be a response surface in which the parameters are the variables (K , n , m).
4. The objective function is unimodal and the search technique proceeds to a neighborhood of the global minimum.

The non linear optimization technique used in determining optimum value of the variables K , n , m was a "steepest gradient" method³¹ adapted from Fletcher-Reeves³⁷ subroutine package.

$$\text{Given } r_i = KC_i^n p_i^m$$

Error function for the i^{th} data point = ε_i

$$\varepsilon_i = r_i - KC_i^n p_i^m$$

$$\text{Thus } \varepsilon_1 = r_1 - KC_1^n p_1^m$$

$$\varepsilon_2 = r_2 - KC_2^n p_2^m$$

$$\varepsilon_3 = r_3 - KC_3^n p_3^m$$

⋮

⋮

$$\varepsilon_i = r_i - KC_i^n p_i^m$$

Summing up all the errors for N (total data points in a given run)

$$\sum_{i=1}^N \varepsilon_i = \sum_{i=1}^N r_i - \sum_{i=1}^N KC_i^n p_i^m$$

An objective function to be minimized was then defined as

$$F = \left(\sum_{i=1}^N \varepsilon_i \right)^2$$

$$F = \left(\sum_{i=1}^N \varepsilon_i \right)^2 = \left(\sum_{i=1}^N r_i - \sum_{i=1}^N KC_i^n p_i^m \right)^2 \text{ --- (3.4)}$$

Procedural step:

1. A starting point is selected \vec{X}_0
2. The direction of steepest descent is determined by determining the normalized direction vector components at the initial starting point

$$\frac{\nabla F(\vec{X}_0)}{\|\nabla F(\vec{X}_0)\|} \text{ and then move to a new point location}$$

X_1 at a distance d from \vec{X}_0 in the direction

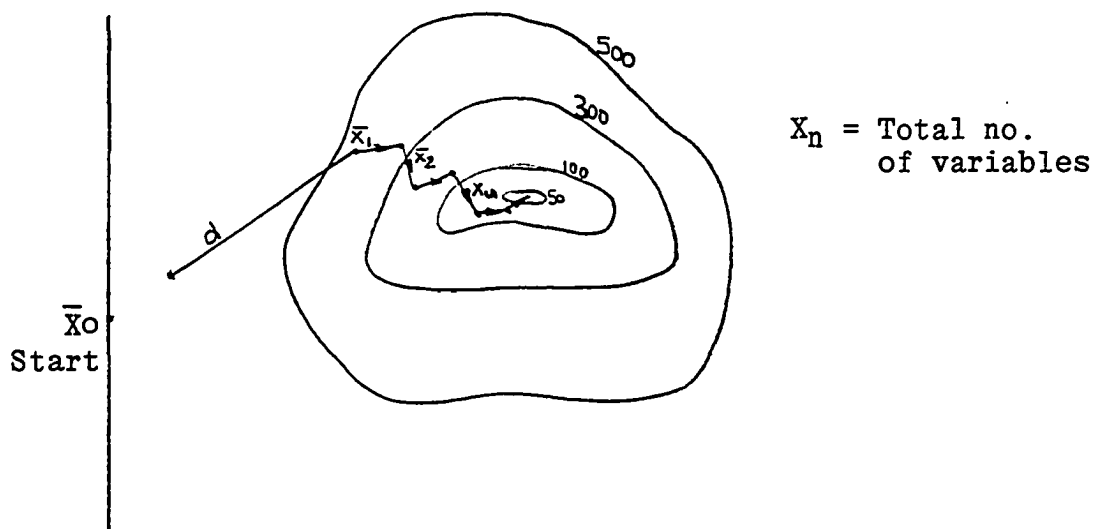
$$S = \frac{\nabla F(\bar{X}_0)}{\|\nabla F(\bar{X}_0)\|} ; S_i = \frac{\partial F / \partial x_i}{\left[\sum_{i=1}^N \left(\frac{\partial F}{\partial x_i} \right)^2 \right]^{\frac{1}{2}}} \text{ where } \partial F / \partial x_i \text{ are the gradient vector components.}$$

$$\text{Thus } \bar{X}_1 = \bar{X}_0 + \frac{d \nabla F(\bar{X}_0)}{\|\nabla F(\bar{X}_0)\|}$$

$$\text{and in general, } \bar{X}_{u+1} = \bar{X}_u + \frac{d F(\bar{X})}{\|\nabla F(\bar{X})\|}$$

$u = N_0$ of iterations along direction of steepest descent until a minimum is obtained.

If d is sufficiently small, selection of these gradient directions will assure $F(X_{u+1}) < F(u)$. At anytime $F(X_{u+1}) > F(u)$, the step size d is automatically reduced and a new direction vector computed to satisfy $F(u+1) < F(u)$. When a minimum is obtained, its precise location is determined by computing a conjugate direction search direction at the new point. When convergence is achieved, as determined from specification of the expected absolute error in movement, the procedure terminates.



Applying the above concept to equation 3.4 .

Gradient of function = ∇F

$$\nabla F = \frac{\partial F}{\partial K}, \frac{\partial F}{\partial n}, \frac{\partial F}{\partial m}$$

$$\left(\frac{\partial F}{\partial K}\right)_{n, m} = 2 \sum_{i=1}^N (KC_i^n p_i^m - r_i) C_i^n p_i^m$$

$$\left(\frac{\partial F}{\partial n}\right)_{k, m} = 2 \sum_{i=1}^N (KC_i^n p_i^m - r_i) K p_i^m C_i^n \log C_i$$

$$\left(\frac{\partial F}{\partial m}\right)_{k, n} = 2 \sum_{i=1}^N (KC_i^n p_i^m - r_i) K p_i^m C_i^n \log p_i$$

Initial direction vector guess $\bar{X}_0 = (n_0, m_0, k_0)$.

New computed improved direction vector $\bar{X}_1 = (n_1, m_1, k_1)$

where $(k_1, n_1, m_1) = (k_0, n_0, m_0) + d \frac{\nabla F(k_0, n_0, m_0)}{\|\nabla F(k_0, n_0, m_0)\|}$

An algebraic illustration of this technique is given in the Appendix.

This solution technique is straightforward, objective and is guaranteed to always converge to a global minimum if the function does indeed possess a minimum. Although this method converges for nearly any set of initial estimates, its convergence can be agonizingly slow for multiparameter problems. This technique like any other type, does not overcome the disadvantages of haphazard selection of experimental data and as such, the point should be stressed that

an adequate understanding of the physical process with justifiable discrimination of certain data points must be understood.

3.2 Diffusion Control Analysis

The proposed methodology for investigating the diffusion limitation process is the unreacted core²⁵ model analysis. In this model, we visualize the reaction as occurring first at the outer surface of the fuel (coke) and the reaction zone then progresses into the solid, leaving behind completely converted material and inert solid (clean sand). The zone of reaction in such a case is narrowly confined to the interface between the unreacted solid and the product. Thus, at any time, there exists an unreacted core of material which gradually shrinks with time.

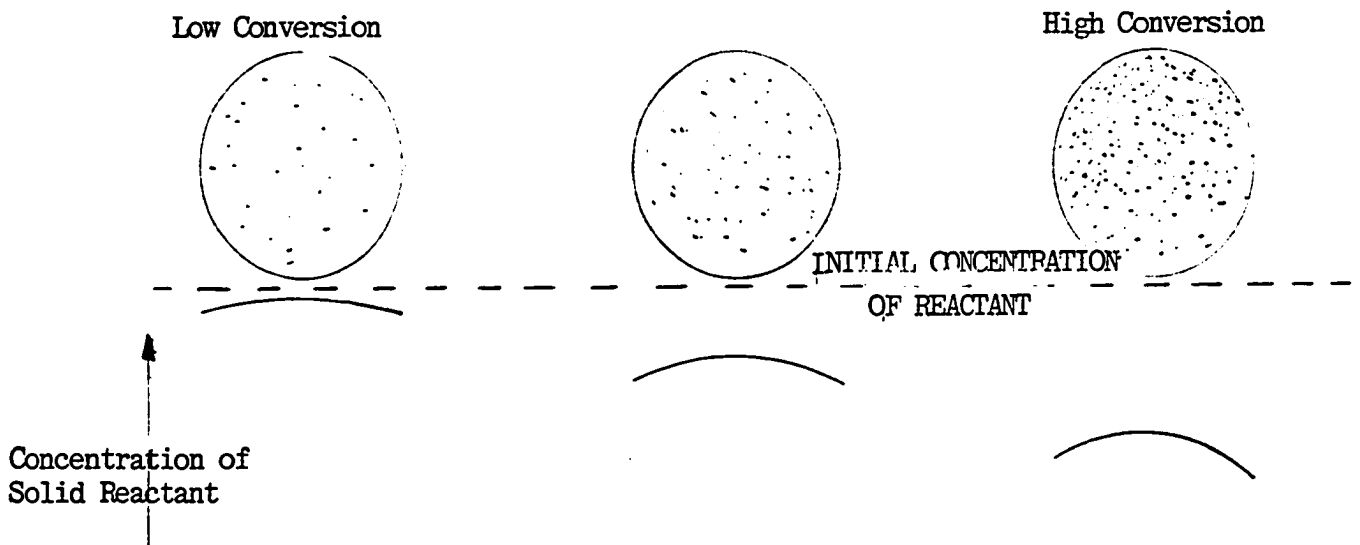
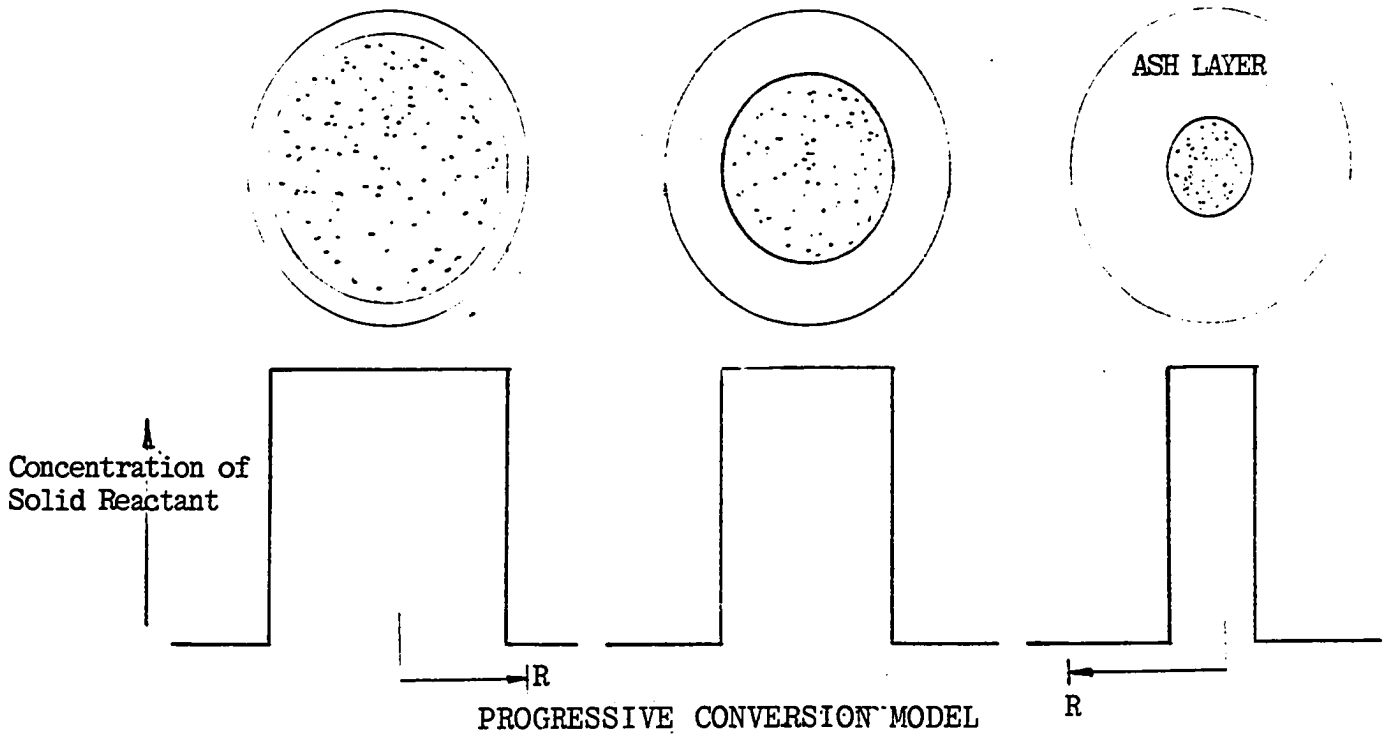
An alternative is the progressive²⁵ conversion model in which we visualize the solid reactant being converted continuously throughout the entire particle and most likely, at different rates at different locations within the particle. Wen and Ishida³² et al. studied various gas-solid systems and concluded that the unreacted core model is the best simple representation for a majority of reacting gas-solid systems provided the following criteria are met:

1. Porosity of unreacted solid is very small and as such, the reaction occurs at the solid-reactant interface. In this case, effective gas diffusivity

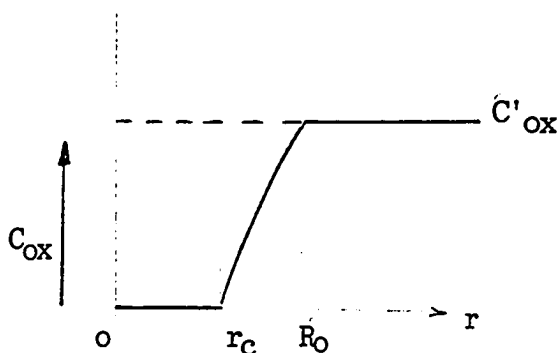
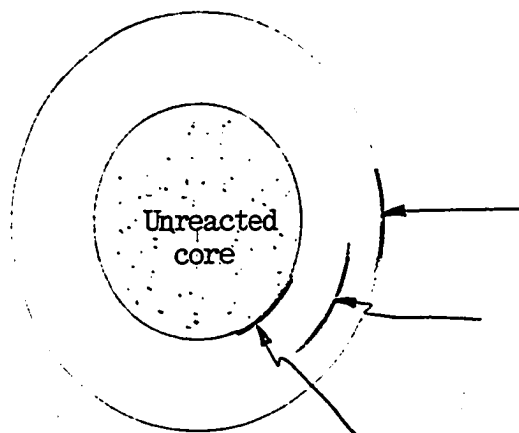
in unreacted solid (D_e') is far less than that of residue-free material (D_e) that is $D_e' \ll D_e$.

2. Chemical reaction rate is very rapid and the diffusion of reactant gas is slow.

UNREACTED CORE MODEL



MATHEMATICAL ANALYSIS



As oxygen diffuses into the 'coke,' it is totally consumed upon initial contact. At any finite time when the surface of the unreacted core is at r_c , the oxygen will diffuse through the space $R_0 - r_c$ and a mass balance on oxygen concentration C_{ox} will satisfy the diffusion equation $D\nabla^2 C_{ox} = 0$. For spherical particles, this becomes:

$$\frac{1}{r^2} \frac{\partial}{\partial r} \left(r^2 \frac{\partial C_{ox}}{\partial r} \right) + \frac{1}{r^2 \sin \theta} \frac{\partial}{\partial \theta} \left(\sin \theta \frac{\partial C_{ox}}{\partial \theta} \right) + \frac{1}{r^2 \sin^2 \theta} \frac{\partial^2 C_{ox}}{\partial \phi^2} = 0$$

Both oxygen concentration and boundary of the unreacted core move towards the center of the particle but since oxygen flow rate is far greater than shrinking of the unreacted core, we can reasonably assume in considering the oxygen concentration gradient at any time that the unreacted core is stationary. Considering oxygen flux in r direction only we have:

$$\frac{d}{dr} \left(r^2 \frac{dC_{Ox}}{dr} \right) = 0$$

Rate of reaction of O_2 at any instant =

$$-\frac{dN_{Ox}}{dt} = 4\pi R^2 Q_{Ox, R_0} = 4\pi r_c^2 Q_{Ox, r_c} = 4\pi r^2 Q_{Ox, r} = \text{Const.}$$

Q_{Ox} = Flux of oxygen

Subscript R_0 , r_c , r = Location of flux front

$$Q_{Ox} = D \frac{dC_{Ox}}{dr} \quad \text{From Fick's Law.}$$

$$-\frac{dN_{Ox}}{dt} = 4\pi r^2 D \frac{dC_{Ox}}{dr} = \text{Const.}$$

$$\therefore -\frac{dN_{Ox}}{dt} \int_{R_0}^{r_c} \frac{dr}{r^2} = 4\pi D \int_{C_{Ox}'}^0 dC_{Ox}$$

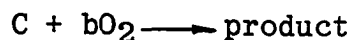
$$-\frac{dN_{Ox}}{dt} \left(\frac{1}{r_c} - \frac{1}{R_0} \right) = 4\pi D C_{Ox}' \text{-----} (3.5)$$

Consider now the case in which the unreacted core shrinks resulting in thicker ash layer which lowers diffusion rate of oxygen.

Hence integrating equation 3.5 with respect to time and other variables should yield required relationship. Since above equation contains three variables r_c , t , N_{Ox} ,

one of them has to be written in terms of the others or eliminated.

Representing the coke combustion as



where b is the stoichiometric ratio of carbon burned per mole of oxygen consumed, we can then say $dN_C = b dN_{Ox}$ based on the stoichiometric relation of the reaction

$$N_C = \rho_c V = \left(\frac{\text{moles } O_2}{\text{Cm}^3 \text{ solid}} \right) (\text{Cm}^3 \text{ solid}) = \rho_c \frac{4}{3} \pi r_c^3$$

$$dN_C = 4\pi \rho_c r_c^2 dr_c$$

$$dN_{Ox} = \frac{4}{b} \pi \rho_c r_c^2 dr_c$$

Substituting above into equation 3.5

$$-\rho_c \int_{R_0}^{r_c} \left(\frac{1}{r_c} - \frac{1}{R_0} \right) r_c^2 dr_c = b D C'_{Ox} \int_0^t dt$$

$$t = \frac{\rho_c R_0^2}{6bDC'_{Ox}} \left[1 - 3\left(\frac{r_c}{R_0}\right)^2 + 2\left(\frac{r_c}{R_0}\right)^3 \right]$$

For complete conversion $r_c = 0$ and time required is

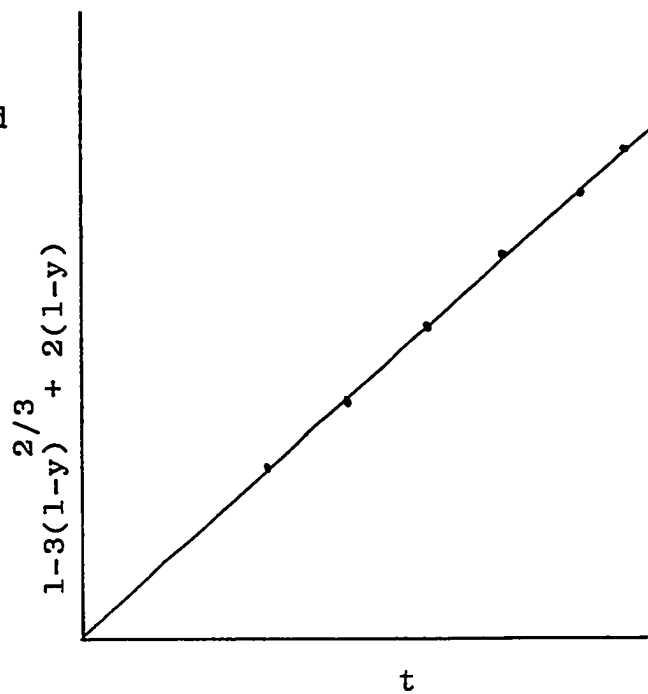
$$\tau = \frac{\rho_c R_0^2}{6bDC'_{Ox}}$$

Extent of conversion = y

$$1 - y = \frac{\text{volume of unreacted coke}}{\text{initial volume of coke}} = \frac{\frac{4}{3}\pi r_c^3}{\frac{4}{3}\pi R_0^3} = \left(\frac{r_c}{R_0}\right)^3$$

$$t = \tau \left[1 - 3(1-y)^{2/3} + 2(1-y) \right] = \tau \left[1 - 3\left(1 - \frac{CB}{CI}\right)^{2/3} + 2\left(1 - \frac{CB}{CI}\right) \right]$$

Isothermal conditions

Anticipated
result:

The above analysis shows that to determine whether or not diffusion is the controlling mechanism requires less complex computation and analysis than the other methods.

CHAPTER IV

EXPERIMENTAL APPARATUS AND MATERIALS

Two sets of experimental apparatus were used in this study. Most of the constituent components were identical for both experimental set-ups: Simulation and Combustion phases.

4.1 Apparatus for Process Simulation

The main components are as shown in Table 4.1 and a schematic diagram of the process is shown in Fig. 4.1.

TABLE 4.1

MAIN COMPONENTS IN PROCESS SIMULATION APPARATUS

-
-
1. Fire Flood Pot Pressure Jacket.
 2. Fire Flood Pot Linear
 3. Temperature Controllers and Temperature Indicator.
 4. Gas injection and Drying Systems.
 5. Fluid Separation System.
-

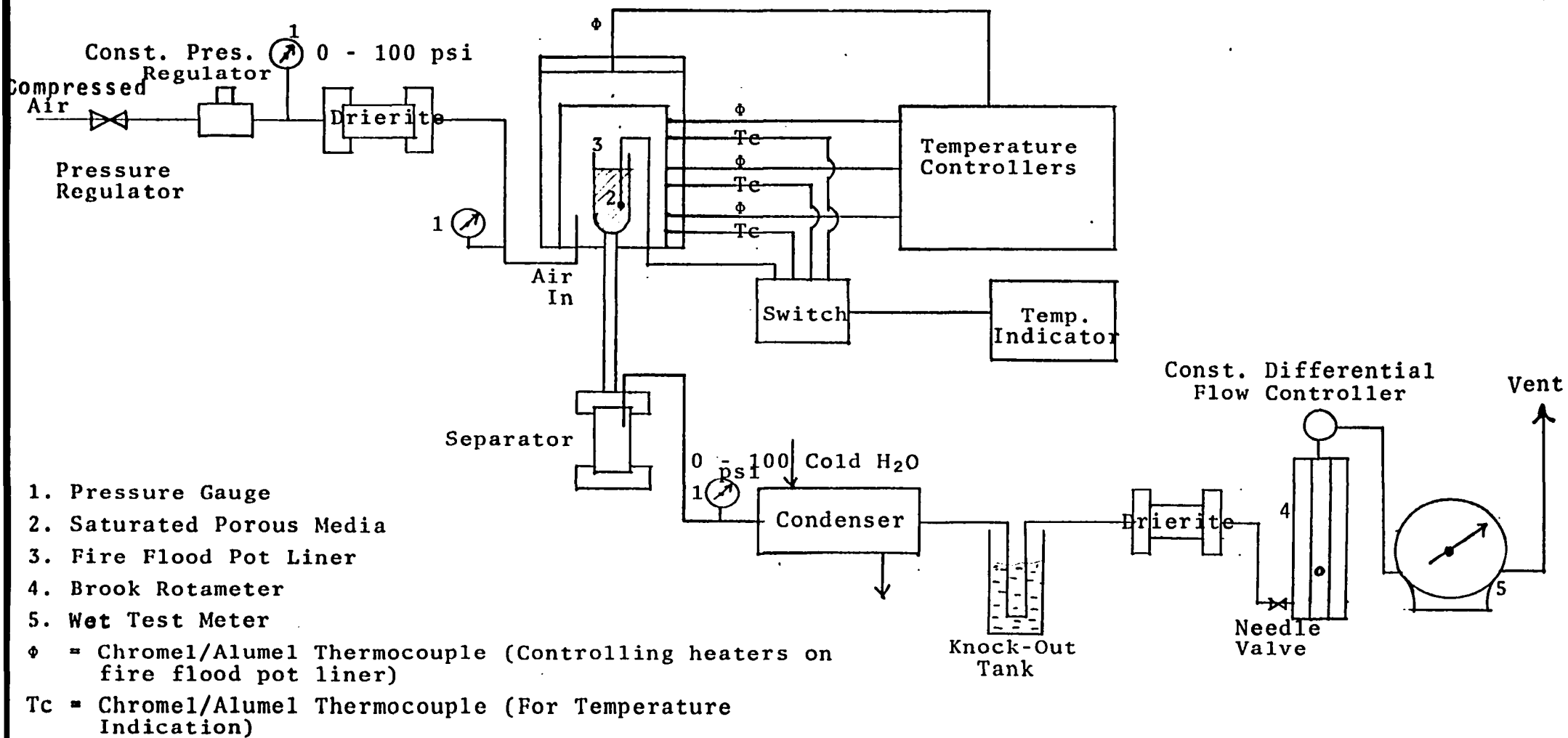


FIGURE 4.1
 SCHEMATIC DIAGRAM OF PROCESS SIMULATION
 EXPERIMENTAL APPARATUS

4.1.1 Fire Flood Pot Pressure Jacket

Figure 4.2 shows the inner detail construction and the outer jacket. As illustrated in Figure 4.2, the unit is equipped with three bands of ring heaters on the wall, each rated at 500 watts. An additional 300 watts heater is attached to the top of the pressure jacket. Each of these heaters has a Chromel/Alumel thermocouple wire connected to a temperature controller so as to control the heat output from these heaters. Three additional Chromel/Alumel thermocouples are attached to the space between the side heaters for monitoring the wall temperature of the jacket. The bottom of the jacket is welded to a flange and the mating flange has two $\frac{1}{4}$ " S.S. and one $\frac{1}{8}$ " S.S. welded nipples. The $\frac{1}{4}$ " S.S. nipples are located at the center and $1\frac{1}{2}$ " radius from the center. The $\frac{1}{8}$ " S.S. nipple is located at $1\frac{3}{4}$ " radius from the center. The $\frac{1}{4}$ " S.S. nipple located at $1\frac{1}{2}$ " radius has a 1" high perforated $\frac{1}{4}$ " S.S. pipe for allowing air into the jacket. The heating jacket is enclosed in an outer jacket and all spaces between the two jackets insulated with Vermiculite. A special $\frac{3}{16}$ " compressed asbestos was used as a gasket between the two mating flanges. See Figure 4.3.

4.1.2 Fire Flood Pot Liner

Detail construction is shown in Figure 4.4. For each simulation run, the liner was packed with oil/water saturated

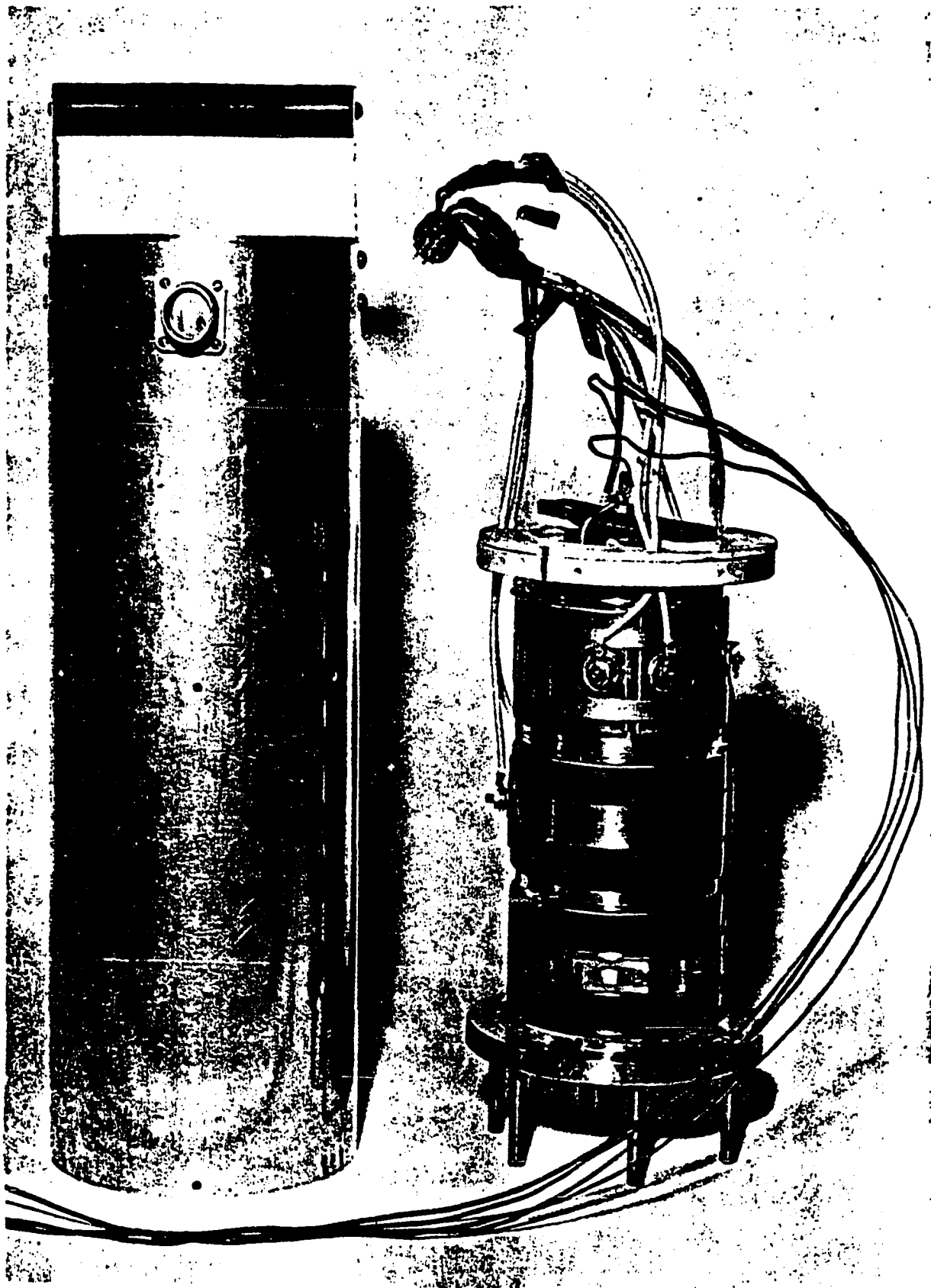


FIGURE FIRE FLOOD-POT PRESSURE
JACKET SHOWING CONSTRUCTION

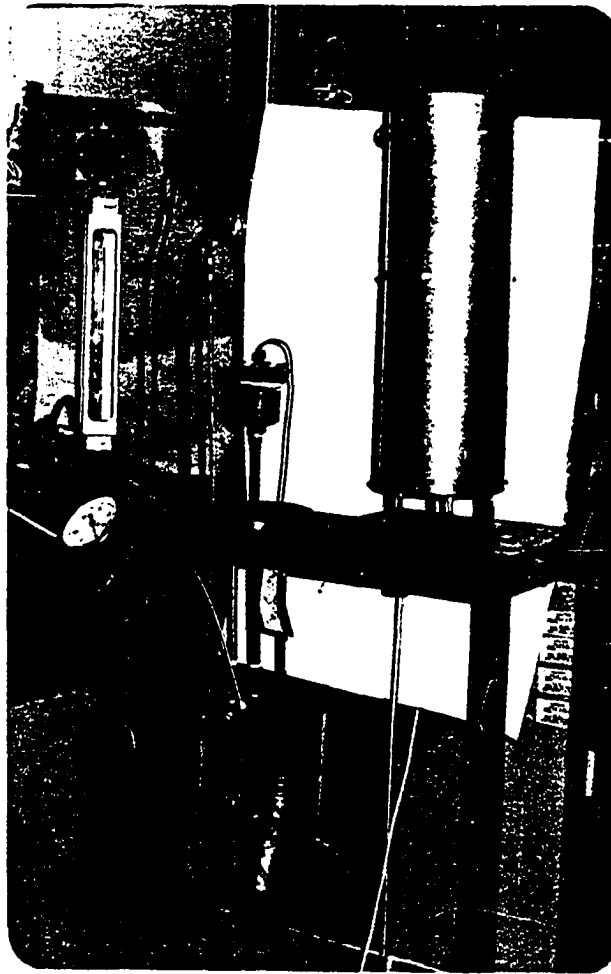


FIGURE 4.3

ASSEMBLED PRESSURE HEATING JACKET,
MATING FLANGE, ASSEMBLED REACTOR

sand and then centrally mounted inside the pressure heating jacket. The porous stainless steel plate supports the porous medium and also, promotes drainage of the produced fluids and gases to the producing $\frac{1}{4}$ " S.S. tube and on to the product separation system.

4.1.3. Temperature Control System

Isothermal temperature over the fire flood pot liner (Simulation process) or over the combustion reactor (combustion process), was achieved within 0.5% accuracy at the desired temperature by using Love Model 49 proportioning controllers. This type of controller cycles the heat on and off automatically at the desired set temperature. Each of the control thermocouples was connected to a Love temperature controller and all the controllers connected in series. The temperature controller wiring is illustrated in Figure 4.5. The other thermocouples from the heating jacket and combustion cell (combustion runs) or heating jacket (simulation runs) were connected to Love Model 101 Sensor Switch. The switch has provision for 12 thermocouples, five of which were used in this study. By connecting the switch to Lovel Model 100 temperature indicator and with proper wiring of the system, it was possible to monitor any temperature from any of the thermocouple wires at any time. A schematic representation of the electrical wiring system is illustrated in Figure 4.6.

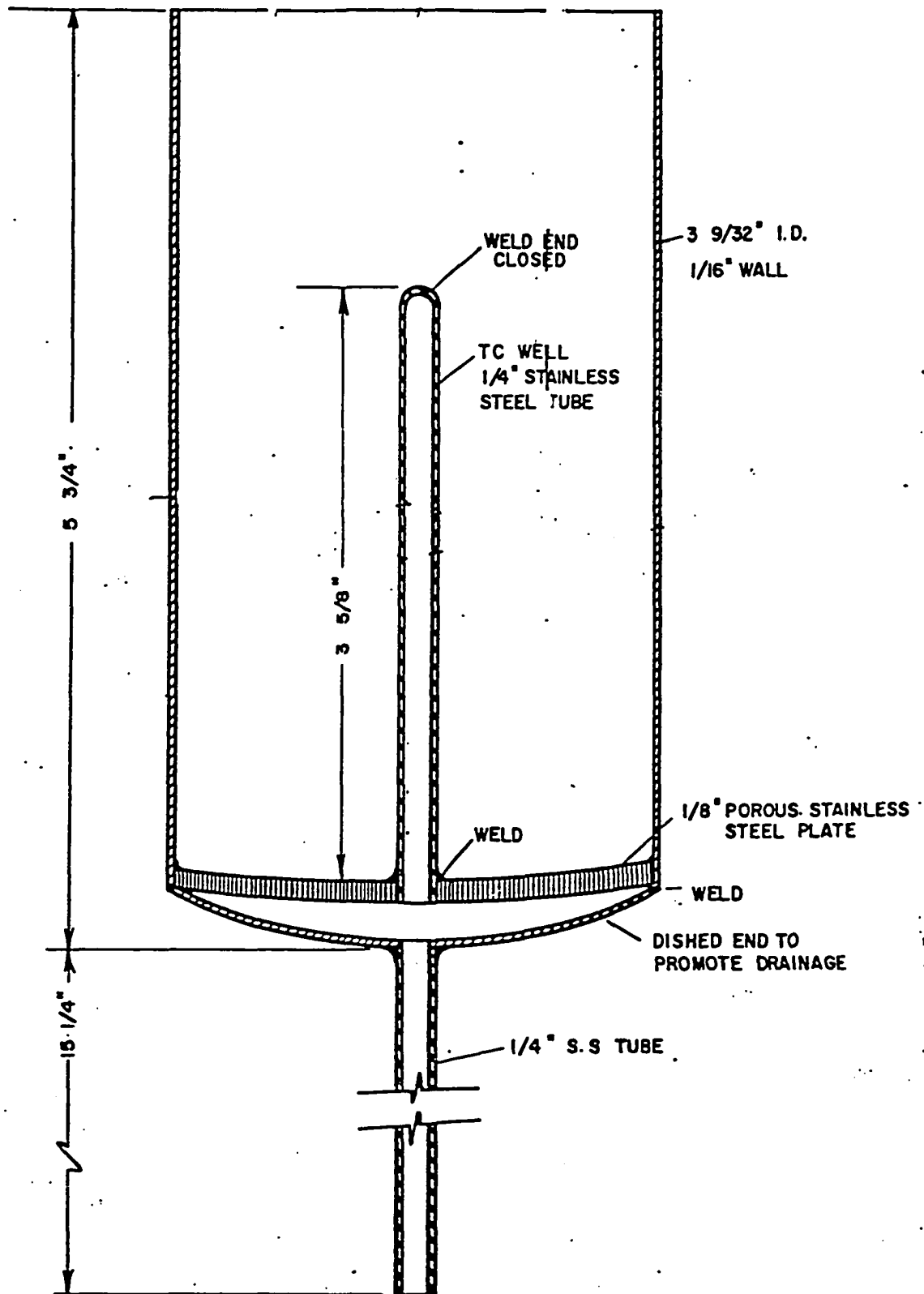


FIGURE 1 - DRAWING OF FIRE FLOOD-POT LINER

Figure 4.5
Controller Wiring

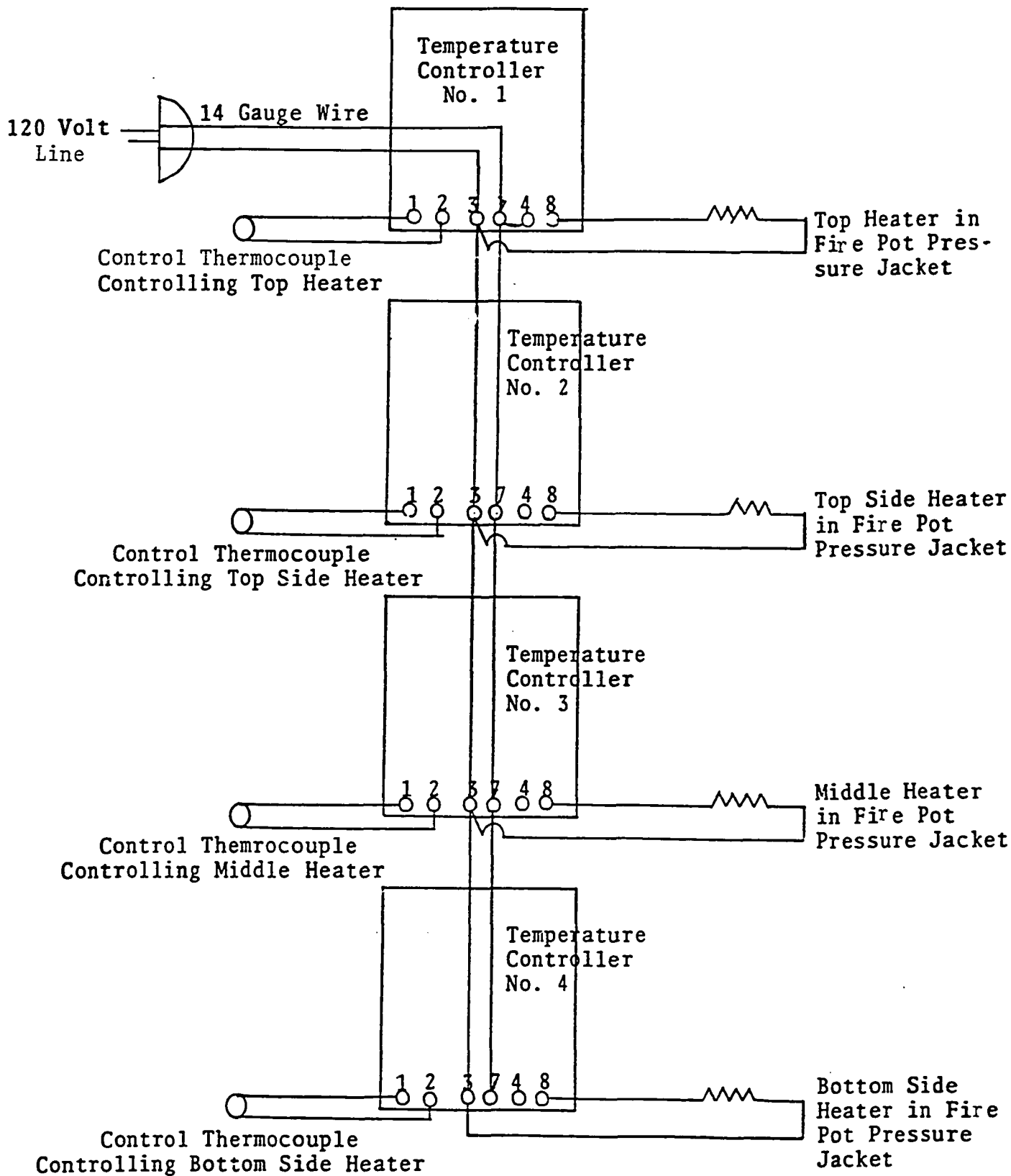
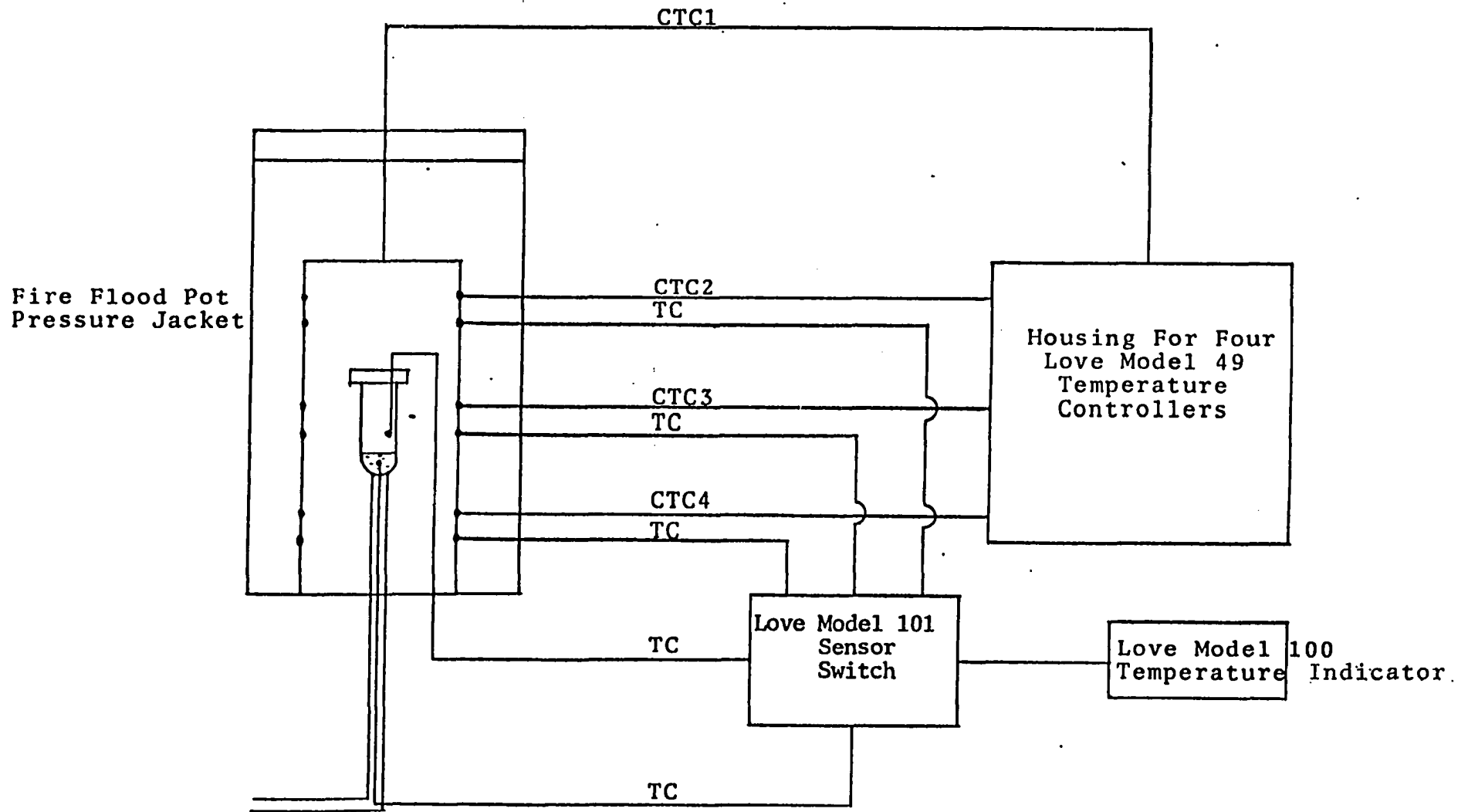


Figure 4.6
Electrical Wiring of Temperature Control System



EXPLANATION OF TERMS FOR FIGURE 4.6

CTC1 Control Thermocouple for Top End Heater.
CTC2 Control Thermocouple for Top Side Heater.
CTC3 Control Thermocouple for Middle Side Heater.
CTC4 Control Thermocouple for Bottom Side Heater.
TC Thermocouples for Temperature Recording.
All Thermocouples are Chromel-Alumel Type.

4.1.4. Gas Flow System

The gases used were (1) compressed nitrogen gas tank equipped with two stage pressure regulators; (2) compressed air line connected to a constant pressure regulator valve; (3) Locally made air-nitrogen gas mixture. This was made by injecting air into a cylinder up to a given pressure and then followed by further injection of pure nitrogen. From the equation below, a rough estimate of the mixture composition was made but the accurate composition was determined from chromatographic analysis.

$$\frac{P_{O_2}}{P_{N_2}} = \frac{n_{O_2}}{n_{N_2}} = \frac{\text{wt. \% } O_2}{\text{wt. \% } N_2} \left(\frac{\text{m.w. of } N_2}{\text{m.w. of } O_2} \right)$$

where

$$P_{O_2} + P_{N_2} = \bar{P} \text{ (system pressure).}$$

When any of this gas was in use, it was made to pass through a glass-wool and drierite system to absorb any moisture present and thereafter, admitted into the combustion reactor (combustion runs) or fire flood pot liner (simulation process). A constant exit flow rate was maintained by using Brooks differential flow regulator. This rotameter is capable of maintaining a constant gas flow rate at a constant pressure regardless of any pressure buildup at the outlet side of the reactor.

4.1.5. Auxiliary Systems

Other equipment used is shown in the schematic diagram of the experimental apparatus. For accurate weighing of the pot liner with saturated porous medium, O Haus heavy duty scale was used. The 15 $\frac{1}{4}$ " long, $\frac{1}{4}$ " S.S. tube extension on the pot liner necessitated the construction of a special gig to enable accurate weight measurement of the pot liner and its contents. See Fig. 4.7. Triple beam balance was used for all weight measurements in combustion studies where higher degree of accuracy was essential.

4.2. Apparatus for Combustion Studies

The equipment for combustion studies was essentially the same as in simulation phase except for the absence of product separation system, replacement of fire flood pot liner with a reactor and addition of gas sampling and analysis system.

4.2.1. Reactor

The exothermic nature of the reaction between coke and oxygen poses a problem when trying to maintain isothermal conditions. Proper design of the reactor could minimize this problem, and this was achieved by using thick walled reactor and small thin layer of coke. Most of the heat liberated during the reaction was absorbed by the mass of

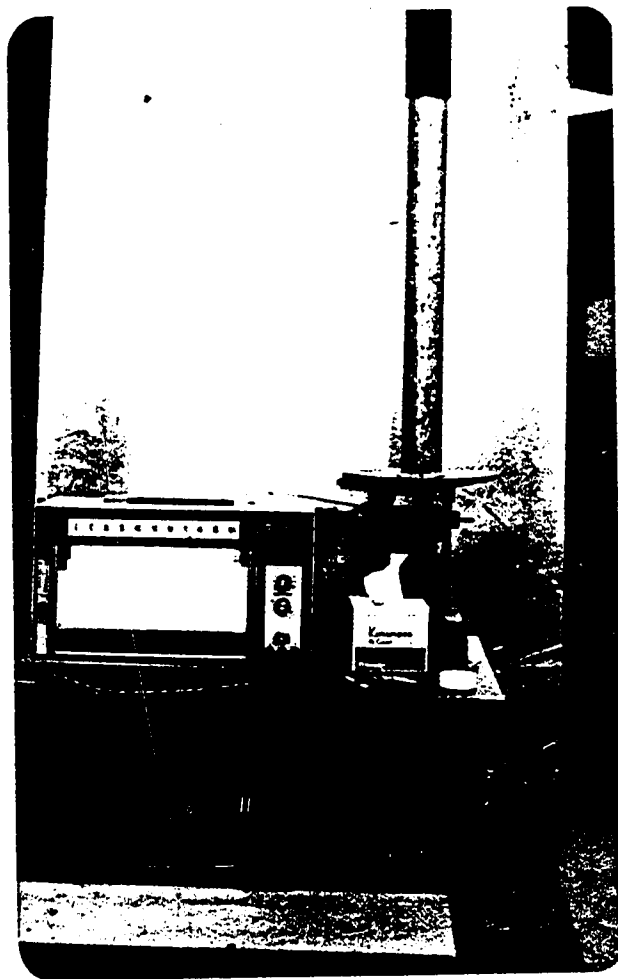


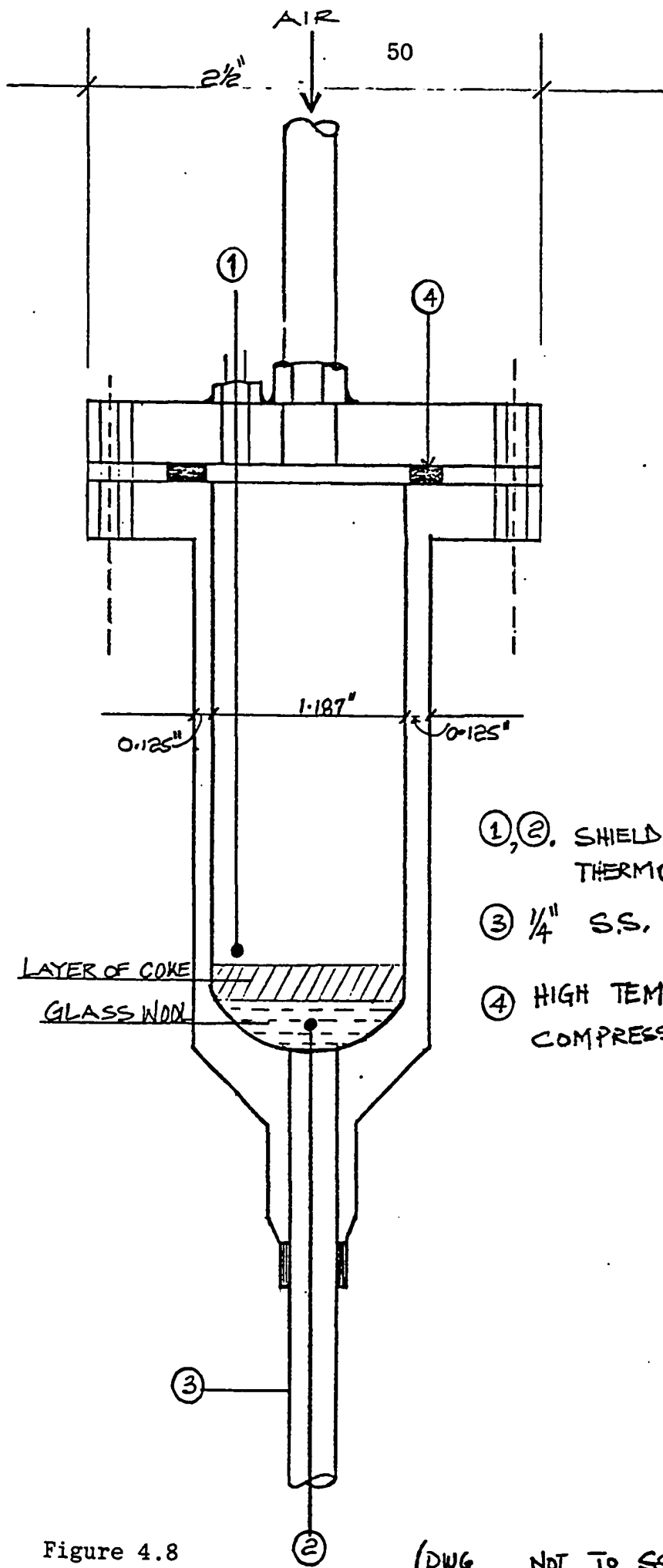
FIGURE 4.7

WEIGHT MEASUREMENTS OF POT LINER USING
HEAVY DUTY OHAUS SCALE

steel and by using thin layer of coke, a near isothermal condition was possible. The thick walled reactor used was a modification of a standard Ruska fluid content still. A flange with six drilled and threaded holes was soldered to the top of the reactor. A mating flange was constructed with matching holes on the circumference. 1/8" stainless steel nipple was welded in the center of the top flange for inlet gas to flow into the reactor. An additional 1/16" S.S. nipple was welded off center on the top flange for a Chromel/Alumel thermocouple wire which indicated the temperature just above the thin coke layer. A gas tight seal inside the reactor was made possible by using 3/16" high temperature compressed asbestos gasket between the flanges. 1/4" S.S. swagelok fitting for 1/4" S.S. tubing was silver soldered to the bottom of the reactor for product gases to flow through. A pictorial presentation is shown in Fig. 4.3 while a schematic representation is on Fig. 4.8.

4.2.2. Gas Sampling and Analysis

A Gow Mac gas chromatograph series 550 was used to analyze the following gases: CO, CO₂, CH₄, O₂ and N₂. The carrier gas used is Helium. A 4cc gas tight syringe was used to collect the product gases for analysis and the output from the thermal conductivity detector monitored on an L&N strip chart recorder. The columns used on the Gas chromatograph were S.S. 5' x 1/4" 13X Molecular Sieve and S.S. 6' x 1/4"



- ①, ②. SHIELDED CHROMEL/ALUMEL THERMOCOUPLES.
- ③ 1/4" S.S. TUBING
- ④ HIGH TEMPERATURE 3/16" COMPRESSED ASBESTOS

Figure 4.8

(DWG NOT TO SCALE)

Porapak Q. Since this G.C. had no series/bypass column switching valve, various column lengths and configurations were tested to evaluate optimum set up arrangement. The best arrangement is shown in Figure 4.9. In this arrangement, the Porapak Q was placed in Column A of the G.C. The Molecular Sieve was connected to the two outlet ports at the back of the G.C. as indicated in Fig. 4.9. A portable oven was placed underneath the Molecular Sieve column and this was used to control the column temperature. With proper adjustment of the oven temperature on the molecular sieve column, CO elution time was reduced from 10-12 minutes to about 4 minutes. This was accomplished at the expense of not having proper base line separation between O₂ and N₂. The amount of eluded component is proportional to the area swept out on the Strip chart. If the carrier gas flow rate, detector and oven temperatures, bridge current are all held constant, then the amount of eluded components will also be proportional to the swept out peak height. Thus, if volume percentage of the produced gases is based on peak height, then inadequate base-line separation between O₂ and N₂ will be of no consequence provided the G.C. is operated at the same constant conditions as the calibration gas. The gas chromatograph was operated under the following conditions:

Helium flow rate	40cc/min
Detector temperature	120°C

FIGURE 4.9(a) & FIGURE 4.9(b)

MODEL 550 GOW MAC GAS CHROMATOGRAPH

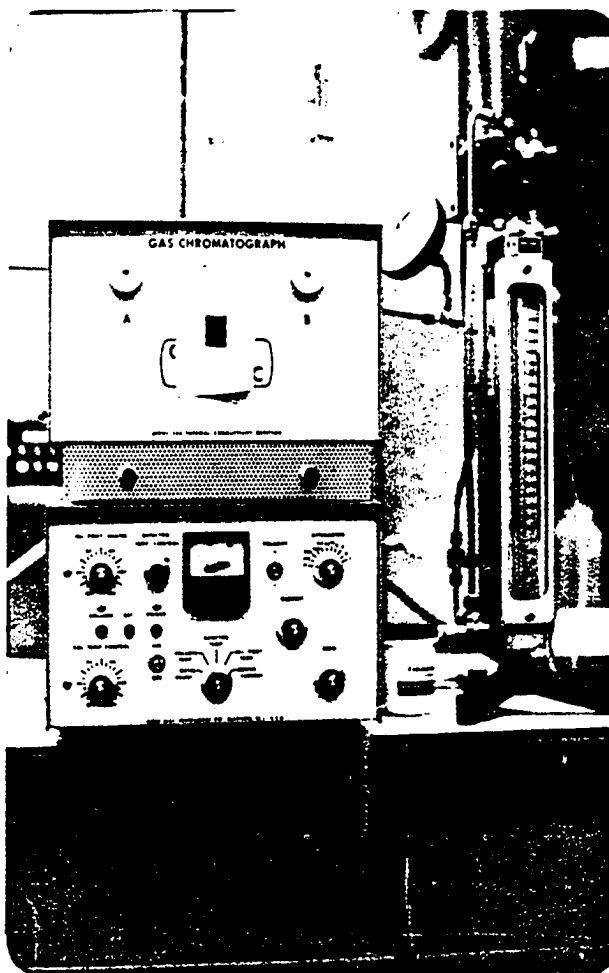


FIGURE 4.9(a)

FRONT VIEW OF GAS CHROMATOGRAPH

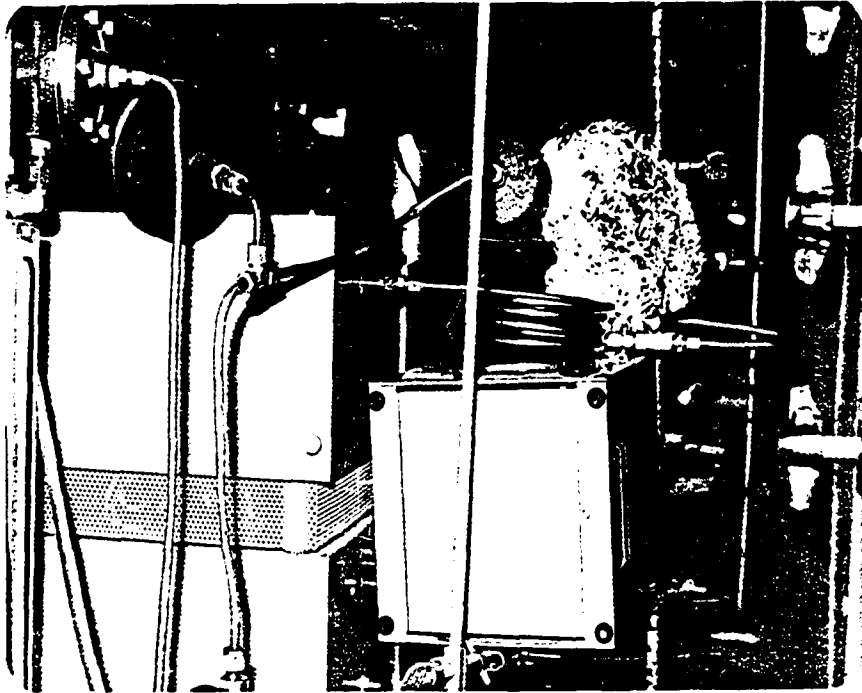


FIGURE 4.9(b)
MODIFICATION OF BACK VIEW OF
GAS CHROMATOGRAPH, SHOWING MOLECULAR SIEVE COLUMN
AND PORTABLE OVEN

Column temperature (Porapak)	75°C
Bridge current	150mA
Sample size	2cc
Recorder	1mV

4.3 Materials

The porous medium was clean Oklahoma sand number 1 with 100 mesh size. Two crude oils used were 15.4°API and 22.7°API.

CHAPTER V

EXPERIMENTAL PROCEDURE

5.1 Process Simulation

To undertake kinetic studies of coke combustion process, the coke has to be formed under displacement situations which essentially will simulate the various heat and mass transport phenomena occurring ahead of a combustion front. This will be accomplished by subjecting the reservoir to a programmed environmental sequence, similar to that experienced by a volume of rock during the approach and passage of a combustion front in a reservoir undergoing in-situ combustion. The temperature profile of a reservoir undergoing in-situ combustion is well documented in the literature,^{17, 33, 34} and the various discrete regions are of particular interest and an attempt was made to simulate them. This represents the simulation phase of the research. A schematic representation of the simulation experimental apparatus is presented in Figure 4.1 with a pictorial representation in Fig. 5.1. Figure 5.2 shows the various discrete regions to be simulated.

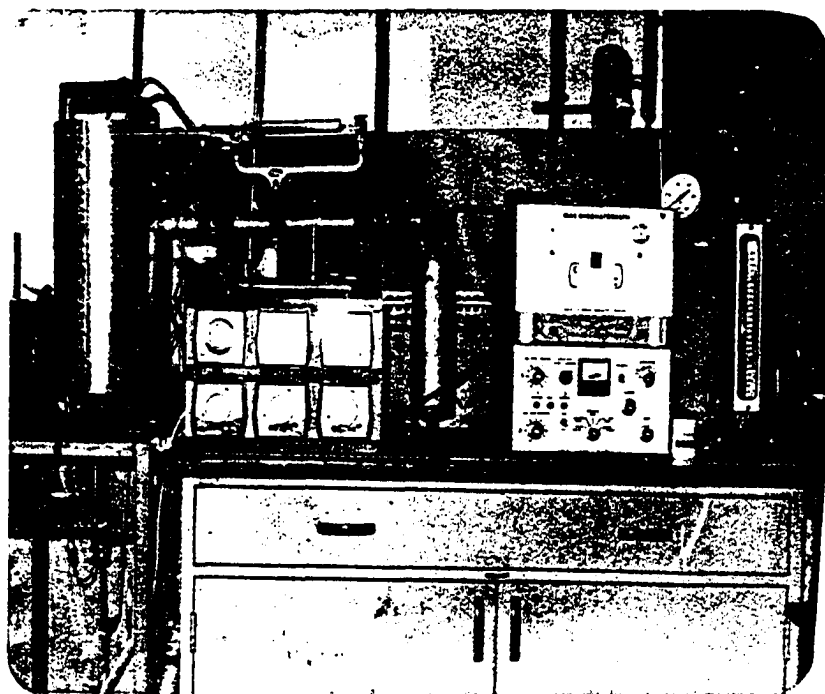


FIGURE 5.1
APPARATUS FOR COMBUSTION TESTS
FRONT VIEW

FIGURE 5.1(a) & FIGURE 5.1(b)

COMBUSTION EXPERIMENTAL APPARATUS

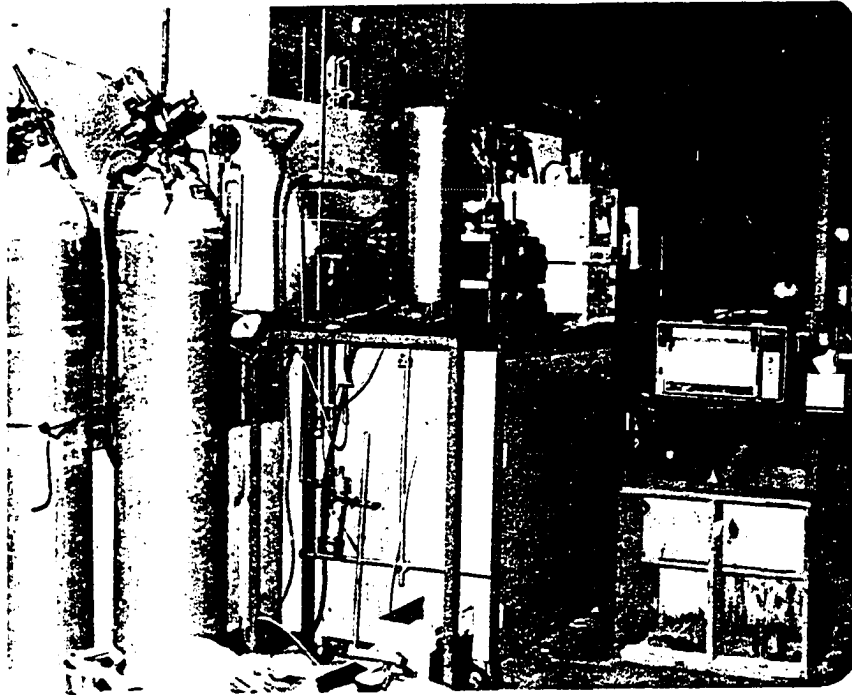


FIGURE 5.1(a)

LEFT SIDE VIEW OF COMBUSTION APPARATUS

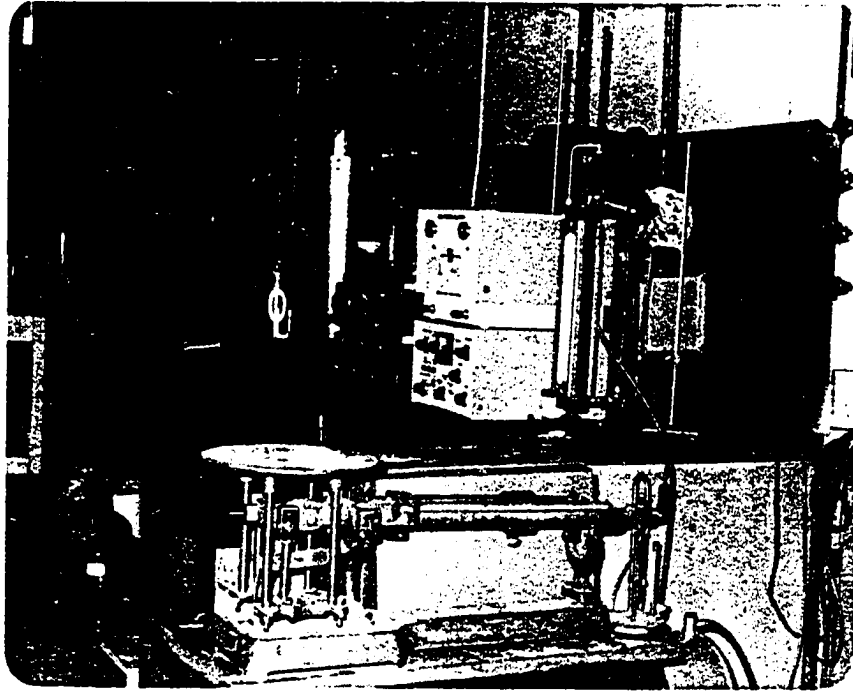
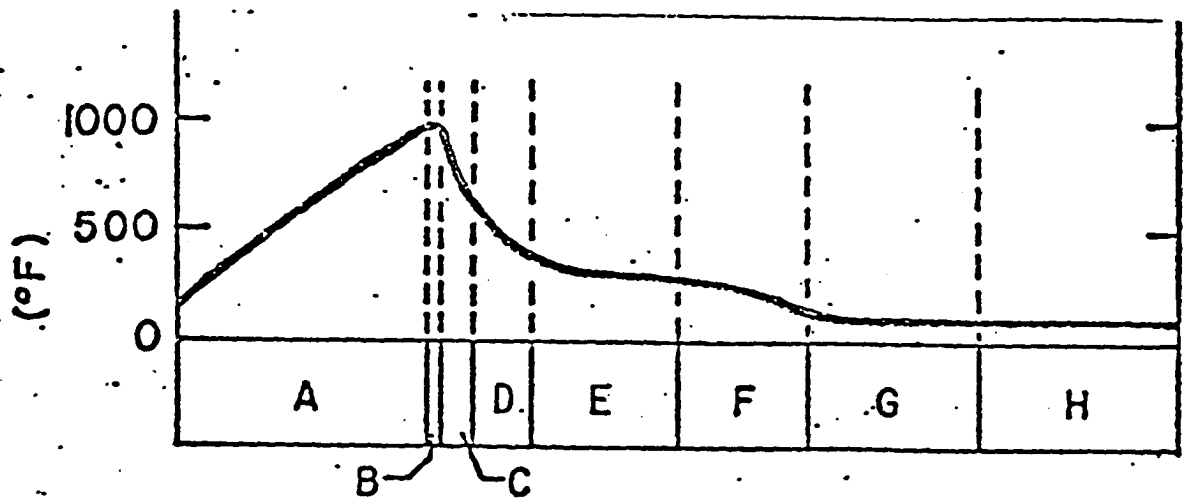


FIGURE 5.1(b)

FRONT VIEW OF COMBUSTION APPARATUS

Fig. 5.2



— DISTANCE FROM INJECTION WELL —

- | | |
|--|------------------|
| A. BURNED ZONE | E. STEAM PLATEAU |
| B. COMBUSTION ZONE | F. WATER BANK |
| C. CRACKING REGION | G. OIL BANK |
| D. EVAPORATION AND
VISBREAKING REGION | H. INITIAL ZONE |

Process To Be Simulated In Model

*Wu, C.H., and Fulton, P.F., "Experimental Simulation of Zones Preceding the Combustion Front of an In-Situ Combustion Process," SPEJ (March, 1971).

Procedure

5.1.1 Weight Measurements

A known weight of clean Oklahoma sand was fed into the fire flood pot liner and with proper tampering and packing, the sand level was always maintained constant at about 1.65" from the top of the pot liner. To obtain accurate weight of the sand in the pot liner, a heavy duty O Haus scale was used. See Figure 4.7. This scale is designed to weigh objects less than 1,100 grams and since the pot liner, sand and jig would weigh more than 1,100 gm, the scale had to be zeroed with the pot liner and jig on it. This was accomplished by sliding the weight on the center beam to such position that resulted in balancing the scale, while at the same time, maintaining the sliding scale weights at zero markings on the scale. The sliding scales were now moved to read 907 gm and clean Oklahoma sand added to the pot liner until a balance on the scale was achieved. Thus, the pot liner now contains 907 gms of sand. The scale reading was once more zeroed with the pot liner, sand and jig on it.

5.1.2 Saturating Porous Medium with Water

A thick rubber stopper with a flask full of water was placed over the pot liner and the $\frac{1}{4}$ " S.S. tubing from the liner was connected to a vacuum pump. A vacuum was then pulled in the porous medium for about 30 minutes, after

which the vacuum line was pinched off and the vacuum pump turned off. The valve on the flask was then opened until water saturated the sand and also completely filled the pot liner. The rubber tubing connecting the pot liner and the vacuum pump was then disconnected and a small rubber plug inserted at the end of the pot liner tubing to prevent drainage of water from the porous medium. The rubber stopper with the flask were now removed and before placing the pot liner on the jig, the small rubber plug was removed. The sliding scales were now moved to new locations where the scale was balanced. The readings on the sliding scales represented the weight of water in sand (pore volume) plus weight of excess water above the sand level and in the pot liner tubing.

5.1.3 Water Displacement in the Porous Medium

The pot liner was now supported by a stand and the drained out water collected in a graduated cylinder. Just before the water level drained to the sand level, a known volume of crude oil was poured into the pot liner. The oil then displaced the water to its irreducible value and thereafter, drained under gravity to a computable saturation value. On a 38°API test crude, the displacement duration was about 6 hrs. while on 22.7°API crude, it took about 2 days to complete the displacement experiment. On 15.4°API crude, it was not practical to have gravity drainage and air injection at low rate was used to displace both

water and crude oil to required oil and gas saturation values. The oil, water and gas saturation values were determined from measurements of oil and water collected. An illustration of the computation involved is shown in Table 5.1. The above procedure simulated initial oil, water, and gas saturations at reservoir (room temperature).

5.4.1 Simulation of Various Discrete Regions

Regions E - F - G

The pot liner with saturated sand was now centrally mounted inside the pressure heating jacket and the compressed air turned on to admit air into the pressure jacket. The air pressure in the pot liner was maintained constant at 20 psig and a constant air injection rate of 12 scf/hr. ft² was also maintained. The combustion cell temperature was now increased from room temperature to 100°F and in a step-wise fashion at a scheduled rate of 100°F/hr until the steam distillation plateau was reached. For these runs conducted at 20 psig, the required distillation temperature was 260°F and this temperature was maintained for 4 hours to vaporize any water present in the porous medium. Simulation of the steam zone in this fashion is not quite rigorous since more steam can pass through a unit rock volume than that generated. Furthermore, at the water bank zone where oil, water and gas are flowing, additional water should be injected into the cell to account for the vaporized water from the steam plat-

TABLE 5.1
COMPUTATION OF INITIAL OIL, WATER
AND GAS SATURATION IN POROUS MEDIA

Crude Type	22.7°API
Weight of water in saturated sand and excess water	= 409.5 gm
Volume of water displaced	= 396.0cc
Volume of oil used	= 161.7cc
Excess water (over sand level and in pot liner tube)	= 241cc
Pore Volume (P.V) = 409.5-241	= 168.5cc
Actual water displaced from P.V. = 396 - 241	= 155cc
Connate water saturation $S_{w_c} = \frac{168.5 - 155}{168.5} = 8\%$	
Total volume of oil displaced	= 37.3cc
Oil saturation $S_o = \frac{161.7 - 37.3}{168.5} = 73.8\%$	
Gas saturation $S_g = 100 - 73.8 - 8 = 18.2\%$	

eau which condenses on hitting this colder zone.

Zone C - D

Depending on the type of coke required, these regions may not be simulated. As the cell temperature exceeds about 650°F, the residual oil in the pot liner cracks to a volatile fraction and non volatile heavy residue consisting of coke, tar and pitch. The coke formed was observed to be very hard black shiny material at 700°F while at 800°F, it became very brittle and very dark. However, in all cases, the coke cemented itself in the pot liner and it required about 15 minutes to chisel it out of the pot liner. The Table 5.2 below is a summary of the temperature history experienced by the porous media in the pot liner.

TABLE 5.2
TEMPERATURE HISTORY EXPERIENCED
BY POROUS MEDIA

Gas Injection Rate	12 scf/hr ft ²						Coking
System Temperature °F	100	200	260	400	500	600 . . .	Temp.
Temperature Residence Time hrs.	1	1	4	1	1	1	2½

Martin et al.¹¹ used 200°F heating schedule that produced temperature history similar to that observed in long combustion tube runs where combustion front rate of advance of approximately 3'/D were noted. Parrish et al.¹⁰ observed

a field combustion front rate of advance of .36 ft/D and Showalter³⁵ also reported a 1'/D rate. Such rates would suggest a much lower heating schedule rate and a 100°F/hr was considered appropriate, but not necessarily the best since any value within reasonable limits can be justified. The end of the heating schedule corresponds to the coking temperature and at the end of a 2½ hr heating residence time, the process was terminated.

5.2 Fuel Concentration

The initial fuel concentration was determined from a weight difference between known weight of a given coke sample and the weight of clean sand left behind after subjecting the coke sample to a 1,500°F temperature in an oven.

5.3 Combustion Process

5.3.1 Preparation of Sample

Each combustion run was started with fresh coke sample that was previously stored in a dessicator. The coke was carefully crushed and 10-20 grams of the sample carefully weighed using triple beam balance and then charged into the combustion cell. The bottom of the combustion cell was covered with glass wool and with proper tampering and packing, the bed thickness remained thin and below 1.3 cm.

Crushing the coke sample could result in distorting the original grain size which could in turn, mask the diffusion

effect of the coke combustion process. As a result of such possible effect, partially coked sample (Zones C-D not simulated in the simulation phase, and sample characterized by being wet, with high oil saturation) was charged into the reactor and heated to the desired combustion temperature in an inert atmosphere. Thus, before the combustion process was initiated, a hard consolidated coke had formed in the reactor.

The two Chromel/Alumel thermocouples were used to detect and measure any temperature variations between the top and bottom of the thin coke layer.

5.3.2 Initiation of Reaction

The reactor with known weight of coke was placed inside a heating jacket and nitrogen was passed through the bed at a rate that was controlled by the needle valve setting in Brooks rotameter. When the cell and flow lines were completely purged of air as determined from analysis of effluent gases, the heaters on the heating jacket were turned on. The controllers on the heaters maintained isothermal condition in the reactor and when the top and bottom temperatures of the thin coke layer inside were the same as the desired run temperature, nitrogen was turned off and ^{compressed} house air or oxygen/nitrogen gas mixture turned on. The inlet gas rotameter was used to measure the constant gas flow rate into the reactor. At this stage, combustion was

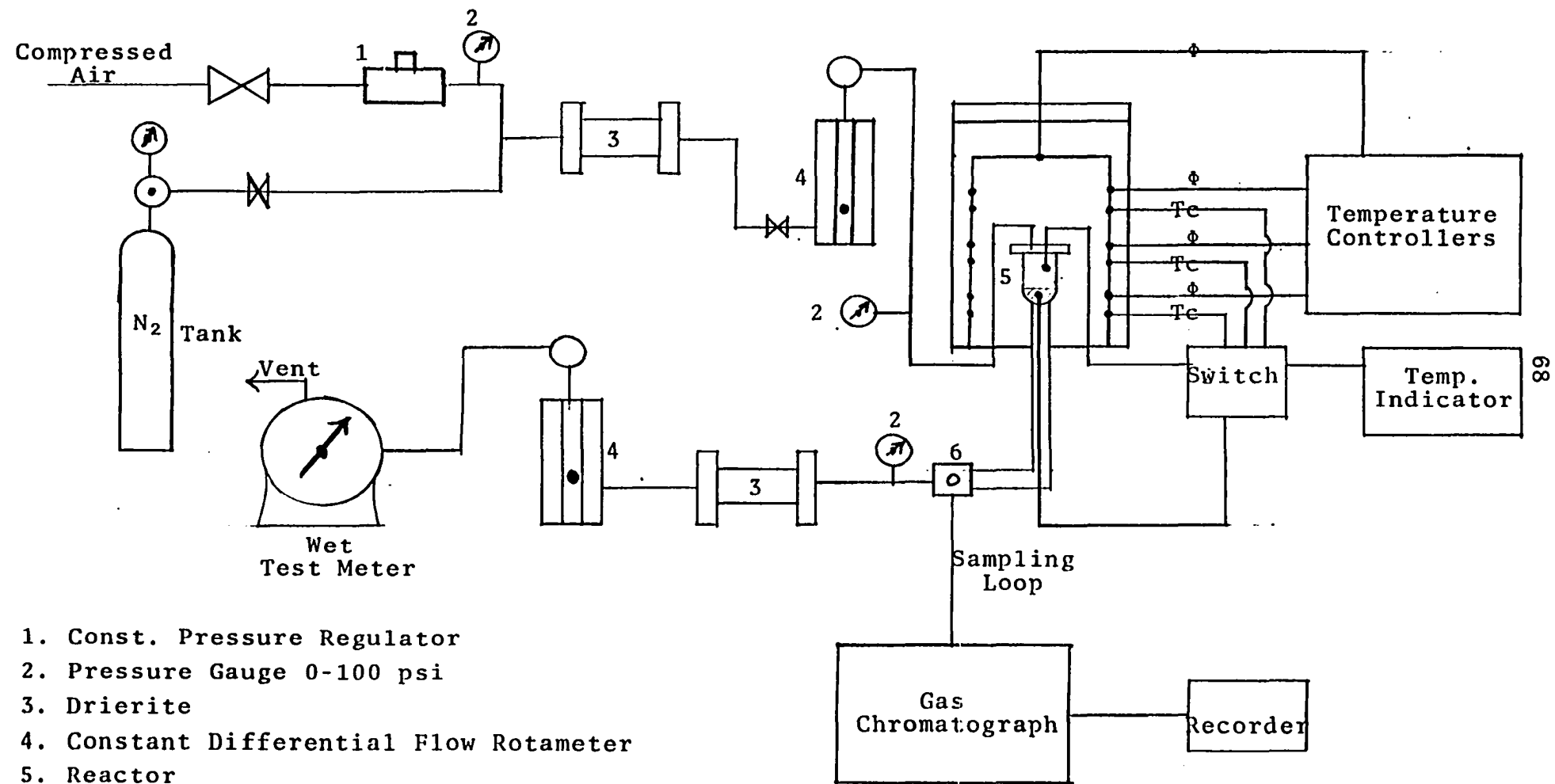
initiated.

5.3.3 Sample Collection

As the coke and oxygen reacted, combustion product gases were produced. These gases flowed through the pot liner tubing, through a modified Imperial T joint having a rubber septum that is located on the flow line (See Figure 5.3), through a drierite system, Brooks constant differential flow rotameter, wet test meter and then vented through a hood to the atmosphere. To simplify computational analysis, the exit gases flow rate was monitored and maintained constant. 2cc of produced gases was taken at frequent intervals from the modified Imperial T joint rubber septum by using a 4cc size gas tight syringe and then analysed for CO, CO₂, CH₄, O₂ and N₂ in a Gow-Mac series 550 gas chromatograph. A schematic representation of the process apparatus is indicated in Figure 5.3.

5.3.4 Sample Analysis

When 2cc of combustion product gases is introduced into the gas chromatograph, various peaks are separated and the first task is to identify the peaks. The peaks could be identified by comparing the elution time with published values for various gases in the literature, but the problem here is that the column lengths, size of column packing, oven and detector temperatures, gas flow rate and pressure and



1. Const. Pressure Regulator
 2. Pressure Gauge 0-100 psi
 3. Drierite
 4. Constant Differential Flow Rotameter
 5. Reactor
 6. Modified Imperial T joint with Rubber Septum
- ϕ = Chromel/Alumel Thermocouple (Controlling heaters on fire flood pot jacket)
 Tc = Chromel/Alumel Thermocouple (for temperature indication).

FIGURE 5.3
 SCHEMATIC DIAGRAM OF COMBUSTION
 PROCESS APPARATUS

other variables must be maintained constant at the values indicated in the literature. Most likely, all these variables cannot be maintained at the above required conditions, and some other technique has to be used to identify the various separated peaks. The technique used was to collect 1cc of combustion product gases plus 1cc of pure Nitrogen and the mixture injected into the G.C. In this case, the nitrogen peak becomes greatly magnified as compared to the result from 2cc of combustion product gases only. By repeating the above procedure with CO, CO₂, O₂ etc., these peaks were also identified.

Chapter 4 contains all the details of the column type used, the arrangement of the columns, and the operating conditions of the Gow Mac gas chromatograph. The volume percentage of the resolved CO, CO₂, O₂ and N₂ had to be computed and this requires calibration of the gas chromatograph.

5.3.5 Calibration of Gas Chromatograph

To calibrate the gas chromatograph, a Scott analysed gas with the following volume percentage composition was used:

CO = 6.55%

CO₂ = 14.8%

O₂ = 9.98%

N₂ = 63.73%

CH₄ = 4.94%

2cc of this Scott analysed gas was introduced into the G.C. and the output monitored on an L&N recorder. The peak heights were then considered to be proportional to the above given volume percentages. The volume percentage of the unknowns in a given 2cc sample of produced gas is then given by $\frac{h'_i}{h_i} * V_i$

where h_i = Peak height of i th component in Scott gas

h'_i = Peak height of i th component in Effluent gas

V_i = Volume % of i th component in Scott gas.

The above analysis is true only if the gas chromatograph is operated under identical conditions during the analysis of both the Scott analysed gas and the effluent sample gases.

5.3.6 Termination of Combustion

At the end of each combustion run, gas injection was switched back to Nitrogen to prevent further oxidation of residual coke. This was only necessary during combustion at low temperatures when combustion time exceeded 25 minutes. For these runs, the unreacted coke was carefully transferred into a crucible and its weight determined by using a triple beam balance. The crucible and its contents were then heated in an oven at 1500°F for 20 minutes. The clean sand residue was again weighed and the weight difference before and after subjecting the coke to 1500°F oven temperature represented the amount of unreacted coke.

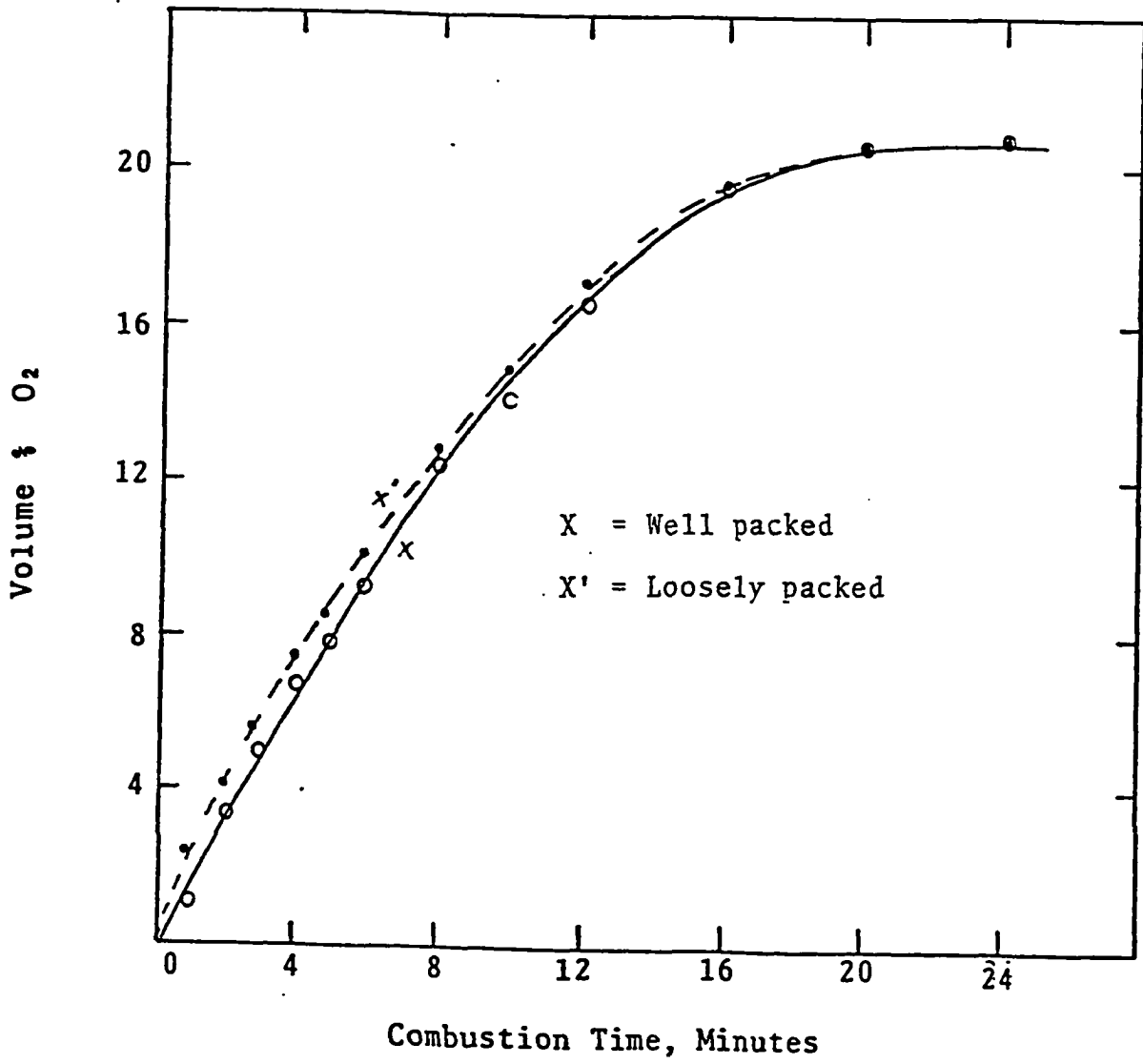
CHAPTER VI

PRESENTATION AND DISCUSSION OF RESULTS

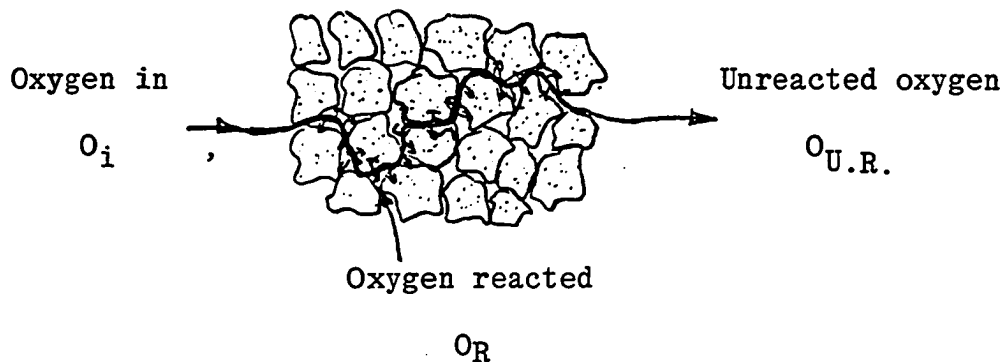
A total of 12 runs were made to observe and explain the poor oxygen utility efficiency at low coke combustion temperature. Oxygen utility is qualitatively described as a measure of the amount of oxygen unreacted during coke combustion process. Low efficiency is synonymous with high volume percent of unreacted oxygen.

The first series of runs represented on Figure 6.1 as X and X' represent samples of coke formed at 700°F and coke combustion temperature of 950°F. This coke was formed from 22.7°API crude and the gas flow rate through the reactor was 110 cc/min. All physical and reaction conditions were identical for both runs except the difference in degree of tamping and packing. In the case of run X, the coked sand was very well packed and tamped whereas in case of run X', the coke was loosely fed into the reactor. The net effect is that run X had thinner bed thickness with less voidage space for air channeling than run X'. Results from monitoring

Figure 6.1

Effect of Channelling on Oxygen Utility

the volume percentage of unreacted oxygen for both runs did show higher values of unreacted oxygen in case X' than that for case X. This is interesting and not totally unexpected because if we assume oxygen consumption rate as being a function of temperature, gas flux, system pressure and carbon concentration, then the reaction rate values should be the same for both runs since all the above named variables are the same. A simple oxygen balance as illustrated in the figure below does demonstrate that.



Mass of unreacted oxygen $O_{U.R.}$ equals $O_i - O_R$. Using the suffix X and X' to represent the run under consideration, then

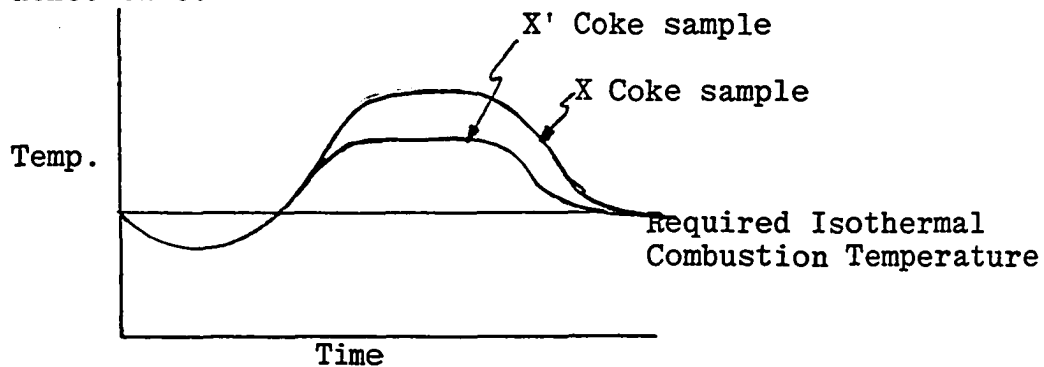
$$O_{U.R.,X} = O_{i,X} - O_{R,X}$$

$$O_{U.R.,X'} = O_{i,X'} - O_{R,X'}$$

Since the oxygen mass flowing into the system is the same for both X and X' and from the above discussions, $O_{R,X}$ and $O_{R,X'}$ are supposedly the same, then volume of unreacted oxygen should be the same for both X and X'. However, since it was observed that $O_{U.R.,X}$ and $O_{U.R.,X'}$ are not the same, this would then imply that the reacted oxygen is not the same

for X and X'. The only reason why this would be true is due to the varying degree of channeling in the reacting bed. In case of X, the gas has to flow through a more tortuous path and the oxygen molecules will have a longer residence time in the reactor, thereby permitting a more efficient coke conversion to CO and CO₂.

For the early time period in the above experiments, the effect of non-isothermal combustion of the system further magnifies the difference between the graphs. To understand this later complication, one has to realize that for a system for example at 950°F, the introduction of cool air into the reactor cell will initially cause a temperature drop, to be followed by a temperature rise above required 950°F due to the exothermic nature of the coke combustion reaction. The degree of departure from the isothermal temperature will depend on the total mass of coke present and the oxygen residence time.



Thus, one of the reasons for poor oxygen utility during in-situ combustion is the presence of air channel paths in the formation as a result of fractures in the formation or high degree of reservoir heterogeneity.

The next series of runs is represented on Figure 6.2 as A, B, C and in Appendix B Table 2. The following is a summary of the properties as indicated in Appendix B:

- A: Coke formed from 15.4°API crude at 600°F coking temperature. Fuel concentration - 2.7 gmC/100 gm sand.
- B: Coke formed from 22.7°API crude at 800°F coking temperature. Fuel concentration - 1.74 gmC/100 gm sand.
- C: Coke formed from 22.7°API crude at 700°F coking temperature. Fuel concentration - 2.45 gmC/100 gm sand.

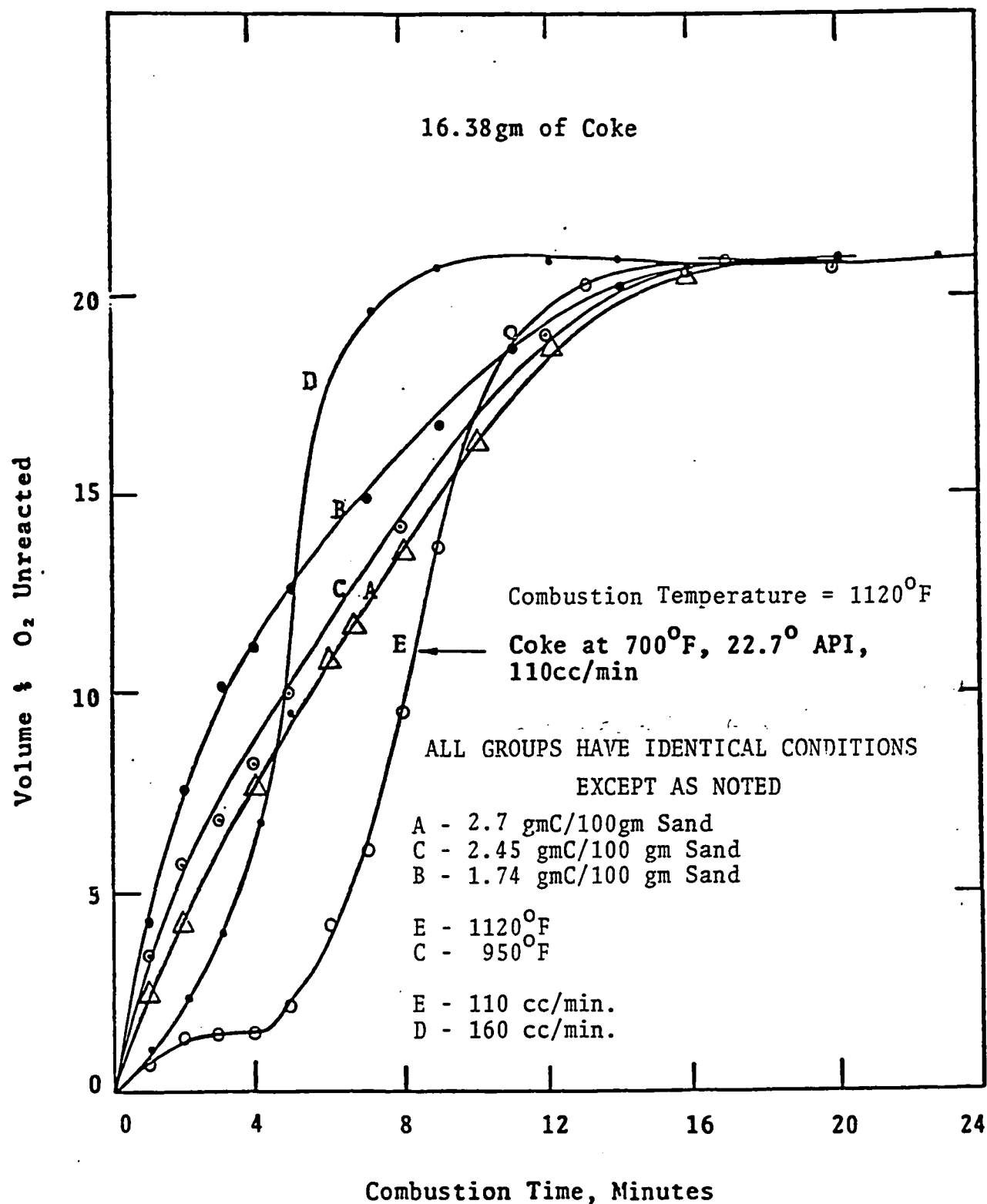
For the above runs, the coke combustion temperature, gas flux and amount of coke feed into the reactor were held constant at 950°F, 110 cc/min and 16.38 gm respectively. The main objective here was to provide coke samples of different concentrations and to maintain the other variables constant in the equation.

$$r = f(T, v, p, c') \dots \dots \dots (1)$$

The observed results indicating poorer oxygen utility efficiency with decreasing carbon concentration was not surprising. This could be explained by examining equation (1) that now becomes $r = f(c)$ since all other variables are held constant. From the hypothesized rate expression describing oxygen coke reaction, $f(c) = C^n$ hence higher rate of oxygen consumption is associated with higher coke concentration. Therefore, from the oxygen mass balance equation $O_{U.R.}$ will be higher for lower carbon concentration.

Figure 6.2

Effect of Coke Concentration (Different Coke) and Temperature
On Oxygen Utility



Although higher coke concentration will improve the poor oxygen utility, one must also realise that the higher coke concentration does represent higher fraction of the intended recoverable crude being converted to unrecoverable oil in the form of coke.

The greatest difference in oxygen utility was observed by comparing run E and C. All the variables in Equation 1 were identical for both runs except for variations in combustion temperatures. The task here is to prove that higher temperatures result in higher oxygen consumption rate and hence, lower values of $O_i - O_R$.

The reaction kinetics of coke combustion process will aid in explaining this observation. Since both coke concentration and reactor pressure are identical then the variation in oxygen consumption rate could only be due to difference in specific rate constant coefficient K . Bousard and Ramey observed a chemically rate controlled coke combustion process and were able to correlate K to Arrhenius equation. Thus $K = Ae^{-E/RT}$. This would indicate that as temperature increases, K would increase resulting in higher oxygen consumption rate and therefore a more efficient oxygen utility. However, this research on the type of coke studied, could not substantiate Bousard and Ramey's findings. In this research, K values did exhibit temperature dependence which qualitatively has the same results as the above authors.

The results on kinetic studies of coke combustion, Fig. 6.4, indicates that increasing gas flux results in higher K values. This would suggest that oxygen utility efficiency should improve with increasing oxygen flux. However, the results depicted by graphs 2, 3, 4 (Fig. 6.3 and Appendix B Table 3) where the only difference in variables is gas flux, is contrary to expected result. It is true that oxygen consumption rate increases with increasing gas flux over the temperature range under investigation but such higher flux rate causes lower oxygen residence time in the reactor and hence, promotes higher degree of channeling. The channeling effects override the increase in oxygen consumption rate with the net effect of lowering oxygen utility efficiency. From a practical standpoint, such high air flux rates are unrealistic if one has to engineer a feasible recovery process, but these results reflect the possible situation around the injection well bore where high fluxes will be experienced.

These studies have demonstrated that oxygen utility efficiency is most drastically affected by temperature variations and this could be explained in terms of temperature sensitivity to coke combustion kinetics at low temperatures.

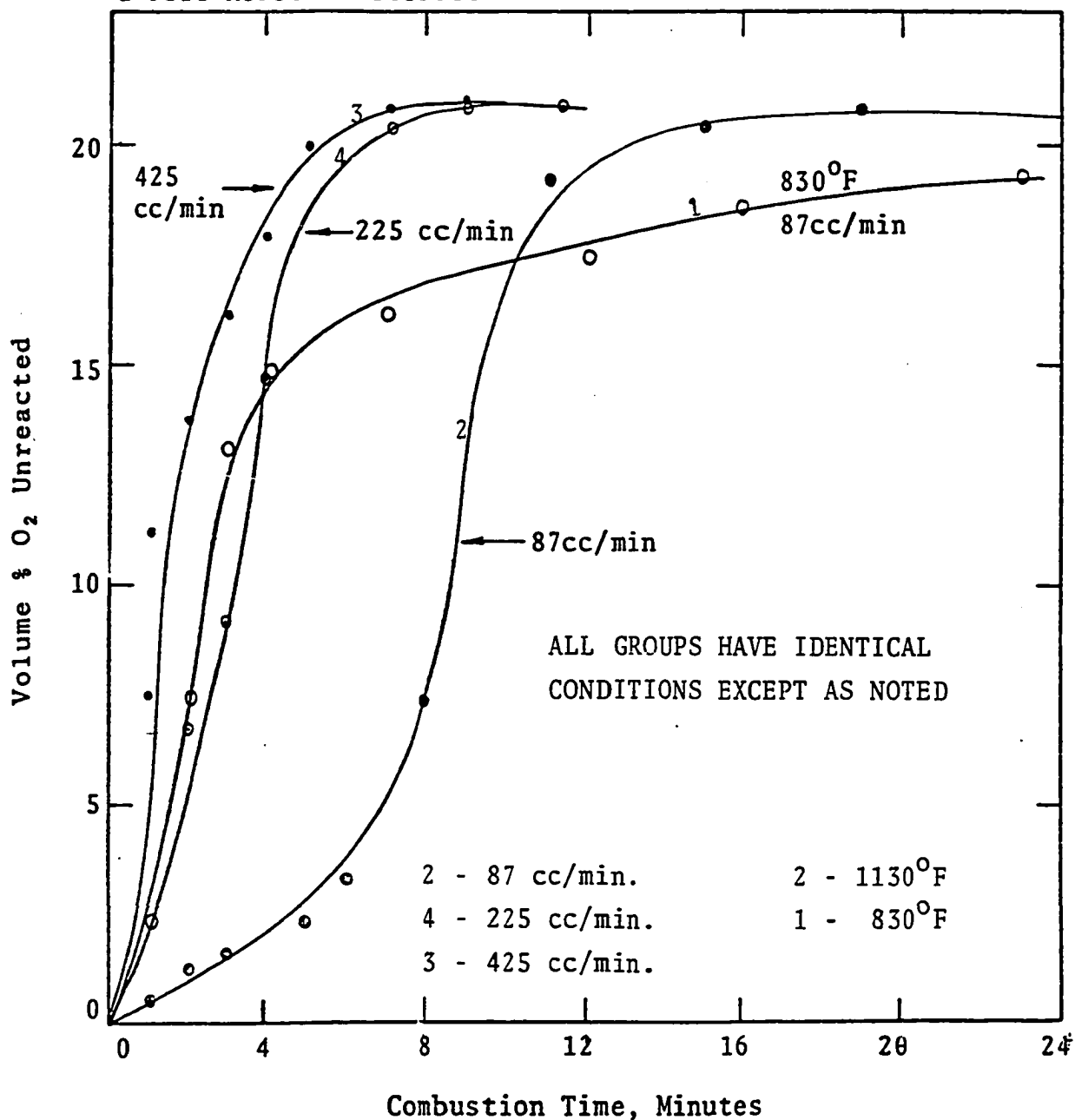
Effect of Temperature & Channelling on Oxygen Utility

Combustion Temp. for 2, 3, 4 = 1130°F

Coke Formed at 600°F; 15.4° API Crude

12 gm of Coke

2 PSIG Reactor Pressure



Best Value of K Vs Gas Flow Rate

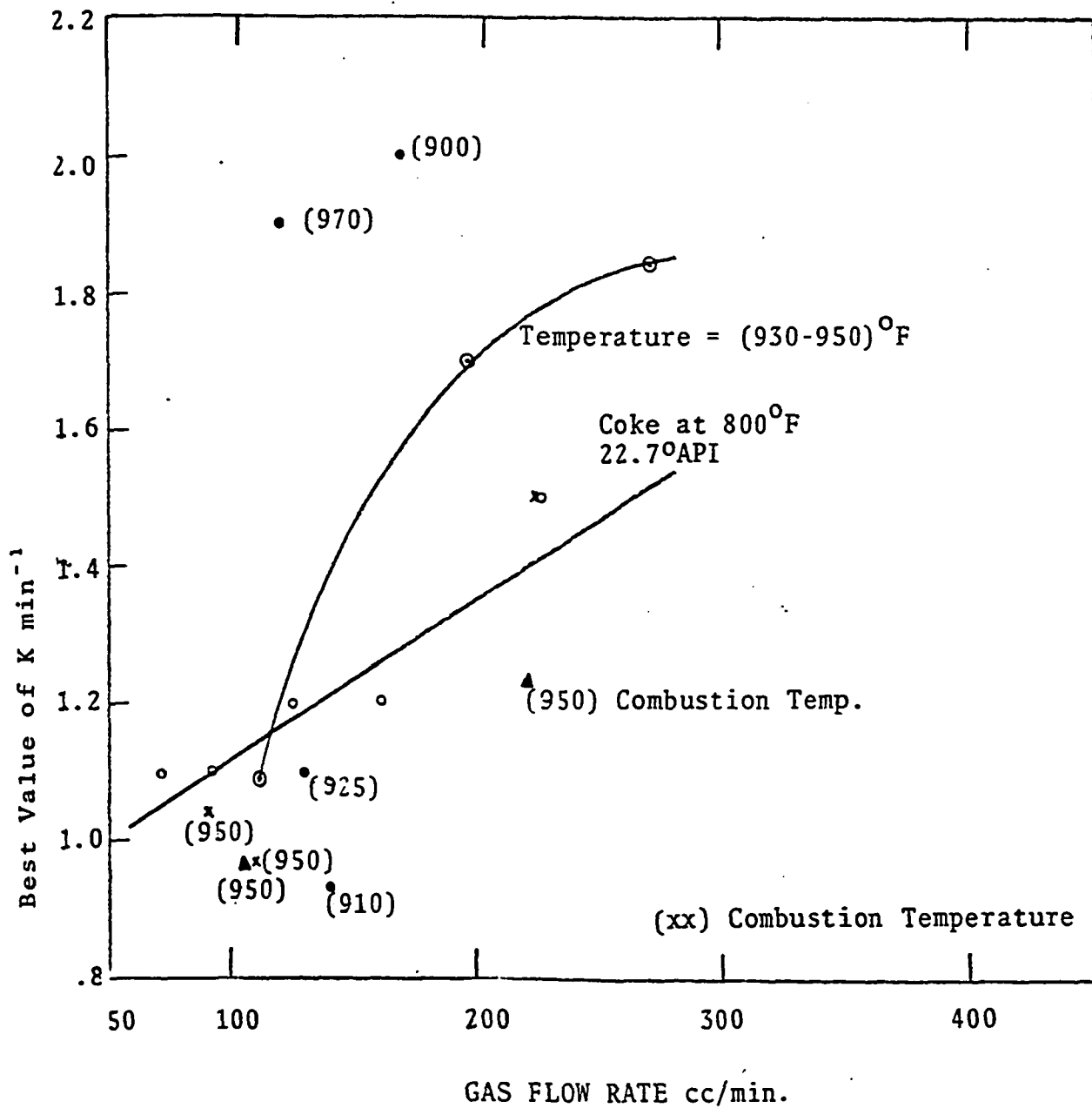


FIGURE 6.4

BEST VALUE OF K VS GAS FLOW RATE

(Specific Rate Const. Coefficient)

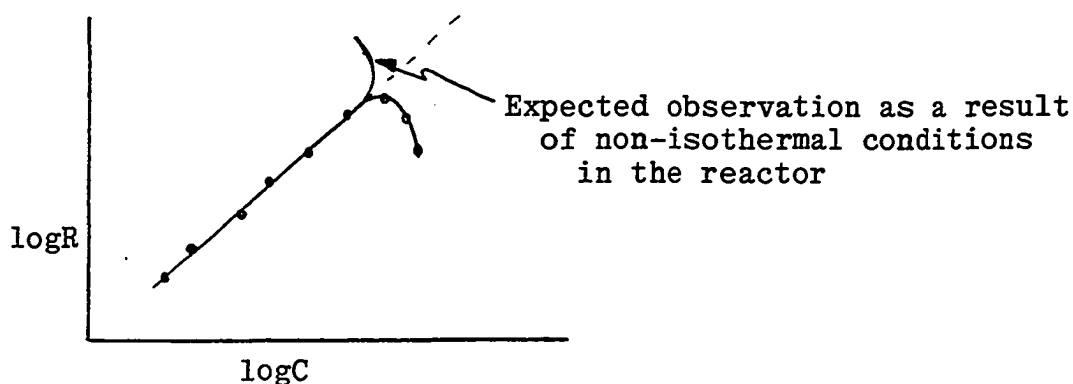
Analysis of Coke Combustion Kinetics

A total of twenty runs were made to determine the controlling mechanism of various types of coke. The results are all tabulated in the Appendix. The first series of runs was made at reactor cell pressure of 20 psig. These runs have not been reported because it was felt that the results would have excessive errors. To achieve 20 psig cell pressure, air at high pressure would have to be introduced into the reactor within a very short period of time. This means excessive reactant within the reactor and any molecule of gas produced as a result of the combustion process would be excessively diluted by the large mass of reactant present. Thus, the effluent gas analysis would not represent the instantaneous composition of the effluent gases under investigation. To avoid this pitfall, the cell pressure was maintained at near atmospheric pressure.

Results of Chemically Rate Control Analysis

As must be stressed, no solution technique to evaluate the variables k , n , m in any hypothesized mechanism describing oxygen coke reaction can overcome the disadvantages of haphazard selection of experimental data. In line with this thinking, a log-log plot of reaction rate against carbon concentration was made, to recognize any trends in the data. An interesting observation was that for the first 4 to 5

minutes, the reaction rates do not follow the trend exhibited by other data. The convex shape of the data points in this region (see Fig. 6.5) were thought to be due to errors involved in effluent gas analysis and temperature fluctuations resulting in non-isothermal conditions in the reactor during this time period. The non-isothermal condition in the reactor could not possibly explain the above consistently observed phenomena because non-isothermal conditions cause temporarily higher temperatures and as such, the data points should deflect upwards as shown below.



Furthermore, the observed phenomena could not be due to errors in measurements since the volume percent of effluent gases of interest is high and as such, the percentage error will be least in this region. By conducting the research at near atmospheric pressure and by ensuring the inlet gas flow rate to be approximately the same as exit flow rate, there will be no pressure build-up in the cell, neither will there be excessive introduction of reactant gas. This ensures an accurate monitoring of the instantaneous concentration of effluent gases.

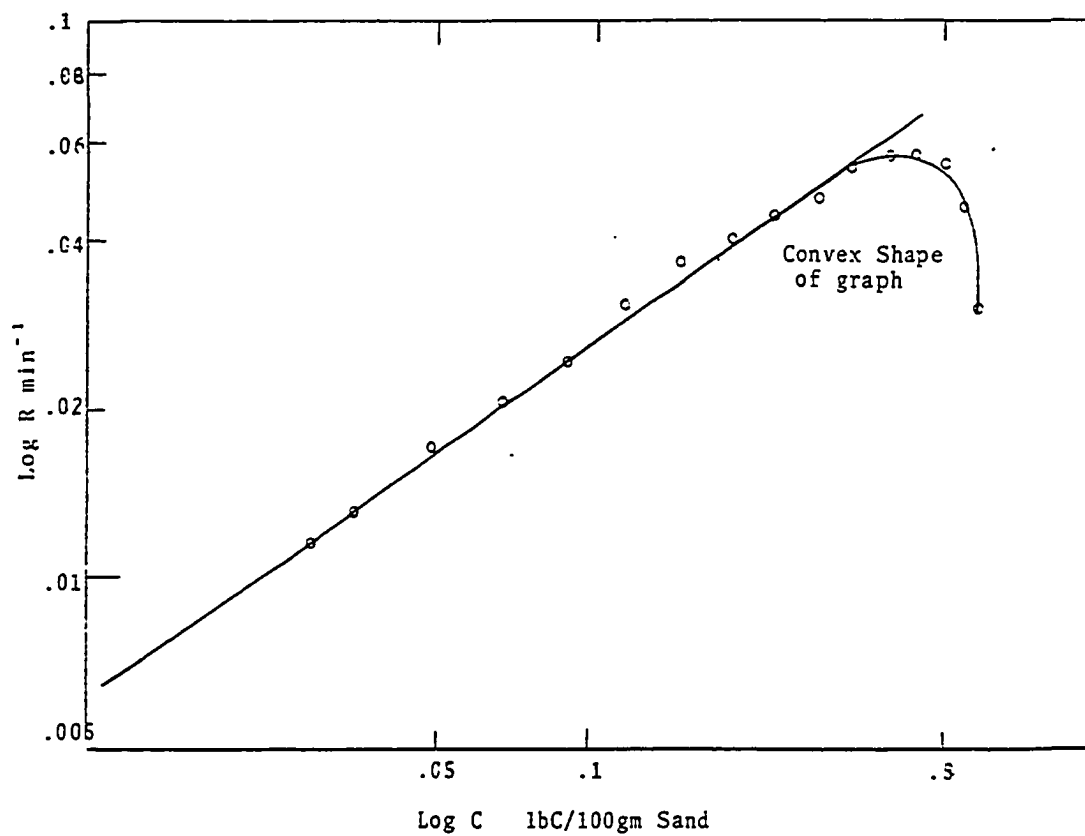


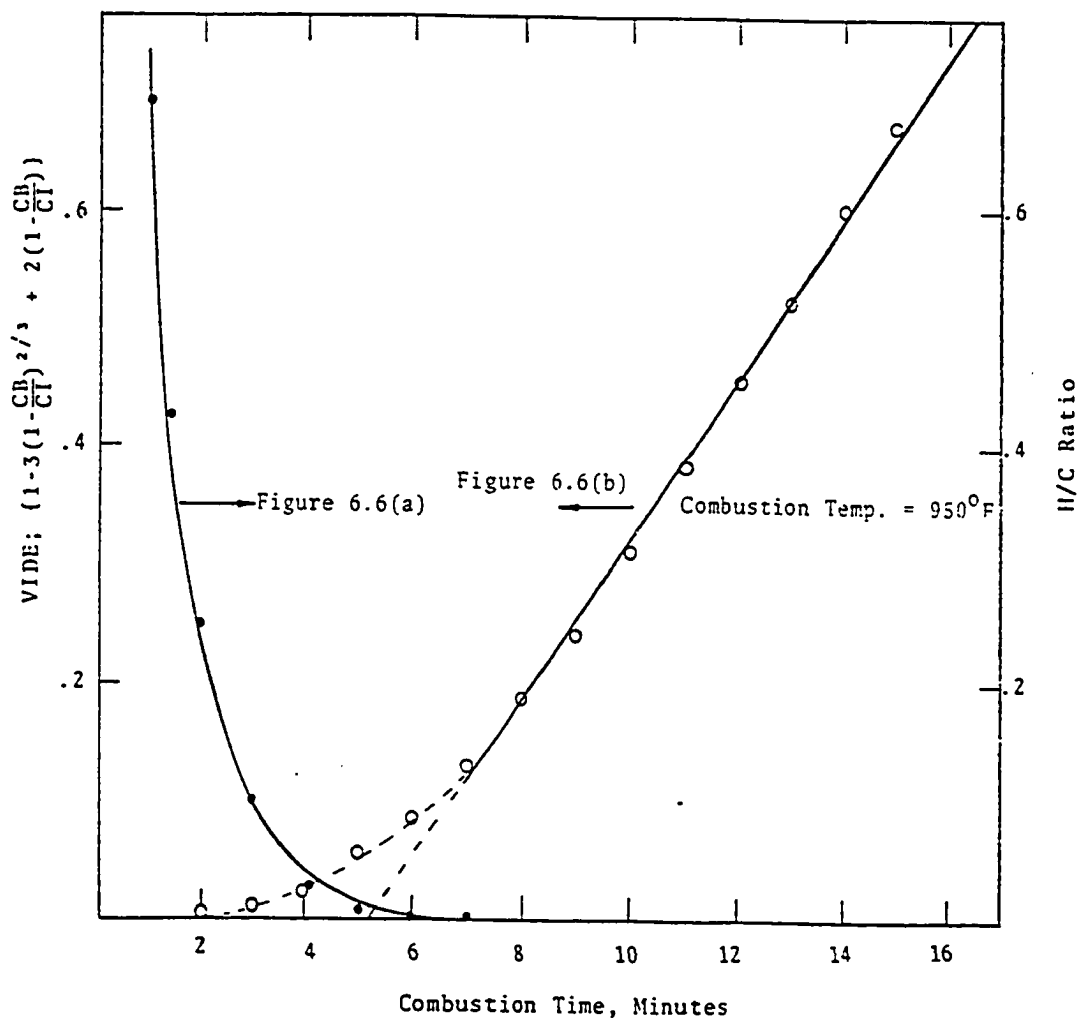
FIGURE 6.5

REACTION RATE VS CARBON CONCENTRATION

The following theory does explain the above observations. The coke under investigation is a highly reactive hydrocarbon residue that contains only carbon and hydrogen with an atomic H/C* ratio of x : CH_x . In a dry forward combustion, x lies between 1 and 1.8.²⁷ On samples of coke formed by pyrolysis, Ramey observed that the hydrogen reacts faster than the carbon and this is in qualitative agreement with conclusions reached by Dart et al. concerning regeneration of clay catalyst pellets. By plotting atomic hydrogen carbon ratio against time for each run as shown in Fig. 6.6, one observes that the H/C ratio decreases, reaching zero between 4-6 minutes and this is the time period corresponding to the observed convex shape of the reaction rate plot. Thus, during the early time period when the H/C ratio is very high, the hydrogen reaction rate is maximum and approaches zero between 4-6 minutes. From 6 minutes onward, the hydrogen concentration is zero and the residue undergoing combustion at this time is essentially pure carbon. Since the reaction rate expression describing coke, oxygen reaction assumes the coke is pure carbon, the required data points ~~to be used in testing the adequacy of the model~~ should be values obtained when H/c ratio is zero. From the above discussions, one can see that the measured reaction rates at the early time periods represent a combination of carbon and hydrogen reaction rates and as such, they are not represen-

*See Appendix C.

Figure 6.6(a) & Figure 6.6(b)
Variable in Diffusion Equation and H/C Ratio Vs Time



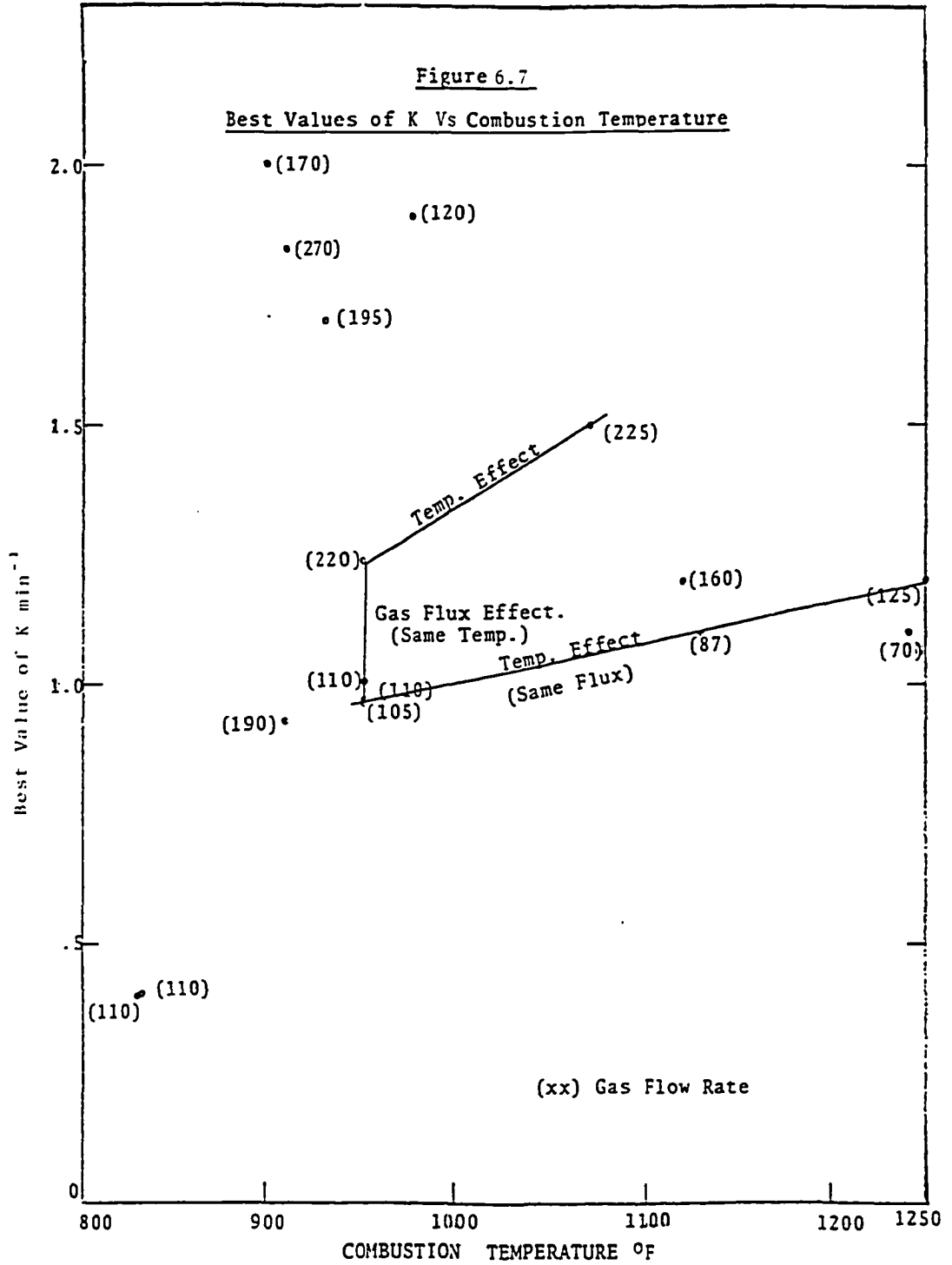
tative of rates for pure carbon combustion.

The tabulated best values of n and m reported in this research (Table 3.1) have values ranging from .6 to 1.3. For isothermal combustion conditions under which these studies were made, the values of n and m should be consistent and with the type of fluctuations observed one has to conclude that the power law reaction rate expression describing coke, oxygen reaction is not quite satisfactory, and it's only an approximation of the kinetic process.

This would imply that results be interpreted qualitatively. Because of the nature of fluctuation in n and m values, the reported values of K could not be given any quantitative interpretation but the results in Fig. 6.4 and 6.7 do indicate the sensitivity of K values on gas flux rate and temperature. Below 900°F, the dependence of K on temperature seems to be very pronounced but above 950°F, the temperature effects appear to be less pronounced. A Langmuir³⁶ type mechanism is proposed to describe the coke oxygen reaction. This mechanism is proposed because the results from the other tested rate expression suggests the presence of two kinetic regimes: the early period when hydrogen is present and the later period characterized by pure carbon combustion. The proposed Langmuir mechanism is

$$R = \frac{-kKC}{1+KC}$$

This mechanism will be able to account for the two observed



kinetic regimes. For example, at the early time period when carbon concentration is high, $KC \gg 1$ and r then equals $\frac{k}{K}$. At later stage, when C becomes very small, $KC < 1$ and r becomes kKC which will represent the second reaction regime characterized by pure carbon combustion.

Results of Diffusion Control Analysis

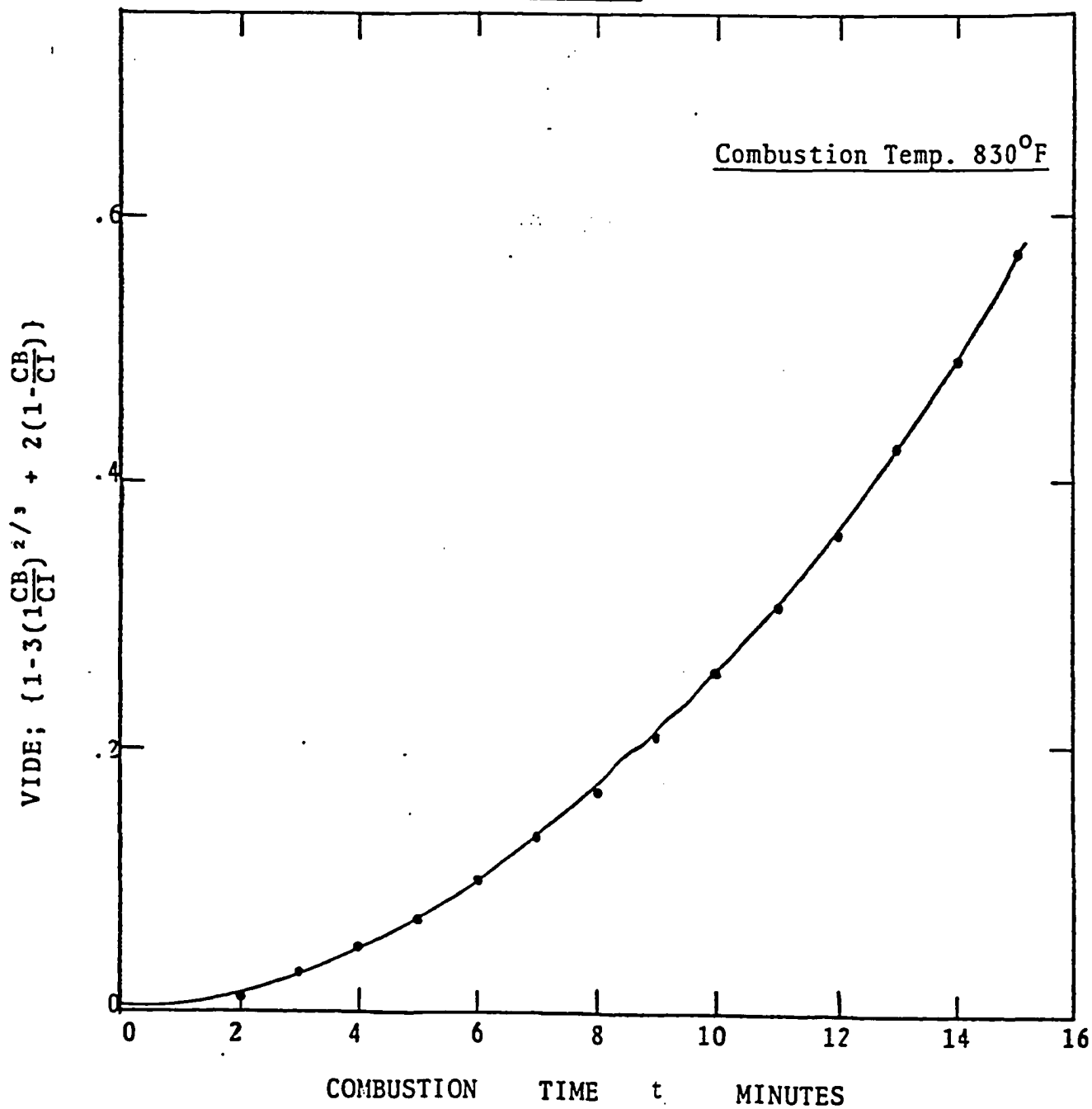
From unreacted core analysis, the variable in the diffusion equation V I D E :- $\left[1 - 3\left(\frac{CB}{CI}\right)^{2/3} + 2\left(\frac{CB}{CI}\right) \right]$ when plotted against time yielded a straight line for temperatures above 950°F. Fig. 6.6b. At temperatures below 900°F, the plot of V I D E against time was a curve. See Figures 6.6b and 6.8. These results indicate diffusion to be the main controlling mechanism at temperatures above 950°F while chemical reaction dominated the process at temperatures below 900°F. For diffusionally controlled process, the V I D E plot should pass through the origin but the reported graph in Figure 6.6b does not pass through the origin. This is not surprising because in deriving the equation

$$t = \frac{\rho_c R_o^2}{6bDC_{Ox}} \left[1 - 3\left(\frac{r_c}{R_o}\right)^2 + 2\left(\frac{r_c}{R_o}\right)^3 \right]$$

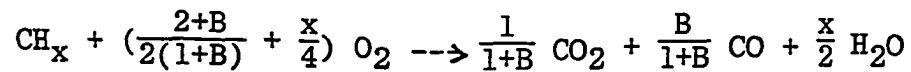
$$t = \tau \left[1 - 3\left(1 - \frac{CB}{CI}\right)^{2/3} + 2\left(1 - \frac{CB}{CI}\right) \right] \text{ where } \tau = \frac{\rho_c R_o^2}{6bDC_{Ox}}$$

The following assumption was made: that the stoichiometric ratio of carbon burned per mole of oxygen consumed is constant and equal to b . By examining the equation pre-

Figure 6.8

Variable in Diffusion Equation Vs TimeVIDE Vs t

sented by Burger²⁷ which describes the stoichiometric relation between coke and oxygen as:



x = Atomic H/C ratio of fuel

B = Volume ratio of CO/CO₂

It becomes evident that the value of b in V I D E equation is not a true constant until such period when H/C = 0. If the origin of the time axis is shifted to such position when H/C = 0, then the V I D E plot would pass through the origin which is the expected result for a diffusion control process.

CHAPTER VII

CONCLUSIONS

Conclusions and Recommendations

For Further Work

Without doubt, in-situ oil recovery is a very complex process and experimental data from the coke combustion kinetics have also proven to be complex. Any hypothesized rate expression describing the nature of the coke oxygen reaction requires non-linear programming techniques to evaluate the variables in the reaction rate expression. A newly developed technique for analysing data using steepest descent optimization theory is presented.

The power law type rate expression does not adequately describe the coke combustion kinetics but the results from this model could adequately be interpreted qualitatively. A Langmuir type mechanism is suggested for further investigation.

At temperatures above 950°F, the coke combustion process is controlled by mass transfer while at temperatures below 900°F, the process is controlled by chemical kinetics.

Regardless of the temperature regime under considerations, both mass transfer and reaction rate control mechanisms do exist but the predominant mechanism is as indicated above.

The diffusional analysis does not require precise definition of the coke-oxygen reaction rate before defining the controlling mechanism and as such, the conclusions from this analysis are more reliable than chemically rate control analysis. Furthermore, in kinetic behavior analysis, the possibility of internal temperature gradient due to the exothermic nature of the coke/oxygen reaction does pose considerable questions on accuracy and degree of reliability of results. Such problems as indicated above are, however, of no consequence in diffusional analysis.

The different cokes do not exhibit any particular trend in chemical properties as could be determined in terms of the controlling mechanism. However, they do exhibit different physical properties.

The atomic H/C ratio decreases with time and at the early time period, the hydrogen burning rate predominates over carbon burning rate. As the H/C ratio tends to zero, we have pure carbon combustion.

The oxygen utility efficiency is dependent on temperature with high efficiency associated with high combustion temperature and low efficiency at low temperatures (less than 900°F). At high specific rate coefficient associated with high temperatures, the coke oxygen reaction is very fast

resulting in low level amount of unreacted oxygen.

At high air flux rate, the oxygen utility efficiency is low and this is due to low residence time of the oxygen in the reactor which results in high degree of channeling.

The oxygen utility efficiency does depend on coke concentration inasmuch as the coke concentration affects the reaction kinetics.

Further work is recommended in this area to show that poor oxygen utility efficiency associated with fractured reservoir formation is due to channelling and reduction in temperature at the far end of the fractured formation face.

BIBLIOGRAPHY

1. Elkins, L. W. API Report No 360-1-G, 1st Annual Meeting of the Division of Production of The API, Los Angeles, May 3-5, 1971.
2. Poetman, F. H. "Secondary and Tertiary Oil Recovery Processes." Interstate Oil Compact Commission, Oklahoma City, Oklahoma, Sept. 1974.
3. Wilson, R. "Tertiary Recovery." Chilton's Oil and Gas Energy (October 1975).
4. Herbeck, W.B. "Miscible Flood Hikes Block 3I's Oil Output." Oil and Gas Journal (October 27, 1969).
5. Walker, J. W. and Turner, J. L. "Performance of Seeligstone Zone 20B-07 Enriched-Gas-Drive Project." J.P.T. (April 1968).
6. Griffith, J.D., Baiton, N. and Steffensen, R. J. "Ante Creek - A Miscible Flood Using Separator Gas and Water Injection." J.P.T. (October 1970):22.
7. Hull, P. "SACROC - An Engineering Conservation Triumph." Oil and Gas Journal (August 17, 1970) 68.
8. C. R. Smith. Mechanics of Secondary Oil Recovery. (New York: Reinhold Publishing Company, 1966).
9. Martin, W. L., Alexander, J. D. and Dew, J.N. "Process Variables of In-Situ Combustion." Society of Petroleum Engineers of AIME, Transactions Vol. 213 (1958).

10. Parrish, D. R., Rausch, R. W., Beaver, K.W. and Wood, H.W. "Underground Combustion in the Shannon Pool, Wyoming." Society of Petroleum Engineers of AIME Transactions Vol. 225 (1962).
11. Alexander, J. D., Martin, W. L. and Dew, J.N. "Factors Affecting Fuel Availability and Composition During In-Situ Combustion." Society of Petroleum Engineers of AIME Transactions Vol. 225 (1962).
12. Wilson, L. A., Wygal, R. J. et al. "Fluid Dynamics During an Underground Combustion Process." Society of Petroleum Engineers of AIME Transactions Vol. 213 (1958).
13. Baily, H. R. and Larkin, B. K. "Conduction-Convection in Underground Combustion." Society of Petroleum Engineers of AIME Transactions Vol. 219 (1960).
14. Chu, C. "Two-Dimensional Analysis of a Radial Heat Wave." Journal of Petroleum Technology Vol. 15 (1963).
15. Wilson, L. A. et al. "Some Effects of Pressure on Forward and Reverse Combustion." Society of Petroleum Engineers of AIME Transactions Vol. 228 (1963).
16. Thomas, G. W. "A Study of Forward Combustion in a Radial System Bounded by Permeable Media." Society of Petroleum Engineers of AIME Transactions Vol. 228 (1963).
17. Tadema, H. J. "Mechanism of Oil Production by Underground Combustion." Proc., 5th World Petroleum Congress Section II (1959).
18. Gottfried, B. S. "A Mathematical Model of Thermal Oil Recovery in Linear Systems." Society of Petroleum Engineers Journal Vol. 5 (1965).
19. Bousaid, I. S. and Ramey, J. "Oxidation of Crude Oil in Porous Media." Society of Petroleum Engineers of AIME Transaction Vol. 243 (1968).

20. Dart, J. C., et al. "Regeneration Characteristics of Clay Cracking Catalyst." Chemical Engineering Progress Vol. 45 (Feb. 1949).
21. Metcalfe, T. B. "Residence Time Distribution of a Complex Reactor." Chemical Engineering Progress Vol. 60, No. 2 (Feb. 1964).
22. Lewis, W. K., et al. "Low Temperature Oxidation of Carbon." Industrial and Chemical Engineering Chemistry Vol. 46 (June 1954).
23. Strijbos, S. "Burning-Out of a Carbonaceous Residue from a Porous Body." Chemical Engineering Science Vol. 28 (1973).
24. Weisz, P. B., and Goodwin, R. "Combustion of Carbonaceous Deposits Within Porous Catalyst Particles 1. Diffusion-Controlled Kinetics." Journal of Catalysts Vol. 2 (1963).
25. Levenspiel, O. Chemical Reaction Engineering. (New York: John Wiley and Sons, Inc., 1972), 2nd Edition.
26. Dabbous, M. K. "In-Situ Oxidation of Crude Oils in Porous Media." Ph.D. dissertation, School of Engineering, University of Pittsburgh, 1971.
27. Burger, J. G. et al. "Chemical Aspect of In-Situ Combustion Heat of Combustion and Kinetics."
28. System/360 Continuous System Modeling Program (360A-CX-16X). Programmer's Manual. IBM Technical Publication No. GH20-0367-4 (IBM Corporation, 1972).
29. Levenspiel, O., Weinstein, N. J., and Li, J.C.R. "Numerical Solution to Dimensional Analysis." Industrial and Engineering Chemistry 48, 324 (1956).

30. IMSL Library 1 Edition 6 (1977). (Fortran IV), IBM System 370/360.
31. Sivazlian, Stanfel. Optimization Techniques In Operation Research. (Englewood Cliffs, New Jersey: Prentice-Hall, Inc., 1975).
32. Ishida, M. and Wen, C. Y. "Comparison of Kinetic and Diffusional Models for Solid-Gas Reactions." A.I.Ch.E. Journal Vol. 14, No. 2.
33. Kuhn, C. S. and Koch, R. L. "In-Situ Combustion, Newest Method of Increasing Oil Recovery." Oil and Gas Journal 52 (August 10, 1953).
34. Wu, C. H., and Fulton, P. F. "Experimental Simulation of Zones Preceding the Combustion Front of an In-Situ Combustion Process." SPEJ (March 1971).
35. Showalter, W. E. "Combustion Drive Tests." Society of Petroleum Engineers of AIME Transactions Vol. 228 (1963).
36. Carberry, J. J. Chemical and Catalytic Reaction Engineering (New York: McGraw-Hill, Inc., 1976).
37. System/360 Scientific Subroutine Package. IBM Technical Publication H20-0205-3. Program FMCG (Fletcher and Reeves Unconstrained Search Technique).

NOMENCLATURE

R	=	Reaction rate, gm Carbon/(100 gm sand)(min)
$\frac{dc}{dt}$	=	Carbon burning rate, gm carbon/(100 gm sand)(min)
K	=	Specific rate constant, (min-atm) ⁻¹
C	=	Carbon concentration, gm Carbon/(100 gm sand)
P	=	Oxygen partial pressure, atmospheres
n	=	Reaction order with respect to Carbon
m	=	Reaction order with respect to oxygen partial pressure
A	=	Arrhenius constant, (min-atms) ⁻¹
E	=	Activation energy, Btu/lb mole
T	=	Combustion temperature, °F
t	=	Combustion time; minutes
CB(t)	=	Mass of carbon burnt at time t, gm Carbon/100 gm sand
F	=	Gas flow rate, cc/min.
C.F.	=	Conversion factor from volume to mass gm C/cc C-100 gm sand)
CI	=	Initial Carbon concentration, gm Carbon/100 gm sand
N	=	Total number of data points for a run
C _{ox}	=	Oxygen concentration
Π	=	System pressure, atmosphere
V.I.D.E.	=	Dependent variable in diffusion equation

d = Step size; distance moved along direction of
steepestdescent subscripts

i = ith species, ith data point

in = inlet

E = Exit

APPENDIX A

ALGEBRAIC ILLUSTRATION OF STEEPEST DESCENT
NON LINEAR OPTIMIZATION TECHNIQUE

ALGEBRAIC ILLUSTRATION OF STEEPEST DESCENT
NON LINEAR OPTIMIZATION TECHNIQUE

The following algebraic expression illustrates the use of the above optimization technique. Although the example presented is a maximization problem, the search procedure is almost the same for a minimization problem. The technique finds the unconstrained maximum of a multivariable, non linear function:

Maximize $f(x,y)$

$$f(x,y) = -2x^4 + 44x^3 - 282x^2 + 440x - y^4 + 28y^3 - 277y^2 + 1140y - 1900.$$

Assume starting point of $\bar{x}_0(2,8)$ and $d = 1$

$$f(\bar{x}_0) = -196.$$

$$\frac{\partial f}{\partial x} = -8x^3 + 132x^2 - 564x + 440.$$

$$\frac{\partial f}{\partial y} = -4y^3 + 84y^2 - 554y + 1140.$$

$$\nabla f(2,8) = \left(\frac{\partial f}{\partial x}, \frac{\partial f}{\partial y} \right) \Big|_{2,8} = (-224, 36)$$

$$f(2,8) = -196$$

$$\|\nabla f(2,8)\| = \sqrt{224^2 + 36^2} = 226.87$$

New vector position \bar{x}_1

$$\begin{aligned} \bar{x}_1 &= \bar{x}_0 + \frac{d\nabla f(x_0, y_0)}{\|\nabla f(x_0, y_0)\|} \\ &= (2,8) + \frac{1}{226.87} (-224, 36) \end{aligned}$$

$$\bar{x}_1 = (1.02, 8.16)$$

$$f(\bar{x}_1) = -68$$

Since $f(\bar{x}_1) > f(\bar{x}_0)$ \therefore There is improvement in value of functions towards achieving maximum values of x and y .

Next determine \bar{x}_2 and $f(\bar{x}_2)$

$$f(1.02, 8.16) = (-6.5, 39.1)$$

$$\|\nabla f(\bar{x}_1)\| = \sqrt{-6.5^2 + 39.1^2} = 39.63$$

$$\bar{x}_2 = \bar{x}_1 + \frac{1}{39.63} (-6.5, 39.1)$$

$$= (1.02, 8.16) + \frac{1}{39.63} (-6.5, 39.1) = (.86, 9.15)$$

$$f(\bar{x}_2) = -23.14$$

Since $f(\bar{x}_2) > f(\bar{x}_1)$, direction of approach is still okay.

$$\nabla f(.86, 9.15) = (45.4, 39.4)$$

$$\bar{x}_3 = (.86, 9.15) + \frac{1}{60.11} (45.4, 39.4)$$

$$\bar{x}_3 = (1.6, 9.8)$$

Since $f(\bar{x}_3) < f(\bar{x}_2)$, there is departure from path of interest and step size is decreased. Another attempt at moving from x_2 is then made.

$$d = \frac{1}{2}$$

$$\bar{x}_3' = (.86, 9.15) + \frac{\frac{1}{2}}{60.11} (45.4, 39.4)$$

$$\bar{x}_3' = (1.3, 9.5)$$

$$f(\bar{x}_3') = -14.6 \quad \text{and again } f(\bar{x}_3') > f(\bar{x}_2)$$

resulting in some improvement over x_2 .

$$\nabla f(1.3, 9.5) = (-94, 34) + \frac{1}{100} (-94, 34)$$

Since $d = 1$ was too long for the previous iteration, we try

$$d = 1/3$$

$$\bar{x}_4' = (1.3, 9.5) + \frac{1/3}{100} (-94, 34)$$

$$x_4' = (.99, 9.6)$$

Again $f(\bar{x}_4') > f(\bar{x}_3')$ and eventually, the process halts at optimum value of $x = 1, y = 10$.

APPENDIX B

EXPERIMENTAL RESULTS AND DATA

Table 1Effect of Channeling on Oxygen Utility

Coke Sample Size:	15.21gms.	
Run:	X (Well Packed)	X' (loosely packed)
Crude Gravity (API ^o)	22.7	22.7
Gas Flow Rate (cc/min)	110	110
Combustion Temperature (^o F)	950	950
Time (min)	% Oxygen by Volume (Unreacted)	
1	1.	2.3
2	3.5	4.2
3	5.4	6.0
4	6.7	7.5
5	7.8	8.4
8	12.3	12.8
10	14.1	14.8
12	16.5	16.8
16	19.8	20.0
20	20.8	20.8
24	21.0	21.0

TABLE 2
EFFECT OF COKE CONCENTRATION AND COMBUSTION
TEMPERATURE ON OXYGEN UTILITY

Coke Sample Size: 16.38 gm.					
RUN:	A	B	C	D	E
Crude Gravity (°API)	15.4	22.7	22.7	22.7	22.7
Coke Concentration (gm c/100 gm sand)	2.7	1.74	2.45	2.45	2.45
Gas Flow Rate (cc/min)	110	110	110	160	110
Combustion Temp- erature (°F)	950	950	950	1120	1120
Time (min)	% Oxygen by Volume (Unreacted)				
1	2.6	4.3	3.4	1.0	.7
2	4.2	7.6	5.7	2.4	1.4
3		10.1	6.8	4.0	1.4
4	7.6	11.2	8.2	6.8	1.5
5		12.6	10.	9.6	2.1
6	10.8				4.2
7		15.		19.6	6.0
8	13.6		14.2		9.5
9		16.7		20.7	13.6
10	16.4				
11		18.7			19.
12	18.7			19.0	20.9
14		20.2		20.9	20.4
16	20.5			20.5	20.9
22	20.9	20.9	20.9	20.9	20.9

TABLE 3
EFFECT OF COMBUSTION TEMPERATURE AND CHANNELING
ON OXYGEN UTILITY

Coke Sample Size: 12 gm.

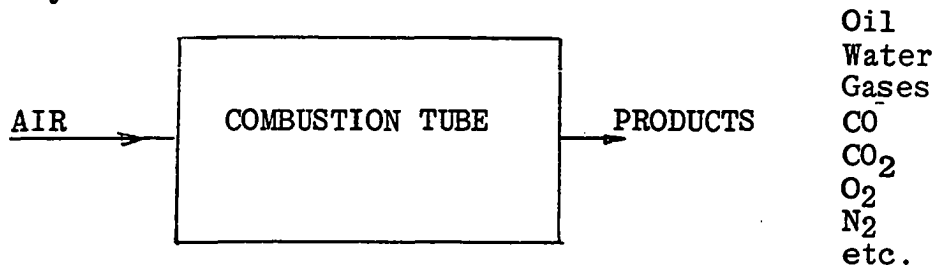
Run:	1	2	3	4
Crude Gravity °API	15.4	15.4	15.4	15.4
Gas Flow Rate (cc/min)	87	87	425	225
Combustion Temperature (°F)	830	1130	1130	1130
Time (min)	% Oxygen by Volume (Unreacted)			
1	2.3	.6	11.0	3.0
2	7.4	1.2	13.8	6.6
3	13.0	1.6	16.0	9.0
4	15.0		17.8	14.6
5		2.3	20.0	
6		3.2		
7	16.0		20.8	20.2
8		7.3		
9		14.0	20.9	20.7
11	17.4	19.0	20.9	20.9
15	18.3	20.3		
19	19.0	20.8		

APPENDIX C

HYDROGEN CARBON RATIO COMPUTATION

COMPUTATION OF HYDROGEN CARBON RATIO
FROM LAB BURNING TEST

Consider a combustion tube filled with coked material at temperature T. With air flowing in at one end and the product gases collected at the other end, the followup analysis can be conducted.



Let V_g = Total volume of gas produced.

V_a = Total volume of gas injected.

N_2 = Fraction of N_2 in produced gas.

N_{2i} = Fraction of N_2 in injected gas.

O_{2i} = Fraction of oxygen in injected gas.

O_2 = Fraction of oxygen in produced gas.

CO = Fraction of carbon monoxide in produced gas.

CO_2 = Fraction of carbon dioxide in produced gas.

Nitrogen mass balance

$$V_a N_{2i} = V_g N_2 \quad \therefore V_a = \frac{V_g N_2}{N_{2i}}$$

$$\text{Oxygen injected} = V_a O_{2i} = V_g N_2 \left(\frac{O_{2i}}{N_{2i}} \right)$$

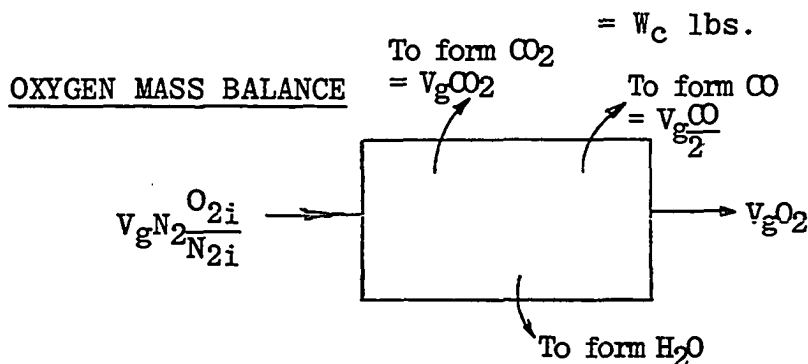
$$\text{Carbon dioxide produced} = V_g CO_2$$

$$\text{Carbon monoxide produced} = V_g CO$$

$$\text{Oxygen produced} = V_g \text{O}_2$$

$$\text{Total volume of carbon oxides formed} = V_g \text{CO}_2 + V_g \text{CO}$$

$$\text{Total mass of carbon burnt} = (V_g \text{CO}_2 + V_g \text{CO}) \left(\frac{1 \text{ lb mol.}}{\text{G.M.V.}} \right) \left(\frac{12 \text{ lb}}{\text{lb mol}} \right)$$



$$\text{Volume of O}_2 \text{ forming water} = \left[\left(V_g N_2 \frac{\text{O}_2 i}{N_2 i} \right) - V_g \text{O}_2 - V_g \text{CO}_2 - \frac{V_g \text{CO}}{2} \right]$$

$$\text{Weight of water formed} = W_w$$

$$W_w = \left[\left(V_g N_2 \frac{\text{O}_2 i}{N_2 i} \right) - V_g \text{O}_2 - V_g \text{CO}_2 - \frac{V_g \text{CO}}{2} \right] \times \left[\frac{1 \text{ lb mol O}_2}{\text{GMV}} \frac{2 \text{ lb mol H}_2\text{O}}{\text{lb mol O}_2} \times \frac{18 \text{ lbs H}_2\text{O}}{\text{lb mol H}_2\text{O}} \right]$$

$$\text{Weight of H}_2 \text{ by combustion} = W_H$$

$$W_H = W_w \left(\frac{2 \text{ lb H}_2}{18 \text{ lb H}_2\text{O}} \right)$$

$$\text{H/C Ratio} = \frac{W_H}{W_c} = \frac{\left[\left(V_g N_2 \frac{\text{O}_2 i}{N_2 i} \right) - V_g \text{O}_2 - V_g \text{CO}_2 - \frac{V_g \text{CO}}{2} \right] 4}{\left[V_g \text{CO}_2 + V_g \text{CO} \right] 12}$$

Hence,

$$\text{H/C Ratio} = \frac{W_H}{W_c} = \frac{\left[\left(N_2 \frac{\text{O}_2 i}{N_2 i} \right) - \text{O}_2 - \text{CO}_2 - \frac{\text{CO}}{2} \right]}{3(\text{CO}_2 + \text{CO})}$$

APPENDIX D

DATA AND RESULTS OF RUNS
(COKE COMBUSTION)

DATA AND RESULTS

RUN # 1

Combustion Temperature	=	950 ^o F	Crude Gravity	=	22.7 ^o API			
Weight of Coke	=	16.31gm	Coking Temperature	=	800 ^o F			
Weight of Sand	=	16.01gm	Reactor Pressure	=	Atmospheric Pressure			
Gas Flow Rate	=	110 cc/min	Conversion Factor	=	3.27 E-03			
(gmC/CC-100gm Sand)								
Time Min.	Volume Percentage of				C lb/100lb	Mean P atm.	r min ⁻¹ X10 ⁻³	Apparent H/C Ratio
	CO ₂	O ₂	CO	N ₂				
0			100		.505	.106		(.5 min)+1.5
1	4.2	3.3	4.8	87.8	.488	.122	3.24	.5
2	6.8	5.5	7.6	80.0	.446	.133	5.18	.1
3	8.1	6.6	8.6	76.7	.39	.139	6.01	.03
4	8.2	8.1	8.8	75.0	.33	.146	6.12	0.0
5	8.0	9.5	8.5	74.0	.27	.153	5.94	
6					0.214	.161	5.15	
7					.166	.169	4.36	

DATA AND RESULTS

RUN #1

Continued

Time Min.	Volume Percentage Of				C lb/100 lb	Mean P atm.	r min ⁻¹ X10 ⁻³	Apparent H/C Ratio
	CO ₂	O ₂	CO	N ₂				
8	5.5	14.3	4.4	75.8	.127	.177	3.56	
9					.094	.183	2.92	
10					.068	.190	2.27	
10.5					.058	.193	1.95	
12	1.8	19.4	.9	77.9				
16	.5	20.7		78.8				
21	.3	21.0		78.7				

DATA AND RESULTS

RUN # 2

Combustion Temperature	=	1130 ^o F	Crude Gravity	=	15.4 ^o API			
Weight of Coke	=	14.70gm	Coking Temperature	=	600 ^o F			
Weight of Sand	=	13.43gm	Reactor Pressure	=	Atmospheric Pressure			
Gas Flow Rate	=	87 cc/min.	Conversion Factor	=	4.0 E-03			
			(gmC/CC-100gm Sand)					
Time Min.	Volume Percentage of				C lb/100lb	Mean P atm.	r min ⁻¹ X10 ⁻²	Apparent H/C Ratio
	CO ₂	O ₂	CO	N ₂				
0				100.	.575			(.5min)+3.1
1	4.0	.6	.8	94.6	.567	.105	1.67	1.3
2	8.0	1.2	2.9	87.9	.539	.108	3.79	.4
3	11.0	1.6	4.7	82.8	.493	.110	5.46	.1
4					.435	.112	6.07	.08
5	13.3	2.3	5.9	78.5	.372	.114	6.68	.07
5.5					.338	.116	6.65	.0
6	13.6	3.2	5.4	77.9	.305	.118	6.61	

DATA AND RESULTS
 RUN #2
 Continued

Time Min.	Volume Percentage Of				C lb/100 lb	Mean P atm.	r min ⁻¹ X10 ⁻²	Apparent H/C Ratio
	CO ₂	O ₂	CO	N ₂				
6.5					.273	.112	6.26	
7					.243	.128	5.92	
7.5					.214	.133	5.57	
8	11.4	7.3	3.6	77.7	.187	.139	5.22	
8.5					.163	.148	4.5	
9					.142	.158	3.77	
11	1.7	19.1	.8	78.5				
15	.8	19.9	.4	78.9				

DATA AND RESULTS

RUN # 3

Combustion Temperature	=	1120 ^o F	Crude Gravity	=	22.7 ^o API			
Weight of Coke	=	14.63gm	Coking Temperature	=	700 ^o F			
Weight of Sand	=	14.28gm	Reactor Pressure	=	Atmospheric Pressure			
Gas Flow Rate	=	150 cc/min.	Conversion Factor	=	3.67 E-03 (gmC/CC-100gm Sand)			
Time Min.	Volume Percentage of				C lb/100lb	Mean P atm.	r min ⁻¹ X10 ⁻²	Apparent H/C Ratio
0	100.							(.5min)+.6
1	8.2	1.0	11.6	79.1	.588	.110	11.6	.1
2	10.2	2.8	12.4	74.6	.463	.119	13.3	.01
2.5					.398	.123	12.8	.0
3	10.2	4.4	10.9	74.6	.335	.127	12.4	.0
3.5					.276	.124	11.5	
4	9.5	7.1	8.4	75.1	.221	.141	10.5	
4.5					.171	.148	9.42	
5	8.1	9.9	6.1	75.9	.126	.155	8.34	

DATA AND RESULTS

RUN #3

Continued

Time Min.	Volume Percentage Of				C		Mean P atm.	r min ⁻¹ X10 ⁻²	Apparent H/C Ratio
	CO ₂	O ₂	CO	N ₂	lb/100	lb			
5.5					.09		.167	6.42	
7	1.0	19.8	.1	79.3	.037		.204	.65	
9	.3	20.8		78.9					

DATA AND RESULTS

RUN # 4

Combustion Temperature	=	830°F	Crude Gravity	=	15.4° API			
Weight of Coke	=		Coking Temperature	=	600°F			
Weight of Sand	=	12.14gm	Reactor Pressure	=	Atmospheric Pressure			
Gas Flow Rate	=	110 cc/min.	Conversion Factor	=	4.3 E-03			
(gmC/CC-100gm Sand)								
Time Min.	<u>Volume Percentage of</u>				C lb/100lb	Mean P atm.	r min ⁻¹ X10 ⁻²	Apparent H/C Ratio
0	100							(.5min)+3.0
1	3.7	2.3	0.4	93.6	.521	.107	1.94	1.3
2	4.9	7.4	1.4	86.4	.497	.132	3.0	.41
3	3.9	12.9	1.0	82.2	.470	.160	2.32	.2
4	3.9	14.6	1.2	80.3	.440	.168	2.41	.05
5	3.4	14.7	1.1	80.8	.424	.169	2.13	.04
7	3.3	15.7	1.3	79.7	.402	.174	2.18	.0
8					.381	.175	2.11	

DATA AND RESULTS

RUN #4

Continued

Time Min.	Volume Percentage Of				C lb/100 lb	Mean P atm.	r min ⁻¹ X10 ⁻²	Apparent H/C Ratio
	CO ₂	O ₂	CO	N ₂				
10					.319	.179	2.0	
12	2.8	17.4	1.2	78.6	.280	.182	1.84	
14					.245	.184	1.70	
16	2.1	18.3	1.2	78.3	.212	.187	1.56	
18					.182	.187	1.48	
20					.153	.188	1.39	
22					.126	.189	1.31	
25	1.6	19.0	.9	78.5	.095	.190	1.18	
30	1.4	19.0	.5	79.1				

DATA AND RESULTS

RUN # 5

Combustion Temperature	=	1070 ^o F	Crude Gravity	=	15.4 ^o API			
Weight of Coke	=		Coking Temperature	=	600 ^o F			
Weight of Sand	=	11.2gm	Reactor Pressure	=	Atmospheric Pressure			
Gas Flow Rate	=	225 cc/min.	Conversion Factor	=	4.68 E-03			
(gmC/CC-100gm Sand)								
Time Min.	Volume Percentage of				C lb/100lb	Mean P atm.	r min ⁻¹ X10 ⁻²	Apparent H/C Ratio
	CO ₂	O ₂	CO	N ₂				
0				100.	.589			(.5min)+1.2
1	6.4	7.3	3.4	83.0	.537	.143	10.3	.3
2	8.9	6.5	5.3	79.3	.411	.145	15.0	.08
2.5					.338	.147	14.3	.04
3	8.6	8.9	4.4	78.1	.268	.151	13.7	.005
3.5					.206	.165	11.1	.0
4	5.4	14.3	2.6	77.7	.157	.178	8.4	.0
4.5					.125	.192	6.37	

DATA AND RESULTS

RUN #5

Continued

Time Min.	Volume Percentage Of				C lb/100 lb	Mean P atm.	r min ⁻¹ X10 ⁻²	Apparent H/C Ratio
	CO ₂	O ₂	CO	N ₂				
5	1.5	19.7	.7	78.0	.104	.205	5.5	
7	.5	21.3		78.2				
10	.3	21.3		78.4				
14	.3	21.3		78.4				

DATA AND RESULTS

RUN # 7

Combustion Temperature	=	930 ^o F	Crude Gravity	=	22.7 ^o API			
Weight of Coke	=	16.38gm	Coking Temperature	=	800 ^o F			
Weight of Sand	=	16.1gm	Reactor Pressure	=	Atmospheric Pressure			
Gas Flow Rate	=	195 cc/min.	Conversion Factor	=	3.26 E-03			
(gmC/CC-100gm Sand)								
Time Min.	Volume Percentage of				C lb/100lb	Mean P atm.	r min ⁻¹ X10 ⁻²	Apparent H/C Ratio
0				100	.498	.109		(.5min)→1.75
1	4.4	8.7	2.6	84.4	.476	.152	4.45	.9
2	6.0	11.6	3.9	78.5	.422	.167	6.29	.08
3	6.0	12.6	4.2	77.2	.358	.172	6.48	.02
4	5.5	14.1	3.8	76.6	.296	.179	4.91	.0
5	4.7	15.7	3.1	76.5	.242	.187	4.96	
6	4.1	17.1	2.3	74.5	.197	.194	4.07	
7					.159	.197	3.43	

DATA AND RESULTS

RUN #7

Continued

Time Min.	Volume Percentage Of				C lb/100 lb	Mean P atm.	r min ⁻¹ x10 ⁻²	Apparent H/C Ratio
	CO ₂	O ₂	CO	N ₂				
8	3.1	18.4	1.3	77.0	.128	.201	2.80	
9					.102	.203	2.40	
10					.08	.206	2.0	
11	2.0	19.9	1.0	77.6	.062	.208	1.59	
12					.0477	.210	1.32	
13	1.4	20.8		77.8	.036	.213	1.05	
14					.027	.214	.81	
15	0.9	21.2		77.9				
18	.3	21.6		78.1				

DATA AND RESULTS

RUN # 8

Combustion Temperature	=	910°F	Crude Gravity	=	22.7° API			
Weight of Coke	=	16.37gm	Coking Temperature	=	800°F			
Weight of Sand	=	16.08gm	Reactor Pressure	=	Atmospheric Pressure			
Gas Flow Rate	=	270 cc/min.	Conversion Factor	=	3.26 E-03			
(gmC/CC-100gm Sand)								
Time Min.	Volume Percentage of				C	Mean P	r	Apparent H/C Ratio
	CO ₂	O ₂	CO	N ₂	lb/100lb	atm.	min ⁻¹ X10 ⁻²	
0				100	.626	.104		(.5min)+1.9
1	3.4	9.2	2.7	84.6	.60	.150	5.37	.5
2	5.2	12.7	4.5	77.6	.53	.167	8.54	.004
3	6.8	13.9	4.6	74.7	.437	.173	10.0	.0
4	5.7				.344	.179	8.63	.0
5	4.7	16.1	3.6	75.6	.264	.184	7.31	
6					.198	.186	5.81	
7	2.8	17.0	2.1	78.2	.148	.189	4.31	

DATA AND RESULTS

RUN #8

Continued

Time Min.	Volume Percentage Of				C lb/100 lb	Mean P atm.	r min ⁻¹ X10 ⁻²	Apparent H/C Ratio
	CO ₂	O ₂	CO	N ₂				
8					.109	.192	3.39	
9	1.7	18.4	1.1	78.8	.08	.196	2.47	
10					.06	.199	1.72	
11	.8	19.5	.3	79.4				
13	.5	19.5		80.0				
17	.3	20.3		79.4				
21	.2	20.6		79.2				

DATA AND RESULTS

RUN # 10

Combustion Temperature	=	1250 ^o F	Crude Gravity	=	22.7 ^o API			
Weight of Coke	=	15.68gm	Coking Temperature	=	700 ^o F			
Weight of Sand	=	15.27gm	Reactor Pressure	=	Atmospheric Pressure			
Gas Flow Rate	=	125 cc/min.	Conversion Factor	=	3.43 E-03			
(gmC/CC-100gm Sand)								
Time Min.	Volume Percentage of				C lb/100lb	Mean P atm.	r min ⁻¹ X10 ⁻²	Apparent H/C Ratio
	CO ₂	O ₂	CO	N ₂				
0				100	.764			(.5min)+1.1
1	9.1	.7	2.3	87.9	.740	.104	4.89	.4
2	12.9	1.4	4.8	81.	.677	.107	7.59	.08
3	14.5	1.4	6.4	77.7	.594	.107	8.96	.01
4	15.1	1.4	6.9	76.7	.503	.107	9.43	
5	15.2	2.1	6.1	76.6	.410	.111	9.13	
6	14.6	4.2	4.4	76.8	.323	.121	8.15	
6.5					.283	.124	7.8	

DATA AND RESULTS
 RUN #10
 Continued

Time Min.	Volume Percentage Of				C lb/100 lb	Mean P atm.	r min ⁻¹ X10 ⁻²	Apparent H/C Ratio
	CO ₂	O ₂	CO	N ₂				
7	14.0	5.2	3.5	77.3	.245	.126	7.5	
7.5					.210	.135	6.6	
8	11.2	8.7	2.3	77.8	.179	.144	5.79	
8.5					.152	.154	4.9	
9	8.3	12.8	1.1	77.7	.130	.164	4.0	
10					.95	.178	2.9	
11	3.5	18.3	.4	77.8				
14	2.6	19.4		78.0				
17	2.1	20.0		77.9				

DATA AND RESULTS

RUN # 15

Combustion Temperature	=	950 ^o F	Crude Gravity	=	15.4 ^o API			
Weight of Coke	=	11.22gm	Coking Temperature	=	600 ^o F			
Weight of Sand	=	10.2gm	Reactor Pressure	=	Atmospheric Pressure			
Gas Flow Rate	=	110 cc/min.	Conversion Factor	=	5.14 E-03			
(gmC/CC-100gm Sand)								
Time Min.	Volume Percentage of				C	Mean P	r	Apparent H/C Ratio
	CO ₂	O ₂	CO	N ₂	lb/100lb	atm.	min ⁻¹ X10 ⁻²	
0				100	.501			(.5min)→2.2
1	3.7	4.4	2.7	89.2	.483	.129	3.62	.8
2	4.6	8.0	3.6	83.9	.442	.147	4.64	.3
3	5.6	10.8	4.4	79.2	.390	.161	5.65	.1
4	6.3	11.5	4.4	77.8	.332	.164	6.05	.03
5	5.8	13.1	3.9	77.2	.274	.172	5.48	.02
6					.221	.178	5.03	.0
7	4.8	15.6	3.3	76.3	.173	.185	4.58	.0

DATA AND RESULTS

RUN #15

Continued

Time Min.	Volume Percentage Of				C		Mean P atm.	r min ⁻¹ X10 ⁻²	Apparent H/C Ratio
	CO ₂	O ₂	CO	N ₂	lb/100	lb			
8					.131		.188	3.82	
9	3.5	17.0	1.9	77.6	.097		.192	3.05	
10					.07		.198	2.35	
11	2.0	19.5	.9	77.6	.05		.201	2.0	
12									
14	.7	21.2		78.1					
20	.2	21.2		78.6					

DATA AND RESULTS

RUN # 16

Combustion Temperature	= 975 ^o F	Coking Temperature	= 800 ^o F
Weight of Sand	= 10.26gm	Reactor Pressure	= 1.9 psig
Gas Flow Rate	= 120 cc/min.	Conversion Factor	= 5.11 E-03
Crude Gravity	= 22.7 ^o API	(gmC/CC-100gm Sand).	

Time Min.	Volume Percentage of				C lb/100lb	Mean P atm.	r min ⁻¹ X10 ⁻²	Apparent H/C Ratio
	CO ₂	O ₂	CO	N ₂				
0				100	.473	.115		(.5min)→1.3
1	8.0	1.2	2.3	88.5	.441	.121	6.32	.4
2	12.6	3.4	3.8	80.2	.360	.134	10.1	.0
3	11.0	7.5	3.5	78.0	.265	.157	8.9	.0
4	8.8	10.2	3.2	77.8	.184	.172	7.36	
5	6.5	12.8	2.0	78.7	.121	.187	5.21	
6	4.6	15.2	1.1	79.1	.077	.20	3.49	
7	3.2	17.0	0.6	79.2	.048	.211	2.33	

DATA AND RESULTS

RUN # 16

Continued

Time Min.	Volume Percentage Of				C		Mean P atm.	r min ⁻¹ X10 ⁻²	Apparent H/C Ratio
	CO ₂	O ₂	CO	N ₂	lb/100	lb			
8	2.2	18.2	0.3	79.3	.03		.217	1.53	
9	1.5	19.2	.1	79.2	.02		.223	1.0	
10	.8	20.0		79.2					
11	.5	20.3		79.2					

DATA AND RESULTS

RUN # 17

Combustion Temperature	=	900 ^o F	Coking Temperature	=	600 ^o F			
Weight of Sand	=	10.35gm	Reactor Pressure	=	3.1 psig			
Gas Flow Rate	=	170 cc/min.	Conversion Factor	=	5.063 E-03			
Crude Gravity	=	15.4 ^o API	(gmC/CC-100gm Sand)					
Time Min.	Volume Percentage of				C lb/100lb	Mean P atm.	r min ⁻¹ X10 ⁻²	Apparent H/C Ratio
0				100	.456	.124		(.5min.)→1.1
1	8.6	2.5	3.0	85.9	.406	.139	10.0	.3
2	8.7	9.0	2.8	79.5	.307	.179	9.9	.04
3	6.7	12.5	2.0	78.8	.220	.20	7.48	.01
4	5.0	15.1	1.4	78.5	.155	.216	5.50	.0
5	3.5	16.6	.8	79.1	.109	.225	3.70	
6	2.4	17.7	.4	79.5	.078	.231	2.41	
7	1.7	18.7	.1	79.5	.059	.237	1.55	

DATA AND RESULTS

RUN #17

Continued

Time Min.	Volume Percentage Of				C lb/100 lb	Mean P atm.	r min ⁻¹ X10 ⁻²	Apparent H/C Ratio
	CO ₂	O ₂	CO	N ₂				
8	1.0	19.4	.1	79.5	.046	.242	.95	
9	.8	20.2		79.0	.037	.244	.82	
10	.6	20.3		79.1	.030	.246	.69	
14	.5	20.4		79.1				
16	.4	20.5		79.1				

DATA AND RESULTS

RUN # 18

Combustion Temperature	=	950 ^o F	Coking Temperature	=	800 ^o F
Weight of Sand	=	10.46gm	Reactor Pressure	=	2.9 psig
Gas Flow Rate	=	140 cc/min.	Conversion Factor	=	5.01 E-03
Crude Gravity	=	22.7 ^o API	(gmC/CC-100gm Sand)		

Time Min.	Volume Percentage of				C lb/100lb	Mean P atm.	r min ⁻¹ X10 ⁻²	Apparent H/C Ratio
	CO ₂	O ₂	CO	N ₂				
0				100	.32	.102		(.5min) ⁻¹ 1.3
1	5.4	8.6	2.9	83.1	.291	.145	5.82	.2
2	4.7	14.0	2.0	79.3	.238	.172	4.7	.09
3	3.8	14.8	1.9	79.5	.195	.176	4.0	.04
4	3.3	15.4	1.6	79.7	.158	.179	3.44	.03
5	2.9	17.1	1.2	78.8	.126	.187	2.88	.0
6	2.4	17.7	1.2	78.7	.099	.19	2.52	
7	21.	18.3	.8	78.8	.076	.193	2.03	

DATA AND RESULTS

RUN # 18

Continued

Time Min.	Volume Percentage Of				C		Mean P atm.	r min ⁻¹ X10 ⁻²	Apparent H/C Ratio
	CO ₂	O ₂	CO	N ₂	lb/100	lb			
8	1.8	18.7	.6	78.9	.058		.195	1.68	
9					.042		.196	1.40	
10	1.3	19.2	.3	79.2	.030		.198	1.12	
11					.020		.199	.91	
12	.9	19.8	.1	79.2					
13									
14	.1	20.3		79.6					

DATA AND RESULTS

RUN # 19

Combustion Temperature	= 1250 ^o F	Coking Temperature	= 800 ^o F					
Weight of Sand	= 10.45gm	Reactor Pressure	= 1.2 psig					
Gas Flow Rate	= 70 cc/min.	Conversion Factor	= 5.05 E-03					
Crude Gravity	= 22.7 ^o API	(gmC/CC-100gm Sand)						
Time Min.	Volume Percentage of				C lb/100lb	Mean P atm.	r min ⁻¹ X10 ⁻²	Apparent H/C Ratio
	CO ₂	O ₂	CO	N ₂				
0				100	.411			(.5min) ⁺ 1.4
1	7.5	.6	.6	91.3	.397	.101	2.86	.5
2	14.6	1.4	1.4	82.6	.354	.104	5.66	.36
3	16.4	1.7	2.2	79.7	.293	.107	6.58	.0
4	17.0	2.1	3.4	77.5	.224	.109	7.21	
5	16.7	2.9	3.2	77.2	.153	.113	7.03	
5.5					.120	.113	6.26	
6	13.4	3.7	2.1	80.7	.09	.117	5.48	

DATA AND RESULTS

RUN # 19

Continued

Time Min.	Volume Percentage Of				C lb/100 lb	Mean P atm.	r min ⁻¹ X10 ⁻²	Apparent H/C Ratio
	CO ₂	O ₂	CO	N ₂				
6.5					.065	.132	4.44	
7	8.6	9.0	1.0	81.4	.046	.146	3.39	
7.5					.031	.159	2.56	
8	4.5	13.7	0.4	81.4	.020	.171	1.73	
8.5					.013	.175	1.31	
9	2.4	15.0	0.1	82.5				
10	1.3	18.0		80.7				

DATA AND RESULTS

RUN # 20

Combustion Temperature	= 925 ^o F	Coking Temperature	= 700 ^o F					
Weight of Sand	= 10.33 gm	Reactor Pressure	= 3 psig					
Gas Flow Rate	= 130 cc/min.	Conversion Factor	= 5.07 E+03					
Crude Gravity	= 15.4 ^o API	(gmC/CC-100gm Sand)						
Time Min.	Volume Percentage of				C lb/100lb	Mean P atm.	r min ⁻¹ X10 ⁻²	Apparent H/C Ratio
0	100				.564	.122		(.5min)→.9
1	10.2	1.2	2.7	85.9	.522	.129	8.5	.24
2	11.8	4.5	3.2	80.3	.429	.149	10.0	.06
3	10.1	7.6	2.9	29.4	.336	.168	8.57	.03
4	8.4	10.1	2.5	79.0	.257	.183	7.19	.02
5	6.8	12.6	2.1	78.5	.192	.198	5.87	.0
6	5.2	14.5	1.6	78.7	.140	.210	4.48	
7	3.6	16.6	1.1	78.7	.102	.222	3.10	

DATA AND RESULTS

RUN # 20

Continued

Time Min.	Volume Percentage Of				C lb/100 lb	Mean P atm.	r min ⁻¹ X10 ⁻²	Apparent H/C Ratio
	CO ₂	O ₂	CO	N ₂				
8	2.4	17.8	.7	79.1	.0766	.229	2.04	
9					.0587	.234	1.55	
10	1.3	19.4	.3	79.0	.0457	.239	1.05	
11					.0359	.240	.89	
12	.9	19.8	.2	79.1	.0279	.241	.72	
14	.7	20.0		79.3				
16	.5	20.2		79.3				
18	.5	20.3		79.3				

DATA AND RESULTS

RUN # 21

Combustion Temperature	=	830 ^o F	Coking Temperature	=	800 ^o F			
Weight of Sand	=	10.4 gm	Reactor Pressure	=	1.9 psig			
Gas Flow Rate	=	110 cc/min.	Conversion Factor	=	5.04 E-03			
Crude Gravity	=	22.1 ^o API	(gmC/CC-100gm Sand)					
Time Min.	Volume Percentage of				C lb/100lb	Mean P atm.	r min ⁻¹ X10 ⁻²	Apparent H/C Ratio
0				100	.39	.107		(.5min)→ 1.3
1	5.8	1.9	3.4	88.9	.365	.118	5.1	
2	4.8	10.3	2.8	82.1	.318	.165	4.21	.14
3	3.7	13.3	1.9	81.1	.281	.182	3.10	.09
4	3.3	15.0	1.5	80.2	.253	.192	2.66	.02
5					.227	.196	2.49	.0
6	2.8	16.4	1.4	79.4	.203	.200	2.33	
7					.180	.201	2.22	

DATA AND RESULTS

RUN # 21

Continued

Time Min.	Volume Percentage Of				C lb/100 lb	Mean P atm.	r min ⁻¹ X10 ⁻²	Apparent H/C Ratio
	CO ₂	O ₂	CO	N ₂				
8	2.7	16.8	1.1	79.4	.158	.202	2.11	
9					.138	.203	2.02	
10	2.5	17.2	1.0	79.3	.118	.204	1.94	
11	2.4	17.3	.9	79.4	.099	.205	1.83	
12	2.3	17.6	.8	79.3	.081	.207	1.72	
13					.065	.208	1.55	
14	1.9	17.9	.6	79.6	.05	.208	1.39	
16	1.7	18.4	.5	79.4				
18	1.6	19.0	.3	79.1				

DATA AND RESULTS

RUN # 22

Combustion Temperature	=	950 ^o F	Crude Gravity	=	15.4 ^o API			
Weight of Coke	=	15.56 gm	Coking Temperature	=	700 ^o F			
Weight of Sand	=	15.21 gm	Reactor Pressure	=	Atmospheric			
Gas Flow Rate	=	105 cc/min.	Conversion Factor	=	3.45 E-03			
(gmC/CC-100gm Sand)								
Time Min.	<u>Volume Percentage of</u>				C lb/100lb	Mean P atm.	r min ⁻¹ x10 ⁻²	Apparent H/C Ratio
	CO ₂	O ₂	CO	N ₂				
0				100	.603	.106		(.5min)+1.8
1	4.4	1.0	3.9	90.7	.588	.111	3.01	1.1
2	6.7	3.5	5.9	83.9	.550	.124	4.57	.25
3	8.0	5.4	7.1	79.4	.50	.133	5.47	.1
4	8.3	6.7	7.5	77.6	.444	.140	5.73	.05
5	8.3	7.8	7.4	76.5	.387	.145	5.69	.02
6	8.1	9.0	7.1	75.8	.331	.151	5.51	.0
7					.279	.159	4.98	

DATA AND RESULTS

RUN # 22

Continued

Time Min.	Volume Percentage Of				C 1b/100 1b	Mean P atm.	r min ⁻¹ X10 ⁻²	Apparent H/C Ratio
	CO ₂	O ₂	CO	N ₂				
8	6.8	12.3	5.5	75.5	.231	.168	4.46	
9					.189	.172	4.06	
10	5.6	14.1	4.5	75.8	.150	.177	3.66	
11					.117	.183	3.04	
12	3.9	16.5	2.8	76.8	.0894	.189	2.43	
13					.067	.193	2.05	
14	2.7	18.4	1.9	77.	.0484	.198	1.67	
15					.0336	.202	1.30	
16	1.6	19.8	1.0	77.7				
18								
20	.5	21.2		78.3				

DATA AND RESULTS

RUN # 23

Combustion Temperature	=	950 ^o F	Crude Gravity	=	15.4 ^o API			
Weight of Coke	=	17.95 gm	Coking Temperature	=	700 ^o F			
Weight of Sand	=	17.52 gm	Reactor Pressure	=	Atmospheric Pressure			
Gas Flow Rate	=	220 cc/min.	Conversion Factor	=	3.0 E-03			
(gmC/CC-100gm Sand)								
Time Min.	Volume Percentage of				C lb/100lb	Mean P atm.	r min ⁻¹ X10 ⁻²	Apparent H/C Ratio
	CO ₂	O ₂	CO	N ₂				
0				100	.576	.105		(.25min)+2.0
1	7.6	5.8	5.3	81.3	.533	.134	8.52	.14
2	8.5	7.5	6.6	77.4	.441	.142	9.97	.027
3	8.5	9.0	7.0	75.4	.340	.150	10.2	.0
3.5					.291	.155	9.37	.0
4	7.4	11.2	5.5	75.8	.246	.161	8.51	
4.5					.207	.168	7.42	

DATA AND RESULTS

RUN #23

Continued

Time Min.	Volume Percentage Of				C		Mean P atm.	r min ⁻¹ X10 ⁻²	Apparent H/C Ratio
	CO ₂	O ₂	CO	N ₂	lb/100	lb			
5	5.6	14.2	4.0	76.1	.172		.176	6.3	
5.5					.143		.181	5.44	
6	4.2	16.5	2.7	76.6	.118		.187	4.55	
6.5					.0964		.190	4.0	
7	3.2	17.8	1.9	77.1	.078		.194	3.37	
7.5					.063		.196	2.87	
8	2.3	18.9	1.3	77.5	.049		.199	2.38	
8.5					.038		.201	2.05	
9	1.6	19.8	1.0	77.7	.029		.204	1.72	
10	1.1	20.4		78.3					
11	.7	20.9		78.4					
14	.3	21.5		78.8					